# Vortex Interactions and the Barotropic Aspects of Concentric Eyewall Formation

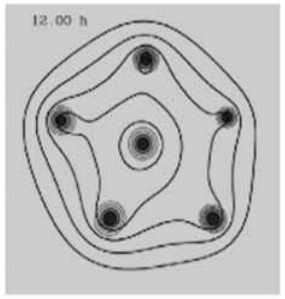


Hung-Chi Kuo
Department of Atmospheric Sciences
National Taiwan University
Taipei, Taiwan

Institute of Mathematical Sciences
NUS
November 14 2006

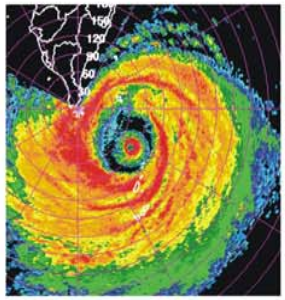

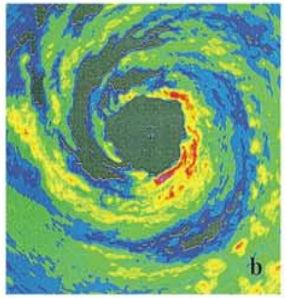


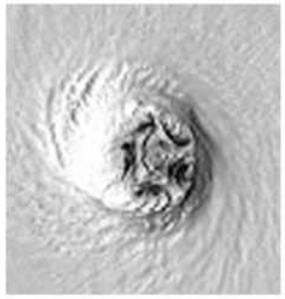

# 象神颱風侵襲後的台北市

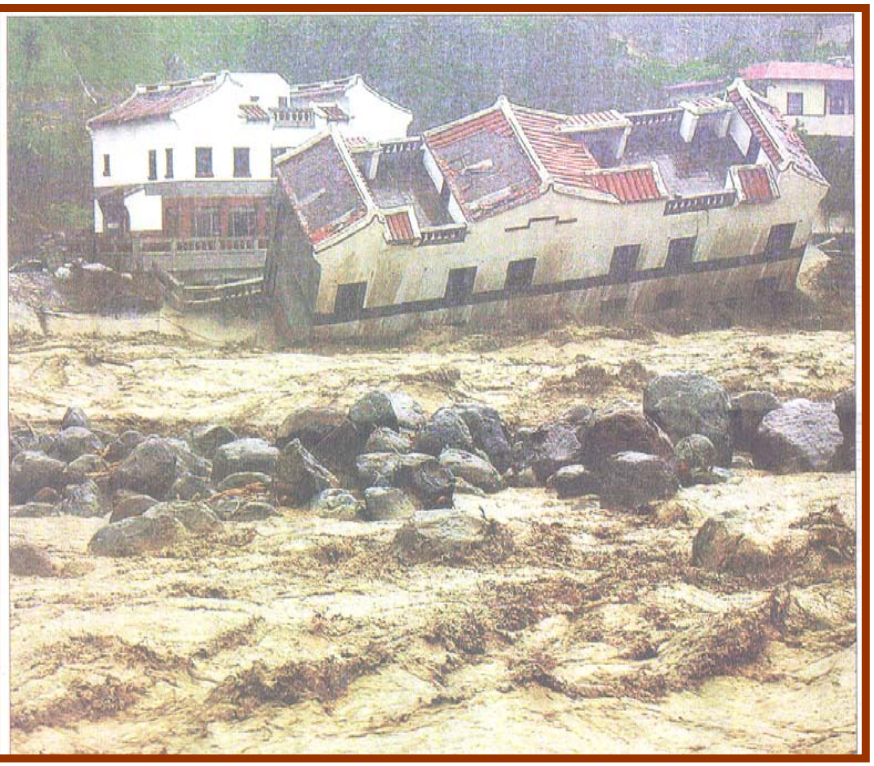

桃芝颱風（2001）

納莉颱風（2001）

**CWB is capable of 24 hr and 100km scale ppn (phase locked with topography)**

**0 to 12 hr and 10 km ppn remain biggest challenges**

**355mm in 5 hr in the city of KaoShung (5 pm to 10 pm at the beginning of the rush hour)**

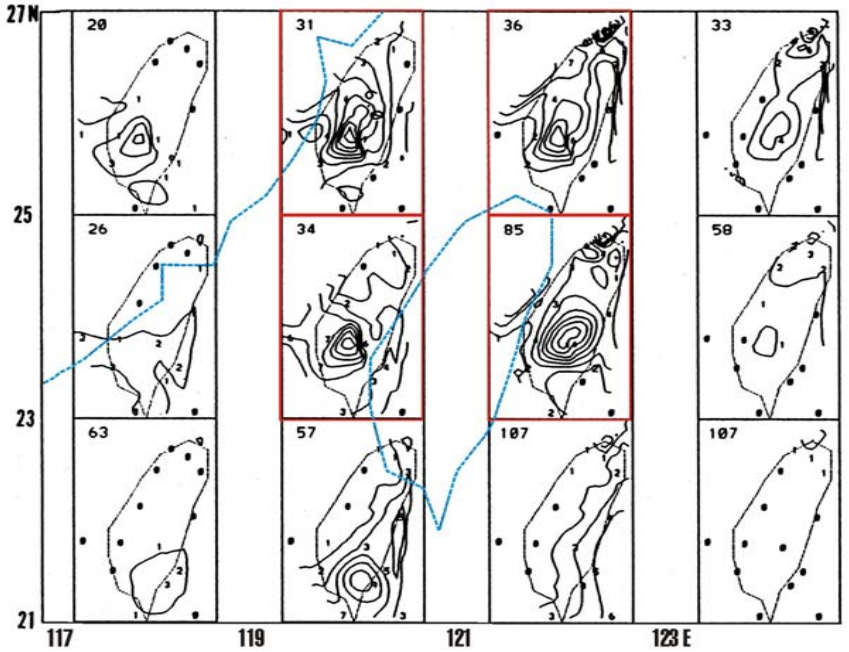


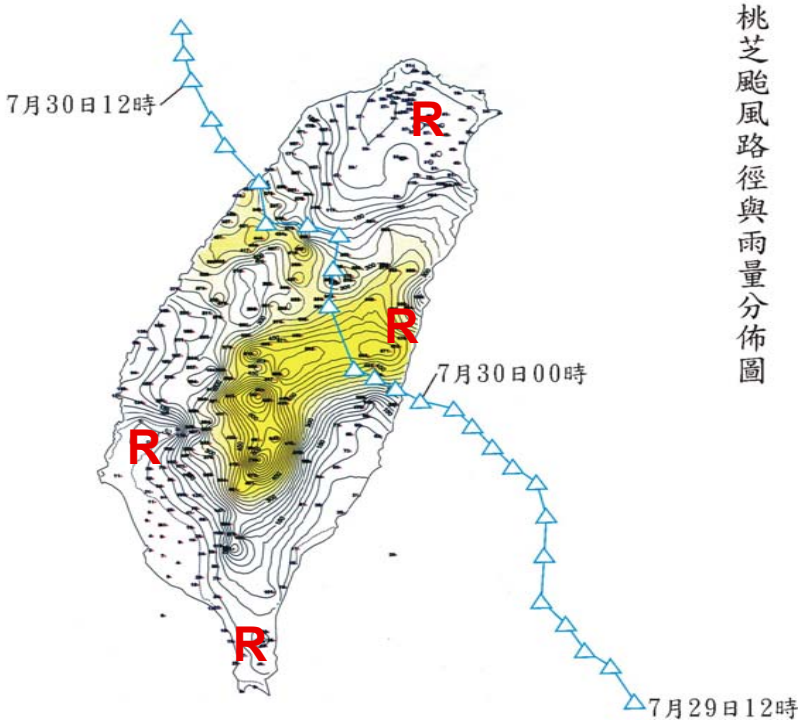

# Concentric eyewalls near Taiwan

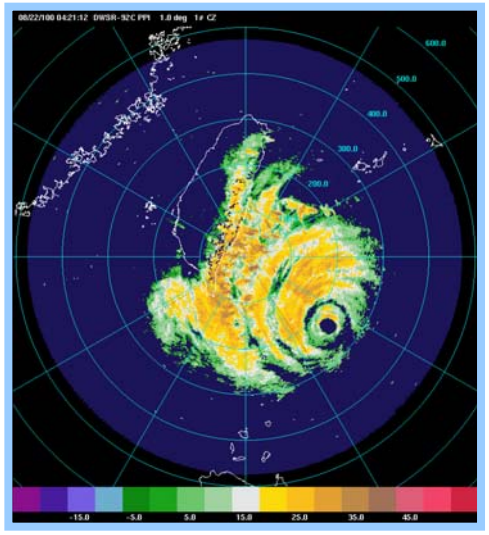

Bilis(2000)

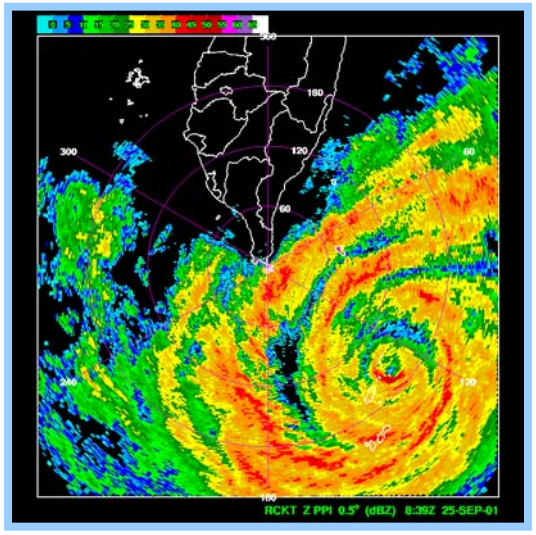


Lekima(2001)

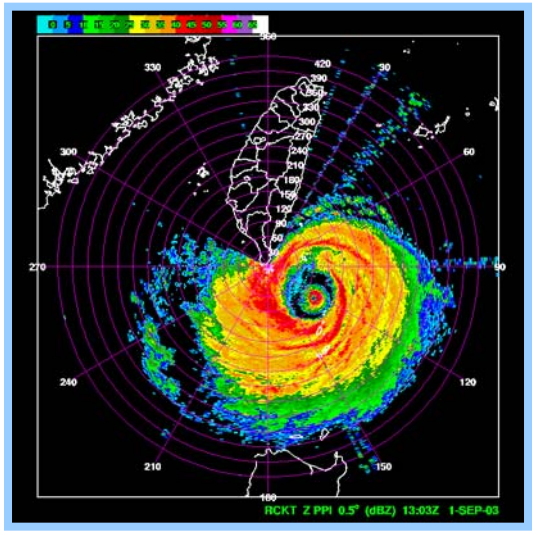


Dujuan(2003)

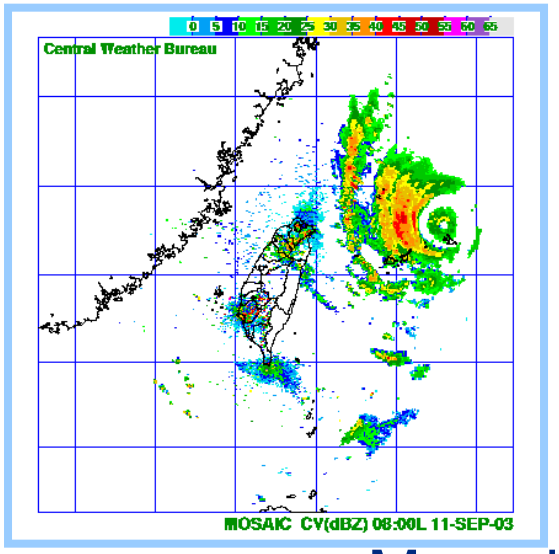


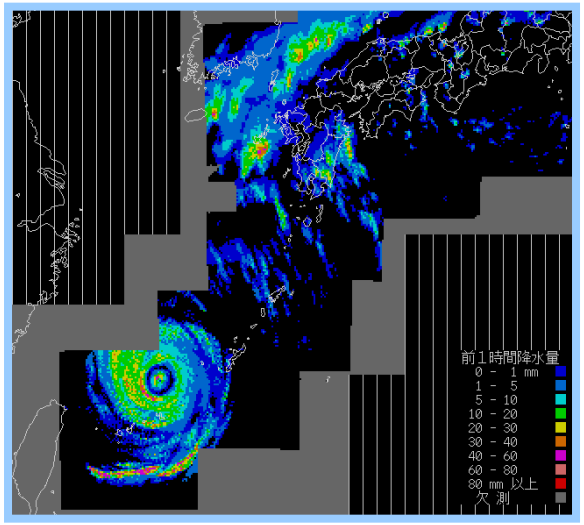


Maemi(2003)

ELDORA

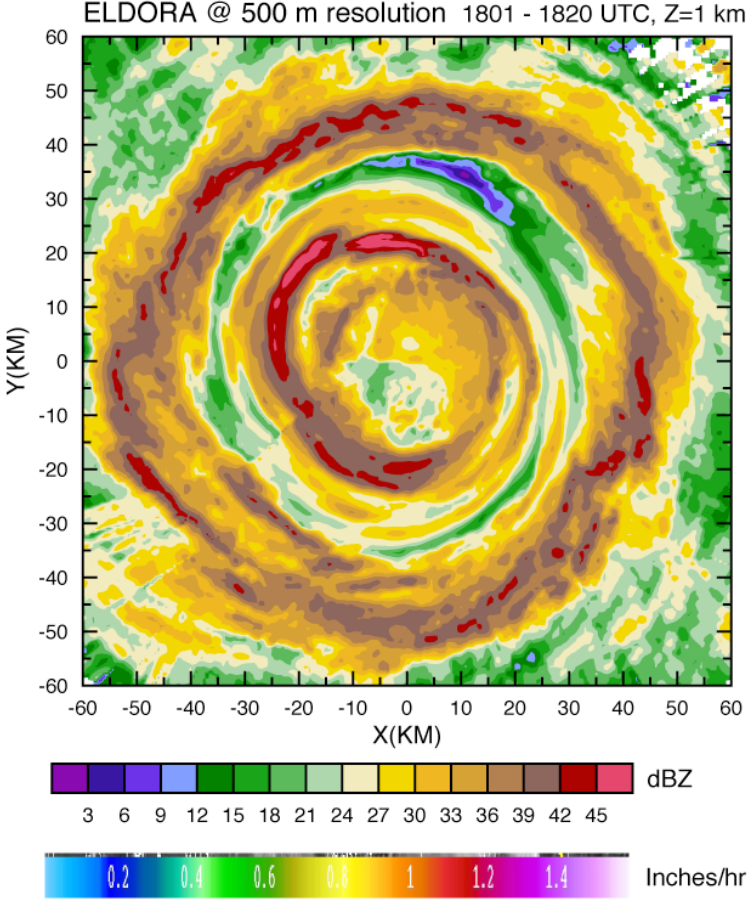


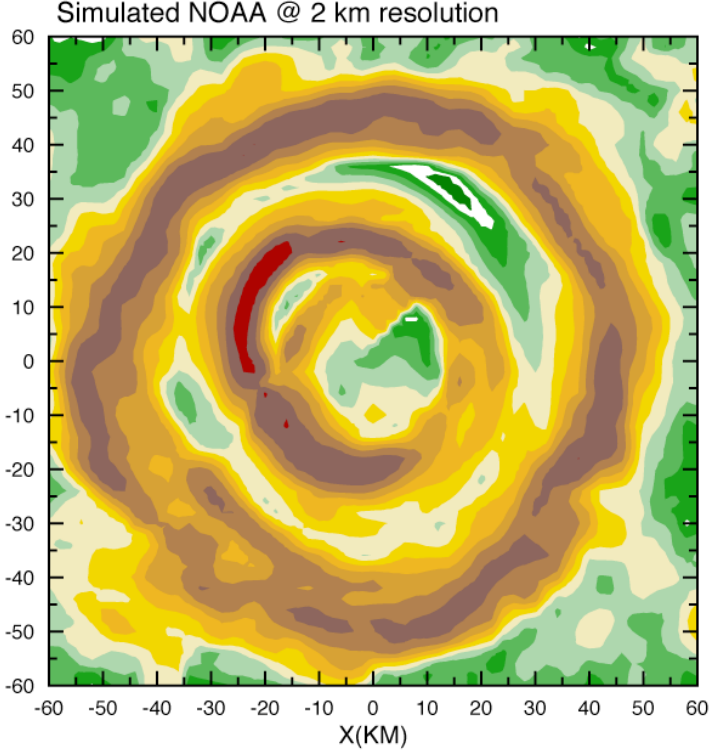


RAINEX

TRMM

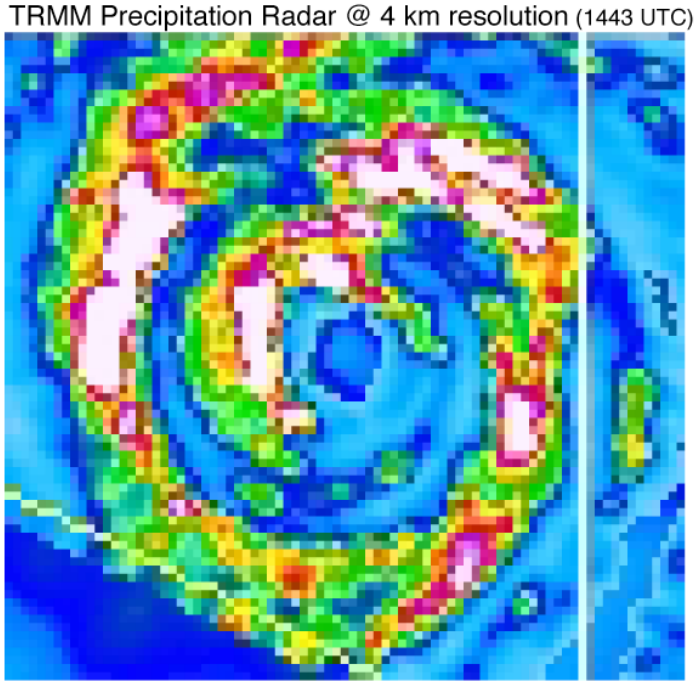

# WNPAC

- 1997~2004
- 197 tropical cyclones
- 182 tropical cyclones examined
- 44 concentric tropical cyclones (25%)
- higher intensity, higher percentage of concentric eyewall

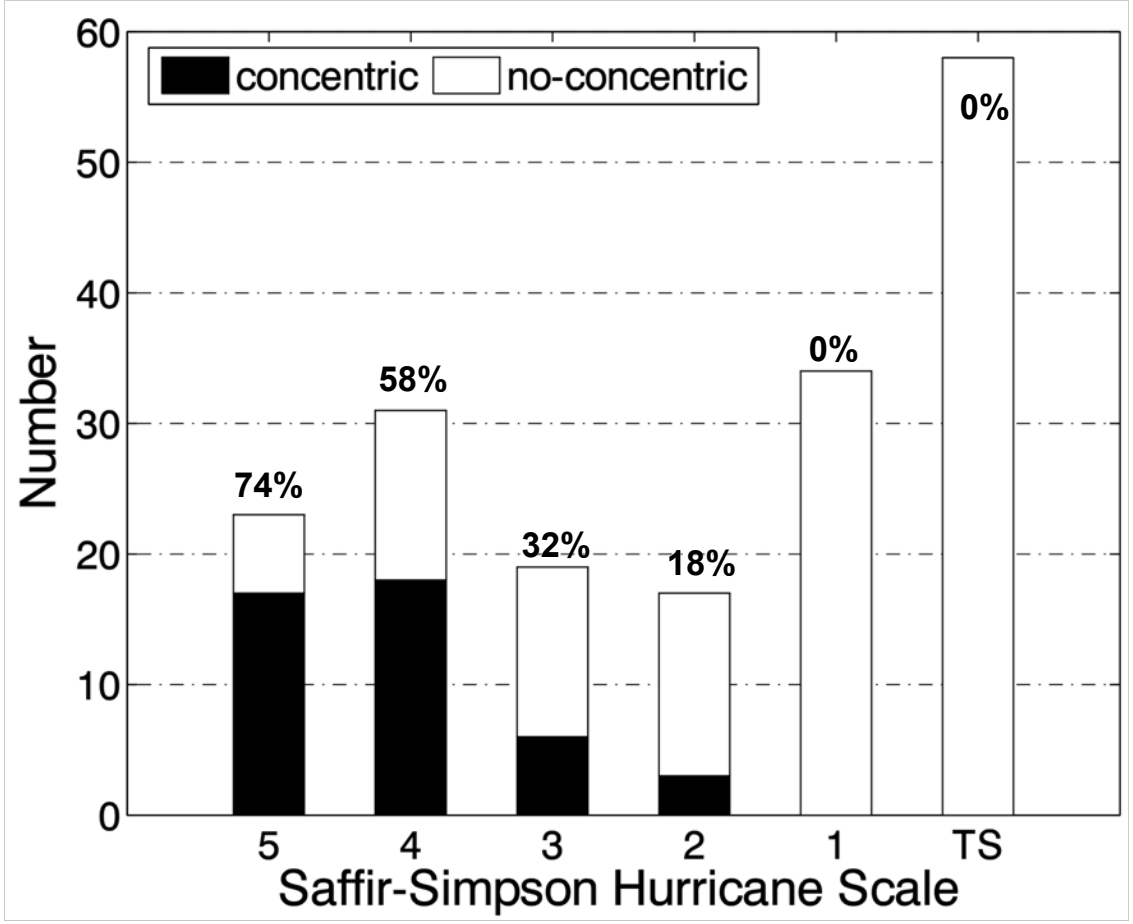


category 5 (135+ kts)
category 4 (114-135 kts)
category 3 (96-113 kts)
category 2 (83-95 kts)
category 1 (64-82 kts)
TS(63- kts)

# *Knaff and Koss*

- color-enhanced IR image of Hurricane Luis (1995) at 2015 UTC 3 Sep

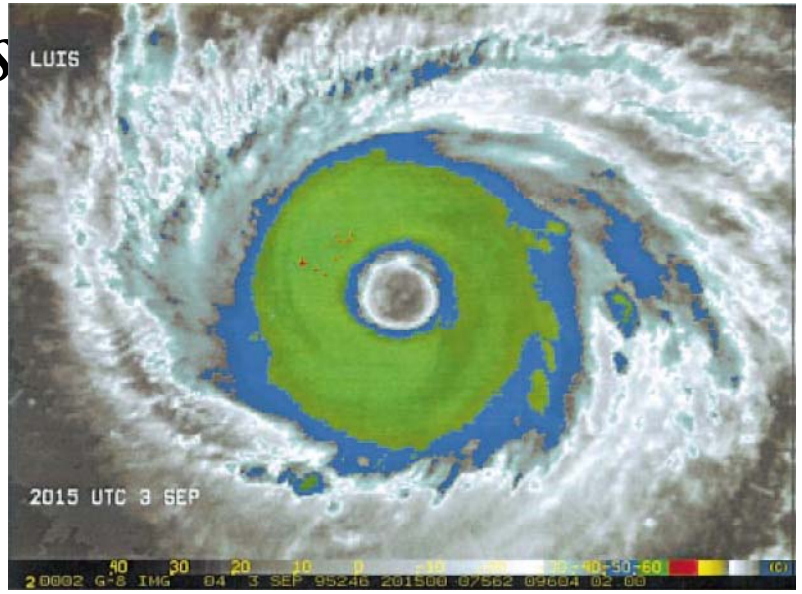


| dimensionless | 24-h weakening |
|---|---|
| ATL(56) | 0.14 |
| Annular hurricanes(6) | 0.05 |

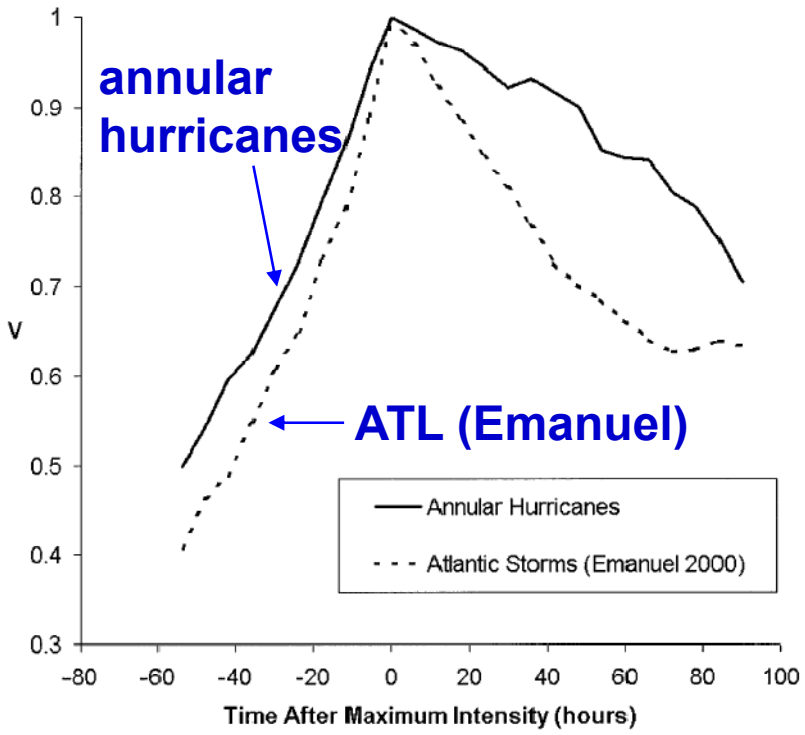

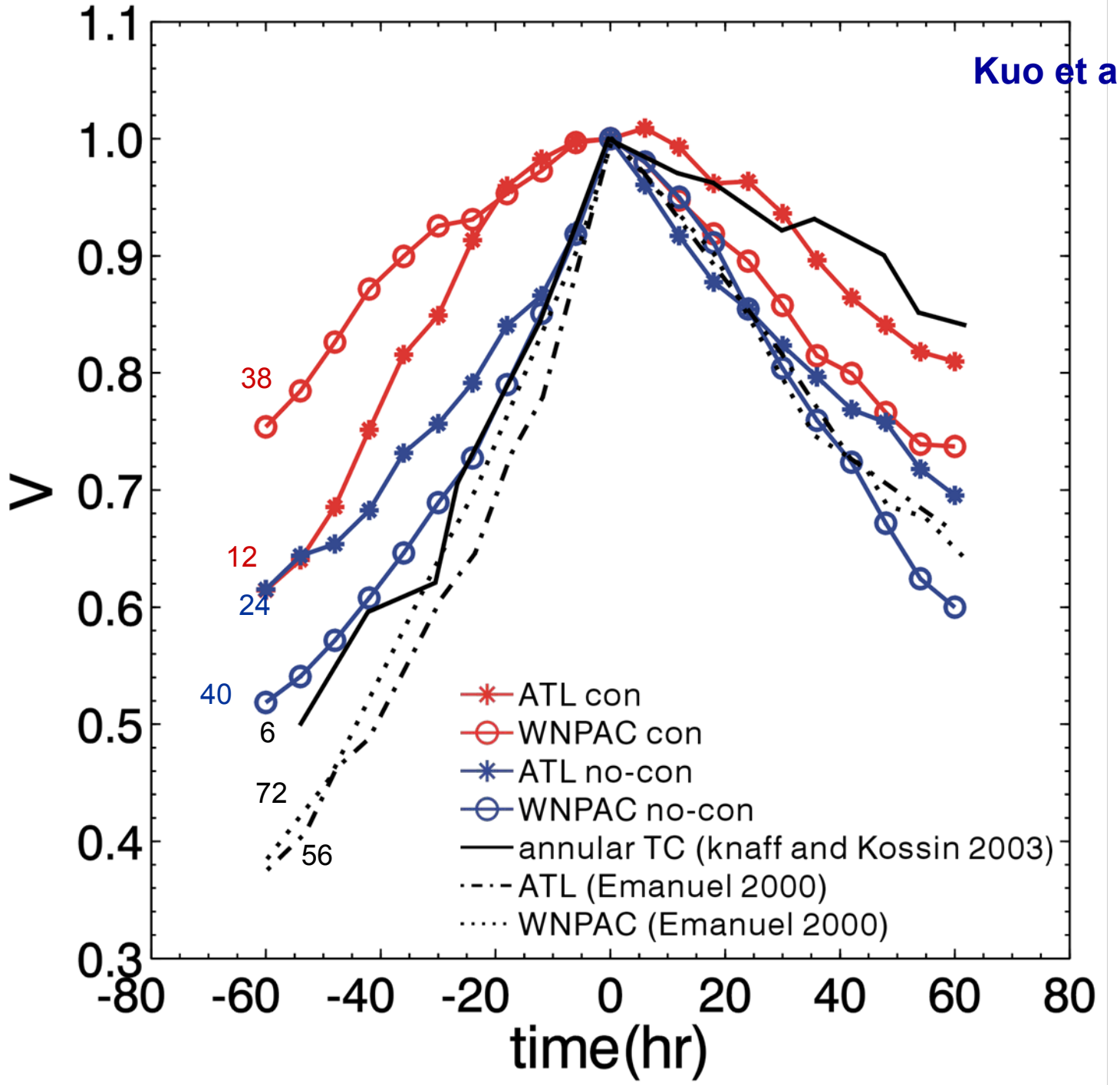
Kuo et al. (2006)
V
time(hr)
1.1
1.0
0.9
0.8
0.7
0.6
0.5
0.4
0.3
-80
-60
-40
-20
0
20
40
60
80
38
12
24
40
6
72
56
ATL con
WNPAC con
ATL no-con
WNPAC no-con
annular TC (knaff and Kossin 2003)
ATL (Emanuel 2000)
WNPAC (Emanuel 2000)

# WNPAC Concentric eyewalls formation locations, intensity, and tracks

Kuo et al. (2006)

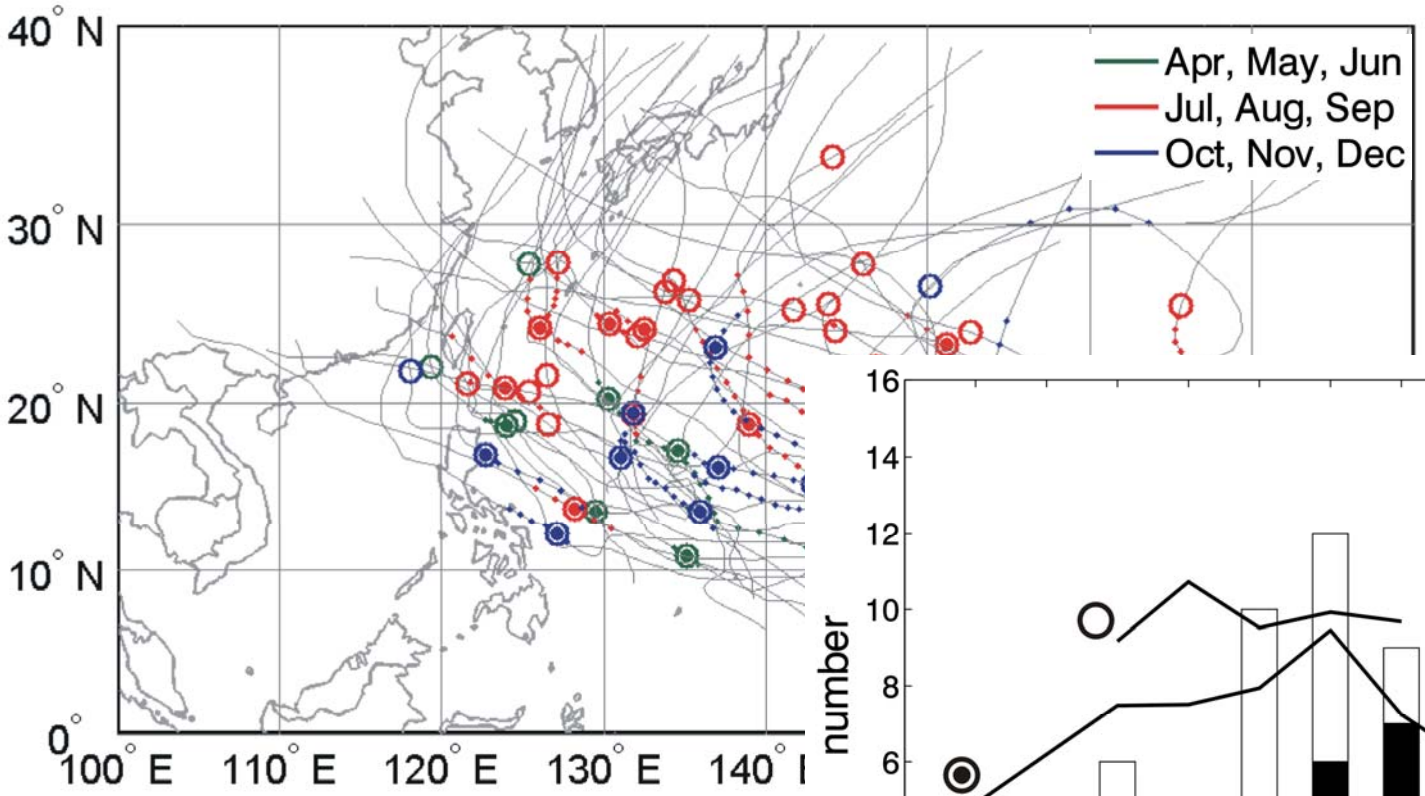


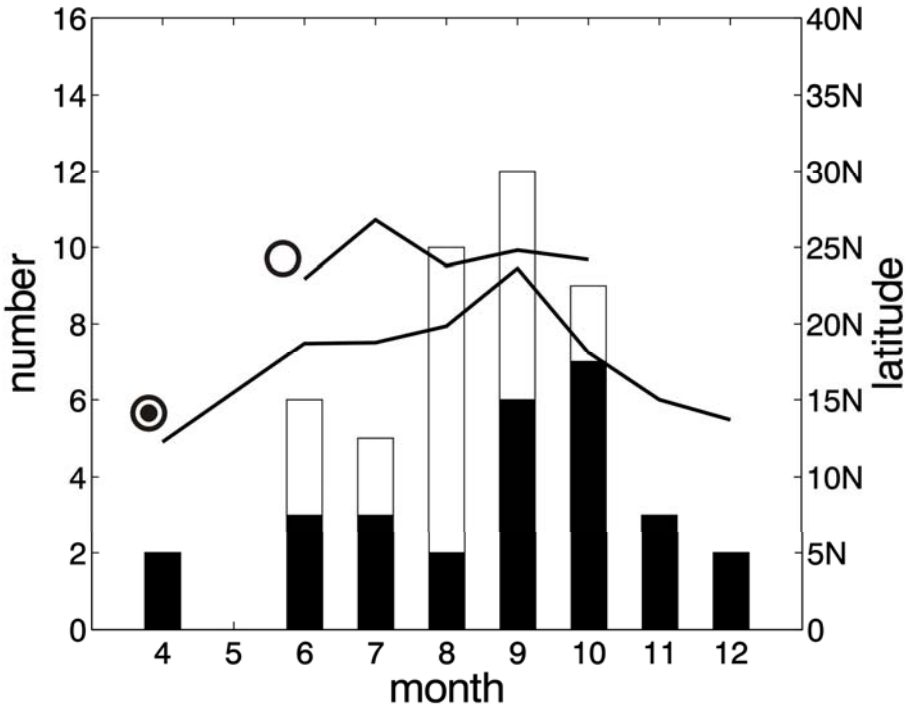


○ : <120 kts

◉ : >120 kts

# Coriolis Force

Non-inertial Frame

3-D

2-D (under rotation)

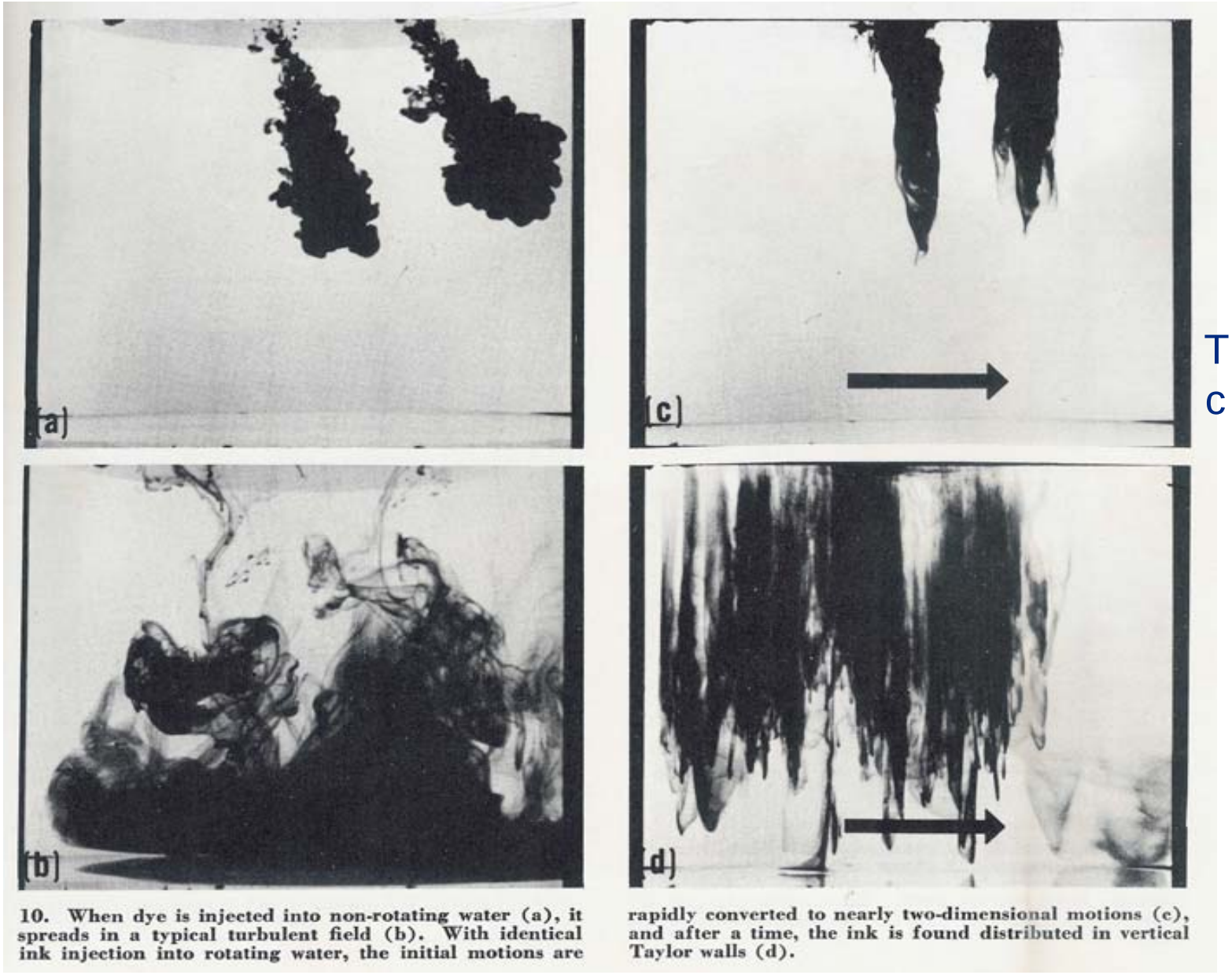


Taylor column

10. When dye is injected into non-rotating water (a), it spreads in a typical turbulent field (b). With identical ink injection into rotating water, the initial motions are rapidly converted to nearly two-dimensional motions (c), and after a time, the ink is found distributed in vertical Taylor walls (d).

3D

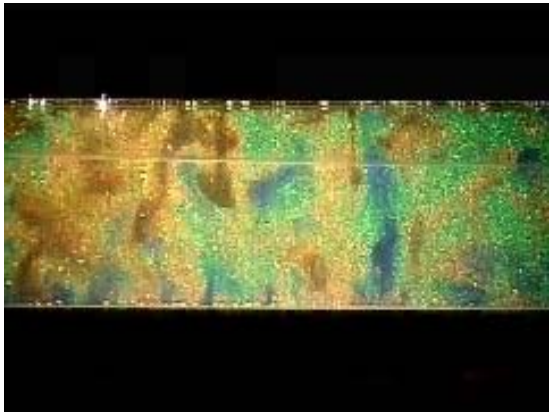

2D (strong rotation)

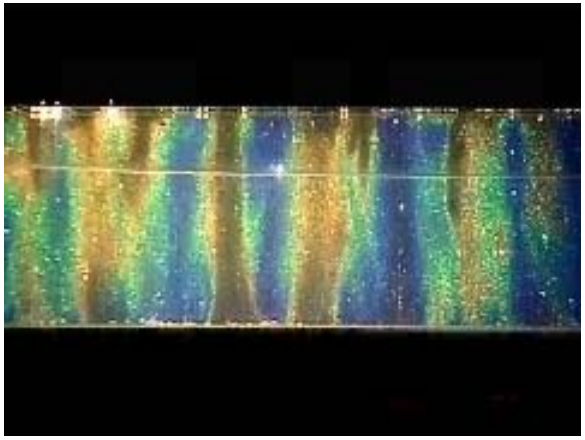

Taylor columns

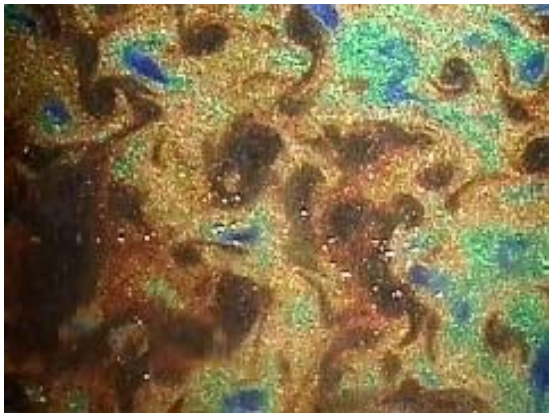

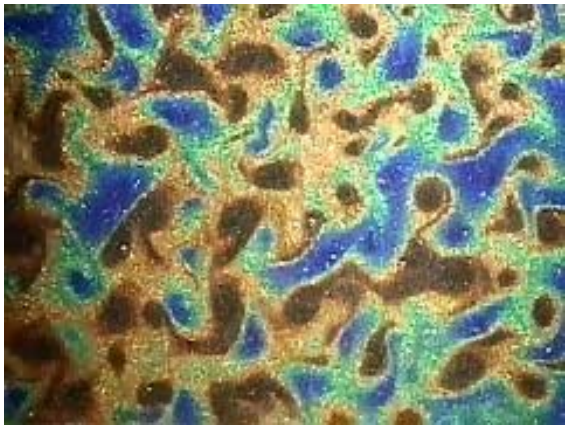

Vortices with sharp edge

$\vec{f} = 2\Omega\cos\phi\,\hat{j} + 2\Omega\sin\phi\,\hat{k}$

$\vec{f} \equiv 2\Omega\sin\varphi\,\hat{k}$

deep atmosphere
(Jupiter??)

shallow atmosphere
(Earth)

$z << a$

traditional
approximation

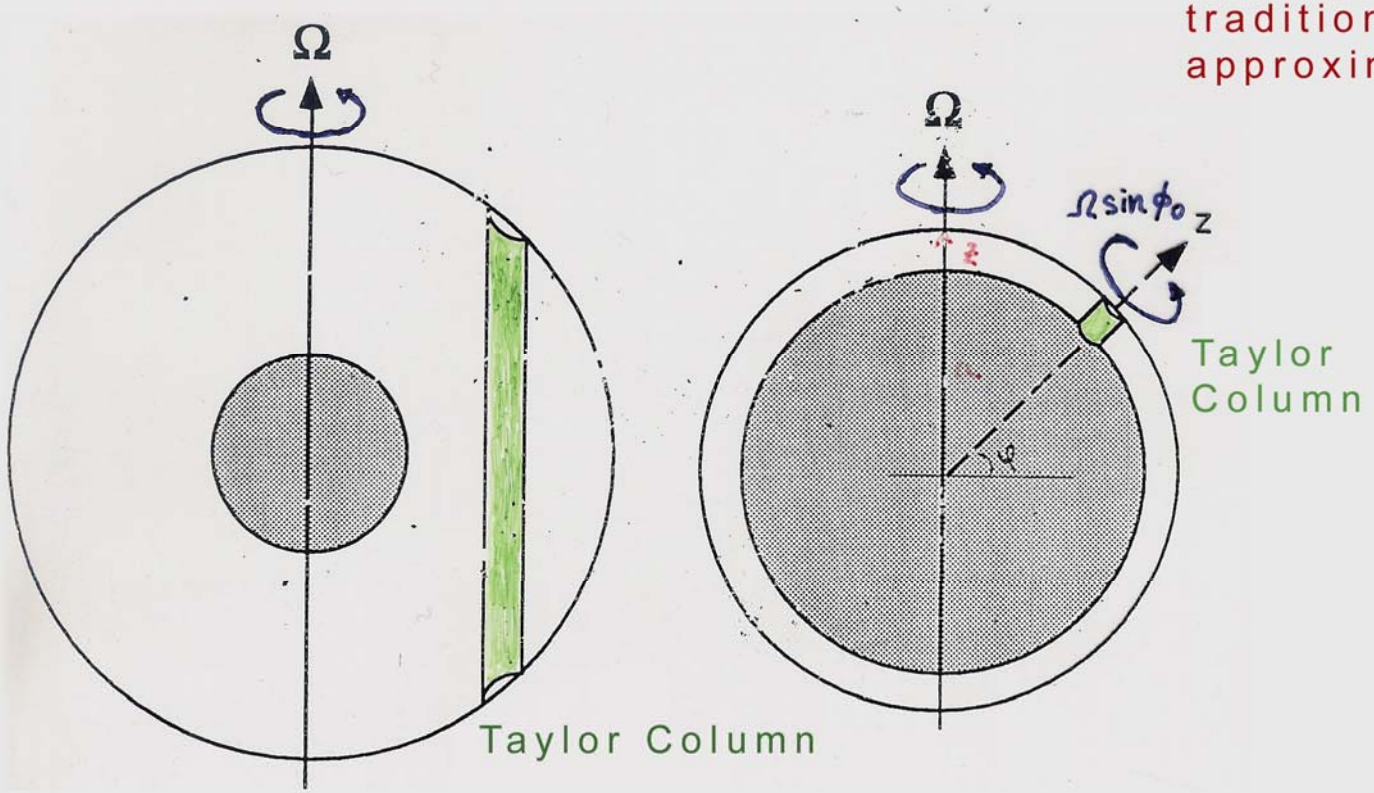

$$\frac{DP}{Dt} = \frac{\partial P}{\partial t} + u\frac{\partial P}{\partial x} + v\frac{\partial P}{\partial y} + w\frac{\partial P}{\partial z} \qquad P = \frac{\vec{\zeta}\cdot\nabla\theta}{\rho}$$

**Potential Vorticity**

$$\frac{\partial}{\partial z} \qquad P \to \zeta$$

$$\frac{D\zeta}{Dt} = \frac{\partial \zeta}{\partial t} + u\frac{\partial \zeta}{\partial x} + v\frac{\partial \zeta}{\partial y}$$

**Barotropic Vorticity**

$$\frac{D\zeta_g}{Dt} = \frac{\partial \zeta_g}{\partial t} + u_g\frac{\partial \zeta_g}{\partial x} + v_g\frac{\partial \zeta_g}{\partial y}$$

$$\zeta_g = \nabla^2\psi \qquad u_g = -\frac{\partial \psi}{\partial y} \qquad v_g = \frac{\partial \psi}{\partial x}$$

**Quasi-Geostrophic Vorticity**

**(Strong Rotation)**

$$\nabla\cdot\vec{V} = 0$$

$$\frac{\partial \zeta}{\partial t} + \frac{\partial(\psi,\zeta)}{\partial(x,y)} = \nu\nabla^2\zeta$$

**Nondivergent Barotropic Equation**

## Non-divergent barotropic model (Nearly Inviscid Fluid)

$$\frac{\partial}{\partial t}\zeta + \mathrm{J}(\psi, \zeta) = \upsilon \nabla^2 \zeta \qquad \boxed{\nabla^2 \psi = \zeta}$$

The energy and enstrophy relations

$$\frac{d\mathcal{E}}{dt} = -2\upsilon \mathcal{Z}$$

$$\mathcal{E} = \iint \frac{1}{2}\left(u^2 + v^2\right) dx\, dy$$ kinetic energy

$$\mathcal{Z} = \iint \frac{1}{2}\zeta^2\, dx\, dy$$ enstrophy

$$\frac{d\mathcal{Z}}{dt} = -2\upsilon \mathcal{P}$$

$$\mathcal{P} = \iint \frac{1}{2}\nabla\zeta \cdot \nabla\zeta\, dx\, dy$$ palinstrophy

Batchelor 1969

**Small viscosity led to large palinstrophy and the large enstrophy cascade**

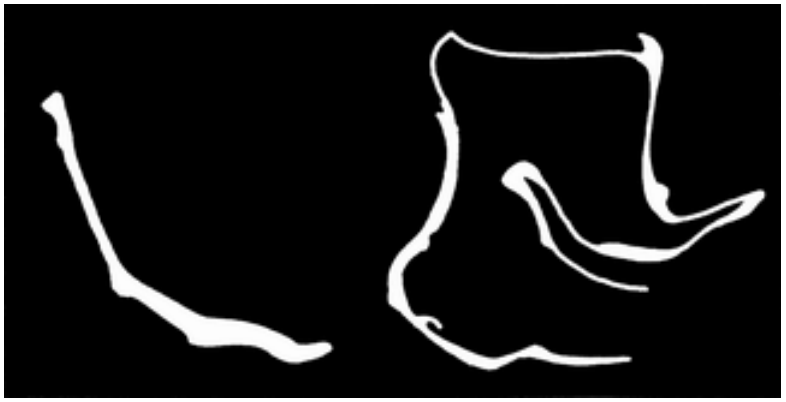

**Stirring**

$E \sim p'^2 / L^2$ (KE) geostrophy

$Z \sim p'^2 / L^4$ (Enstrophy)

KE nearly conserved $L \sim p'$

Enstrophy cascade L ↑ (L increase Z decrease)

Selective Decay of 2D turbulence

The vortices become, on the average,
larger, stronger, and fewer.

Merger and Axisymmetrization Dynamics

# Emergence of coherent structure in 2-D turbulence

The tendency toward successive merger

**Fewer and stronger vortices !!!**

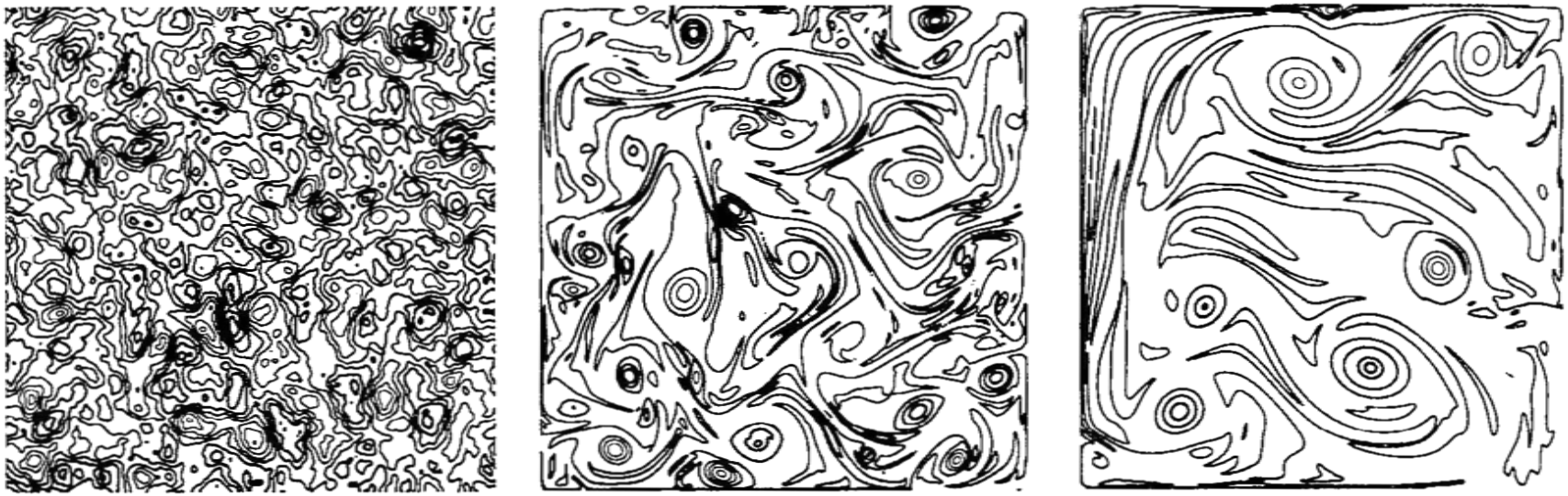

$\tau$

McWilliams 1984

# Waves, turbulence, and coherent vortex

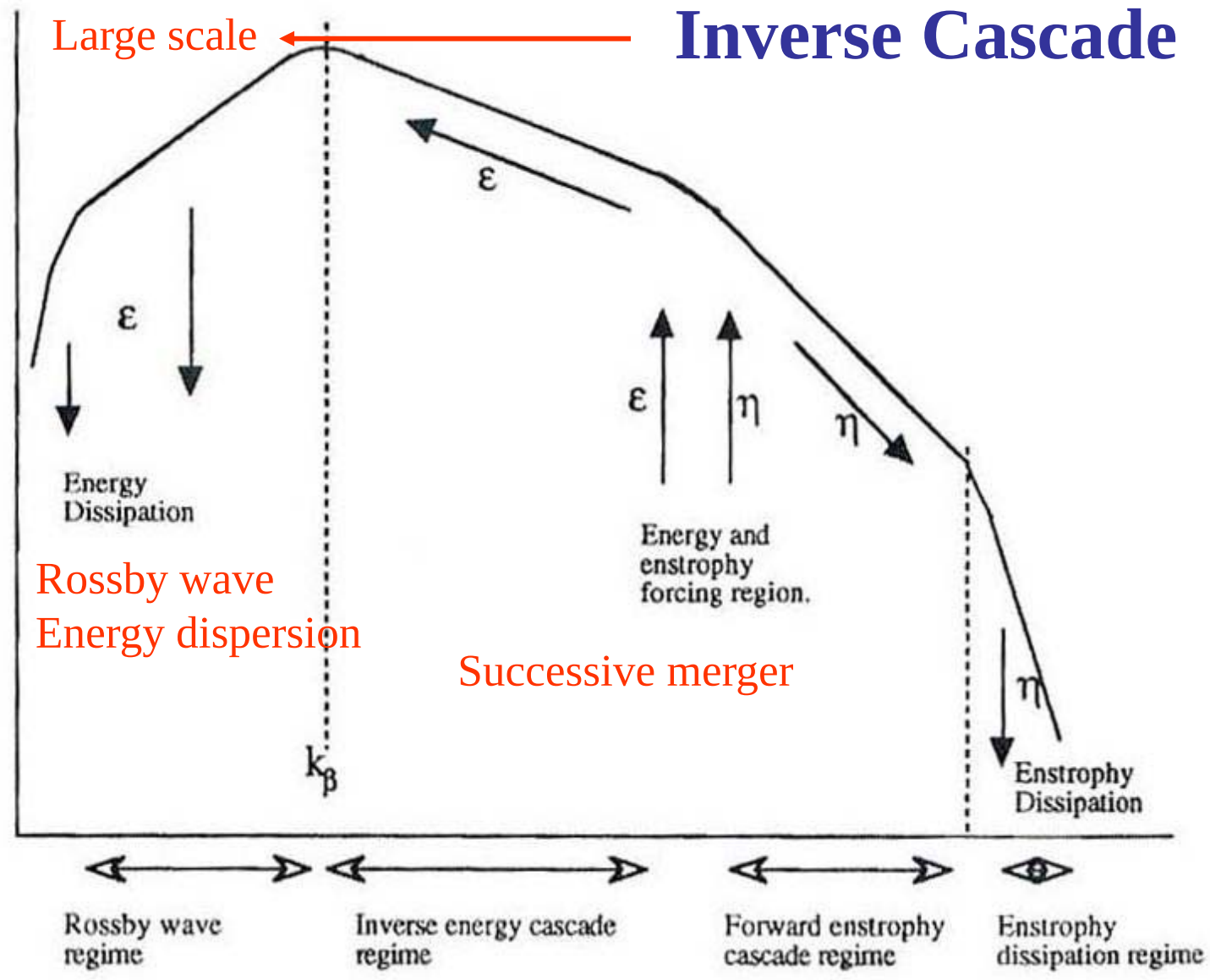

Huang and Robinson 1998

Turbulence

↑

Rhines curve

↓

Waves

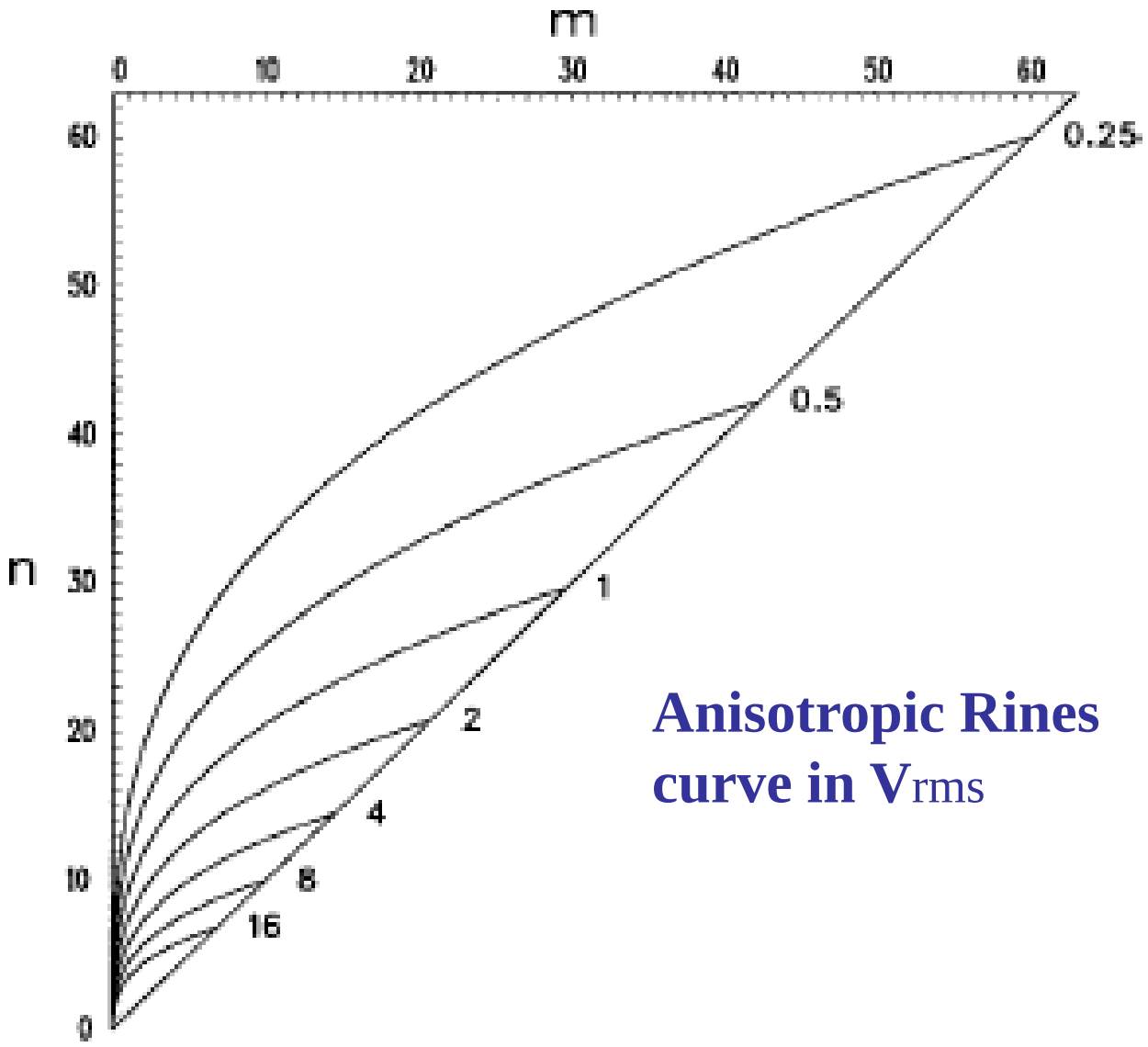


**Anisotropic Rines curve in Vrms**

FIG. 1. Anisotropic Rhines curve on the wavenumber plane based on Eq. (3). Dimensional values of $V_{rms}$ (in m $s^{-1}$) are labeled at right.

Huang and Robinson
1998

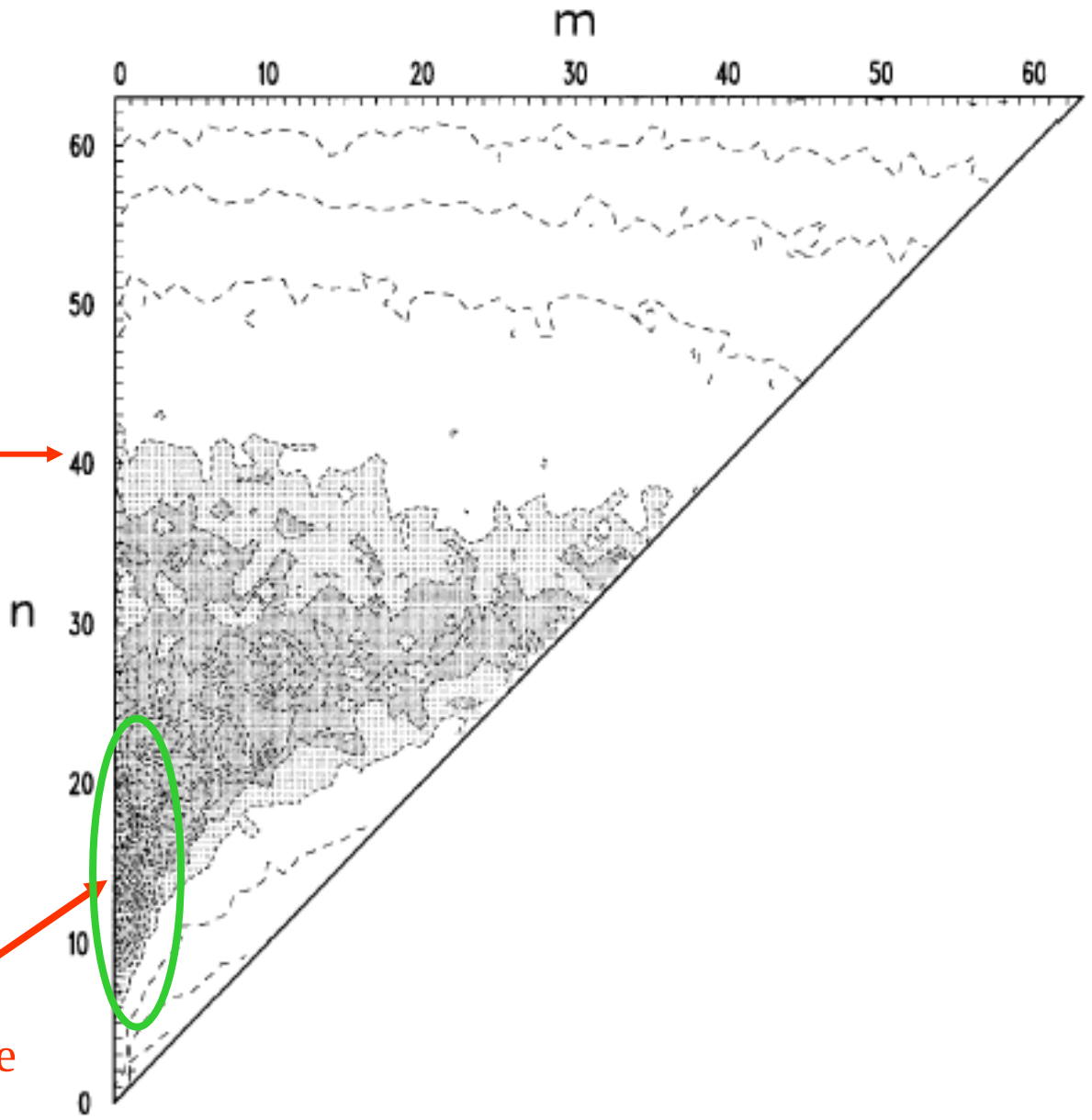


Forcing added

Inverse energy cascade
to zonal Harmonics

FIG. 2. Energy spectrum $E(m, n)$ of an ensemble mean at day 80 of 10 decaying turbulence experiments. The magnitude of the spectrum is normalized by the maximum value on the map. Contour levels are 0.0001, 0.001, 0.01, 0.1–0.9 with increment 0.1. Area with $E(m, n) > 0.1$ is lightly shaded, $E(m, n) > 0.2$ heavily shaded.

## Huang and Robinson 1998

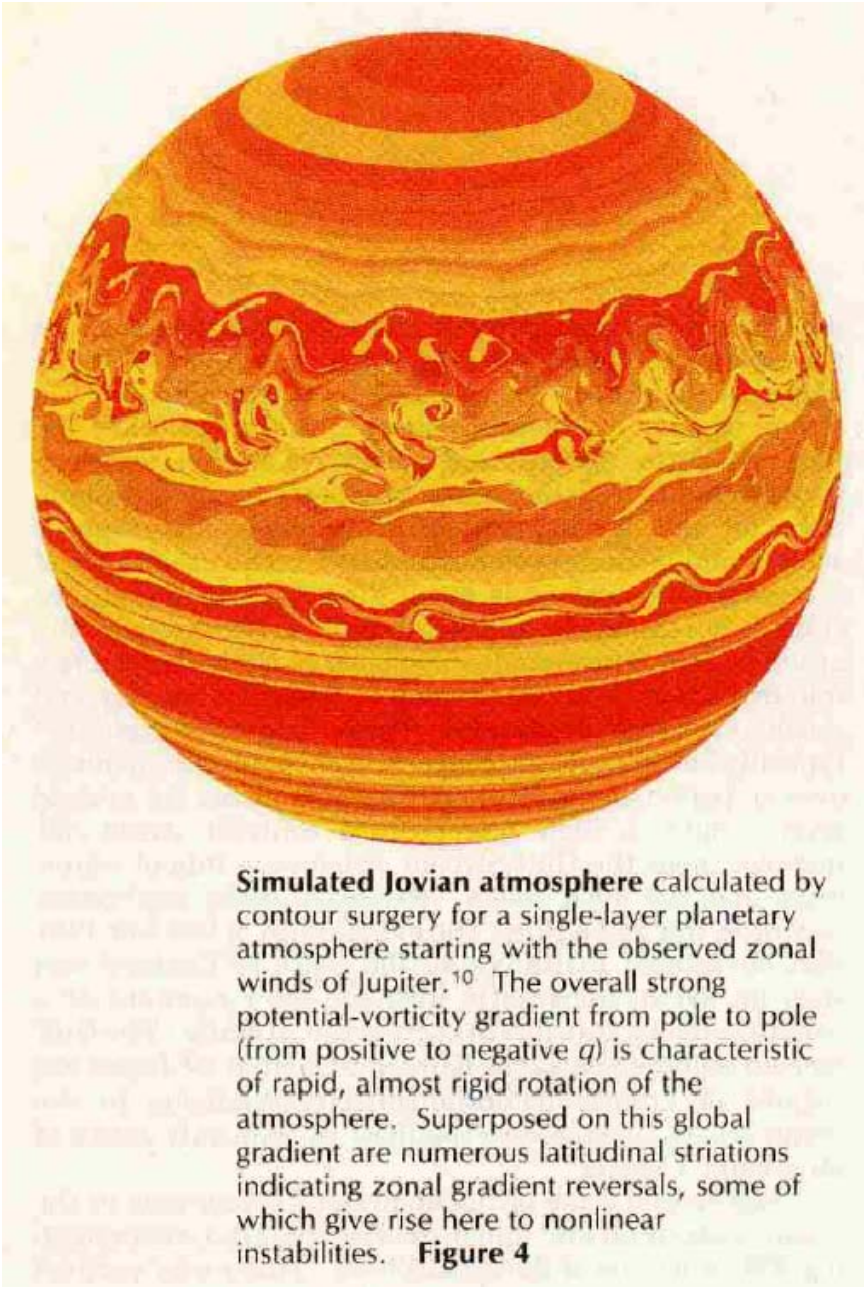

**Simulated Jovian atmosphere** calculated by contour surgery for a single-layer planetary atmosphere starting with the observed zonal winds of Jupiter.[10] The overall strong potential-vorticity gradient from pole to pole (from positive to negative $q$) is characteristic of rapid, almost rigid rotation of the atmosphere. Superposed on this global gradient are numerous latitudinal striations indicating zonal gradient reversals, some of which give rise here to nonlinear instabilities. **Figure 4**

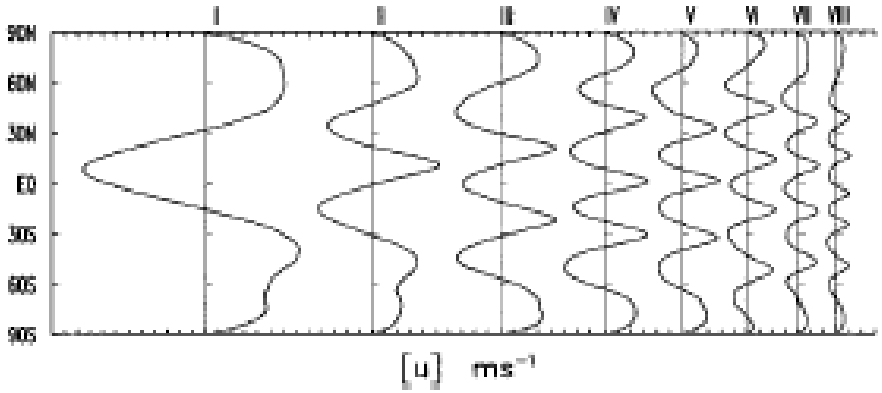


FIG. 4. Time-mean zonal-mean zonal wind profiles for cases I–VIII in Table 1 (the eight open circles in Fig. 3). Each grid on the abscissa represents 1 m $s^{-1}$.

**These alternating Easterly and westerly Jets are similar to observed patterns on Jupiter and Saturn.**

Rotational period 9.84hr

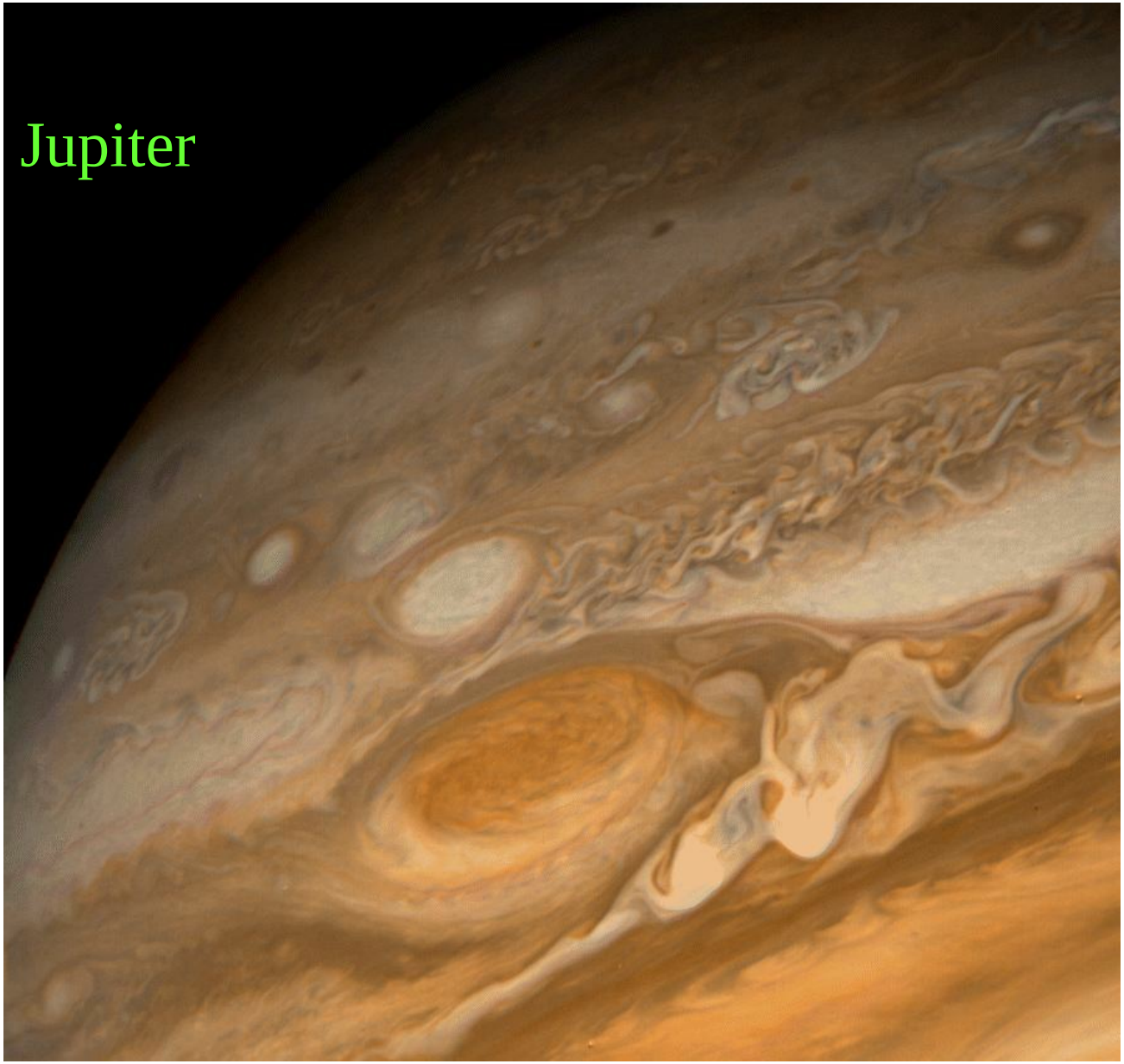


Alternating Zonal Structures

The Great Red Spot

# 賀伯颱風的橢圓形眼　Kuo et al. 1999

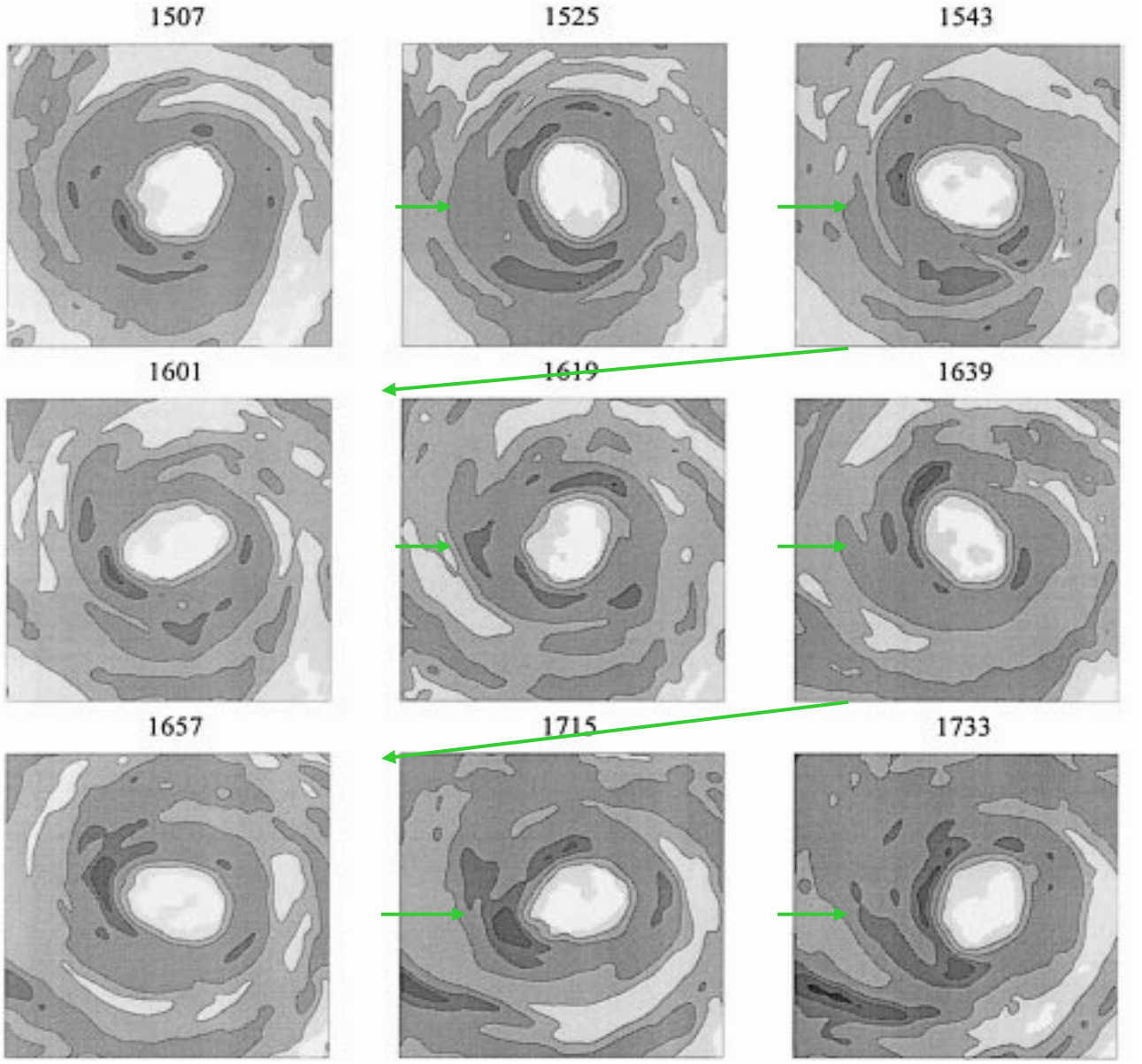


FIG. 1. Horizontal distribution of maximum reflectivity in the vertical column for Typhoon Herb from the Central Weather Bureau WSR-88D (10 cm) radar at Wu-Feng Mountain on 31 Jul 1996. The sequence of images is from left to right and from top to bottom. The time interval between each image is approximately 18 min. The local time of observation is indicated on top of each image. The major axis radius in the eye region is about 30 km and the minor axis radius is about 20 km. The nine images illustrate one eye rotation period of 144 min.

**144 min rotation period**

**Coherent vortex**
**Dispersion resistant**

**Vorticity Dynamics**

**Nonlinear glue**

**Nonlinear Dynamics**

- Kirchhoff vortex ( nonlinear ) Lamb, 1932

$$\frac{x^2}{a^2}+\frac{y^2}{b^2}=1$$

a ~ 30 km  b ~ 20 km

$$\zeta\frac{ab}{(a+b)^2}=\omega$$

P ~ $(2\pi/\zeta)*4$  $\zeta \sim 3*10^{-3}\ s^{-1}$

rotating period **P** = $\frac{2\pi}{\zeta}\frac{(a+b)^2}{ab}$

Vmax ~ 50 $ms^{-1}$

- Kelvin PV wave ( linear )

rotating period **P**

$$c=V_{max}(1-\frac{1}{m}) \qquad m=2$$

angular velocity = $c/r = \frac{V_{max}}{2r}$

$$\sim\frac{2\pi}{\omega}=\frac{2\pi}{2\frac{V_{max}}{r}}*4=\frac{2\pi}{\zeta}*4$$

Same as Kirchhoff vortex !!

# Eye rotation is nonlinear

$$J(\psi,\zeta) \quad >> \quad J(\psi,\zeta)$$

EXP 1 EXP 2

T= 0 min T= 0 min

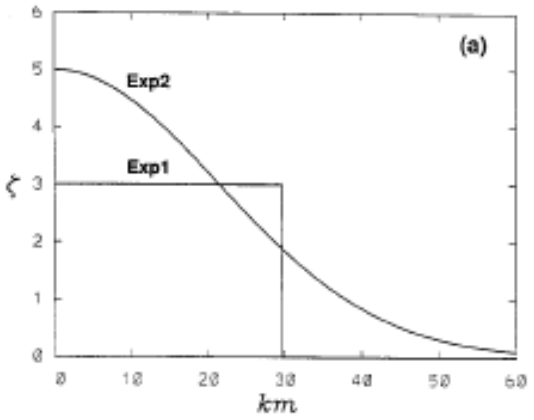


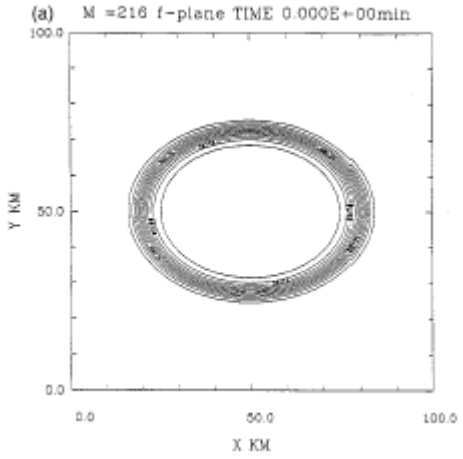


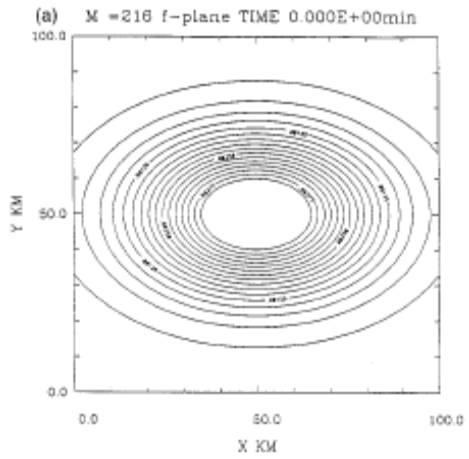


$$\frac{\partial}{\partial t}\zeta + J(\psi,\zeta) = 0$$

T= 144 min T= 144 min

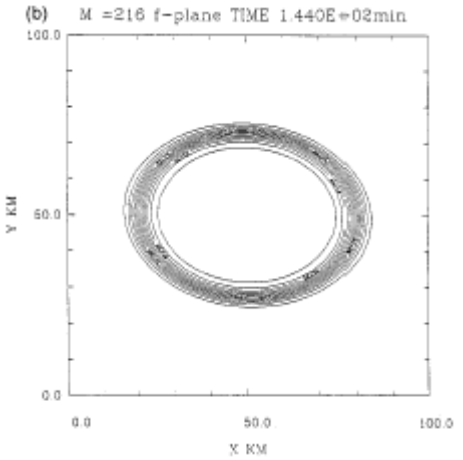


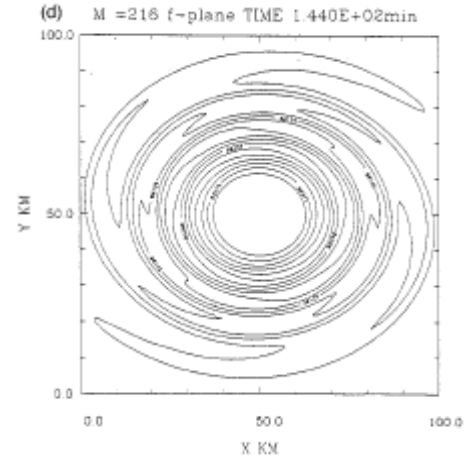

# Bowmen and Mangus (1993)

Observations of deformation and mixing of the total ozone field in the Antarctic polar vortex

## Surf Zone Dynamics

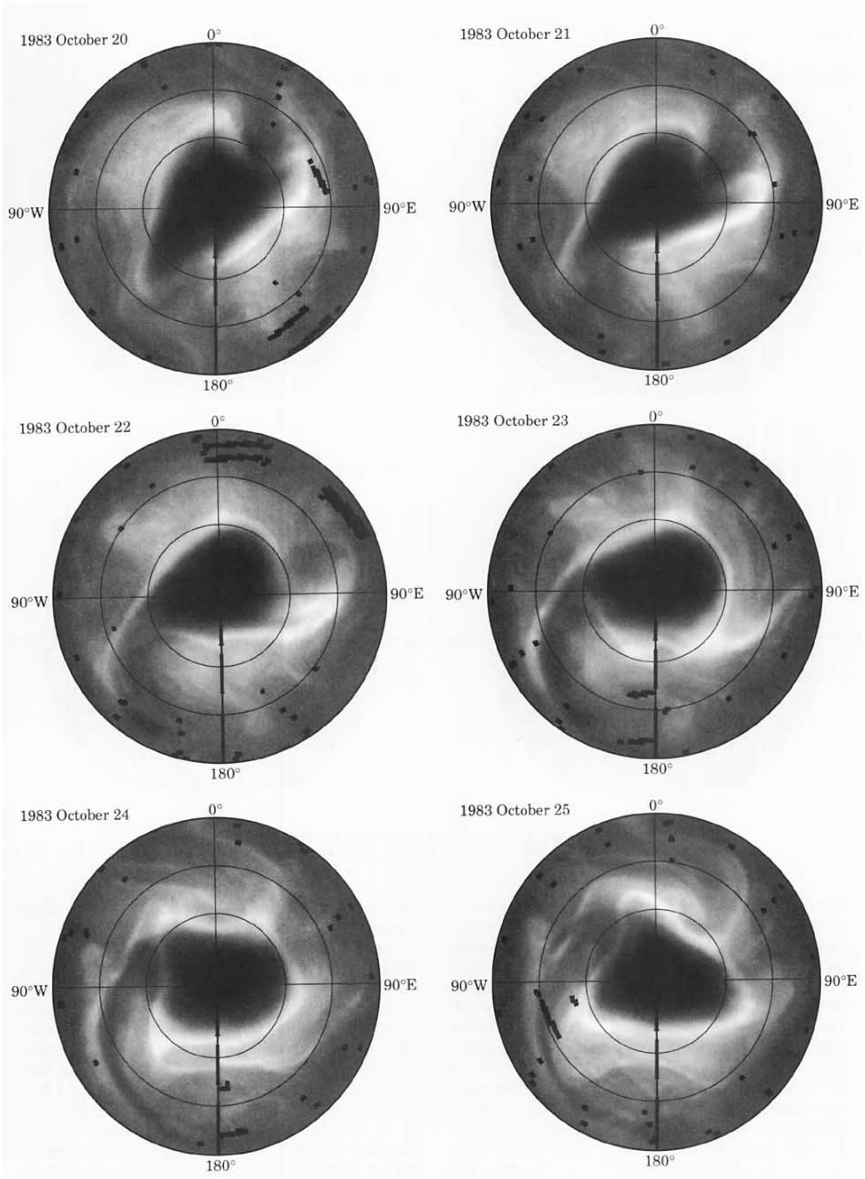


Fig.1: Daily TOMS images of total ozone in the Southern Hemisphere for six consecutive days in October 1983. Latitude circles are drawn at 40˚,60˚, and 80 ˚S. The outermost latitude is 20 ˚S.

# Electron density redistribution in experimental plasma physics

single sign charge

+

axial magnetic field confinement

$$\mathbf{E} = -\nabla\psi$$

$$\nabla \cdot \mathbf{E} = -\nabla^2\psi = \frac{\rho}{\epsilon}$$

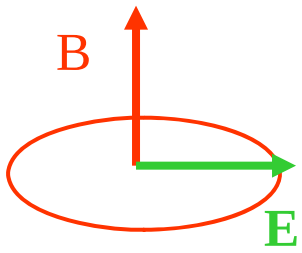


$\vec{E}\times\vec{B}$ drift

**Coriolis force**

Axisymmetrization 軸對稱化

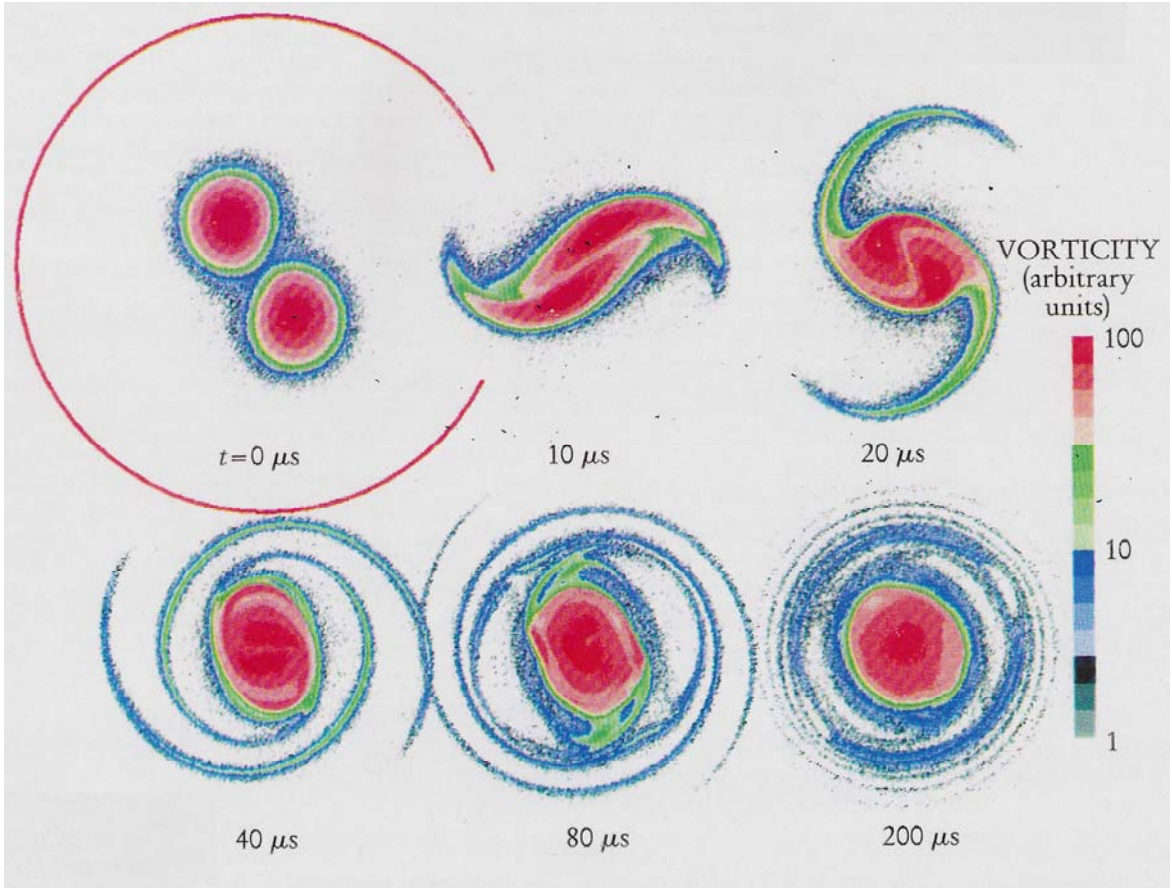


Core is protected, thin filaments from edges

$$\frac{D\theta}{Dt} = \frac{\partial\theta}{\partial t} + \vec{V}\cdot\nabla\theta = \nu\nabla^2\theta$$

$$C = \frac{1}{2}\int \nabla\theta\cdot\nabla\theta \, dV$$

$$\frac{dC}{dt} = \int (\vec{V}\cdot\nabla\theta)\nabla^2\theta \, dV - \nu\int (\nabla^2\theta)\, dV$$

**Stirring** **Mixing**

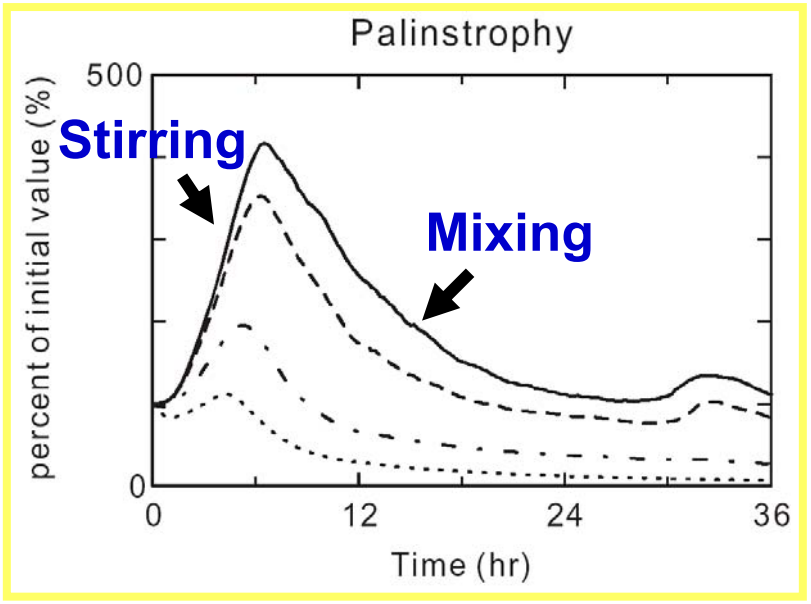


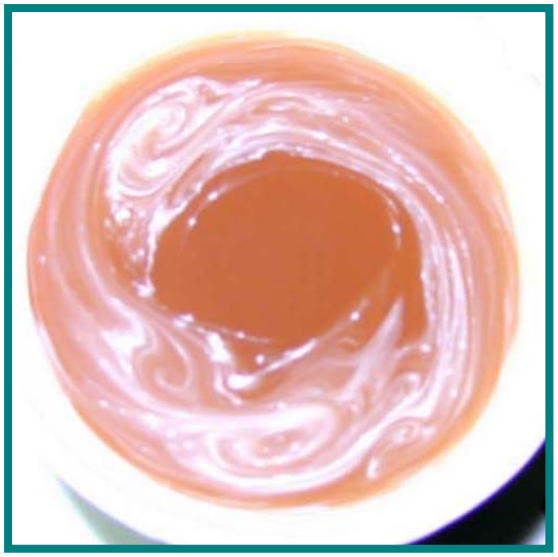

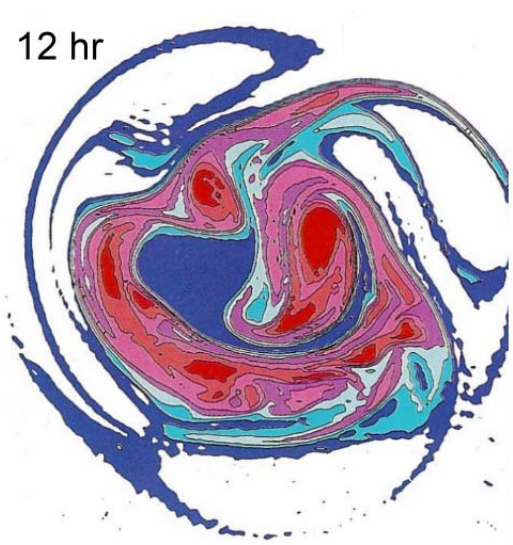


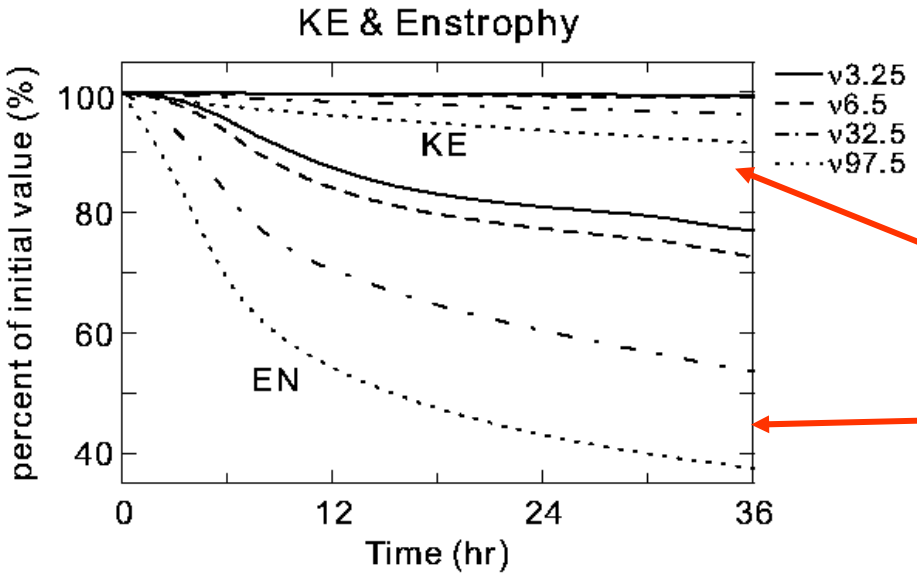


**KE nearly conserved**

**Enstrophy cascade**

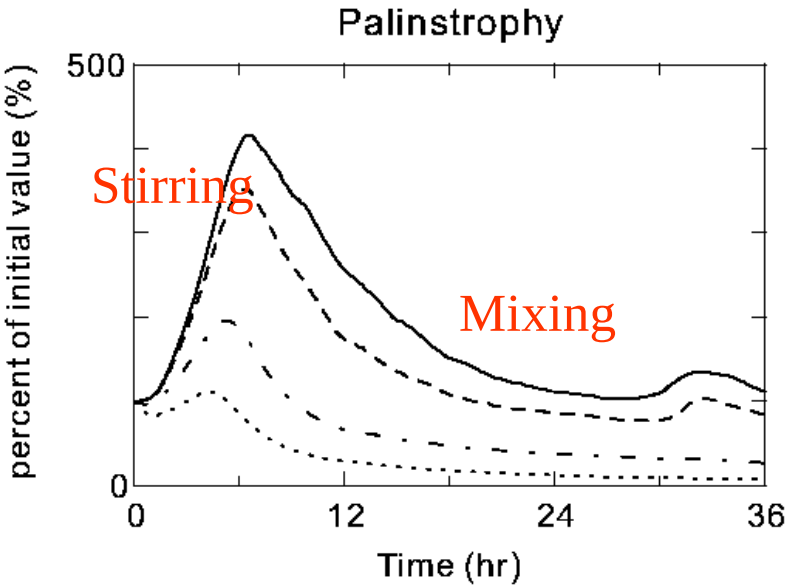


**Selective Decay of 2D turbulence**

# Black and Willoughby (1992) Hurricane Gilbert (1988)

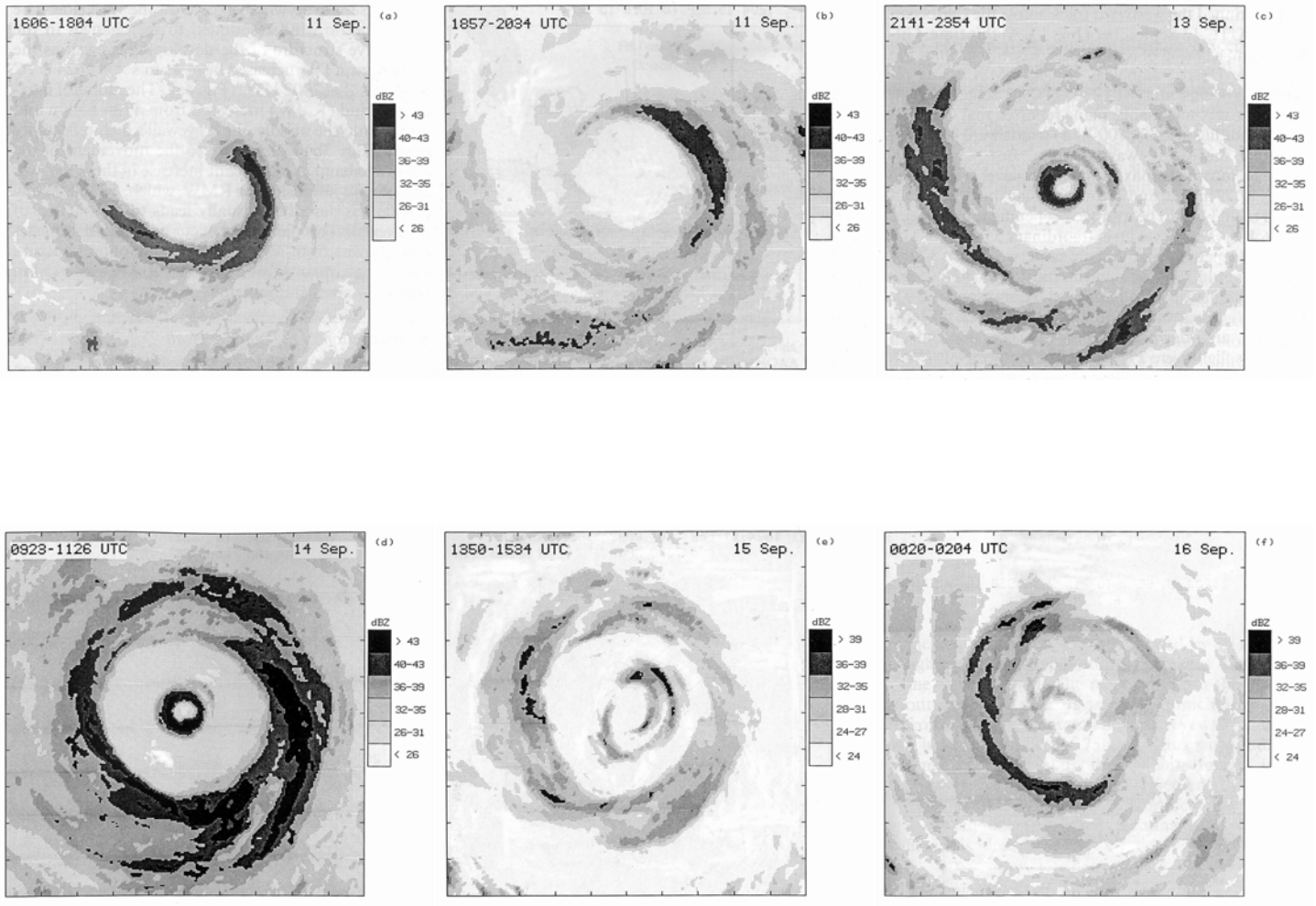

# Black and Willoughby (1992)

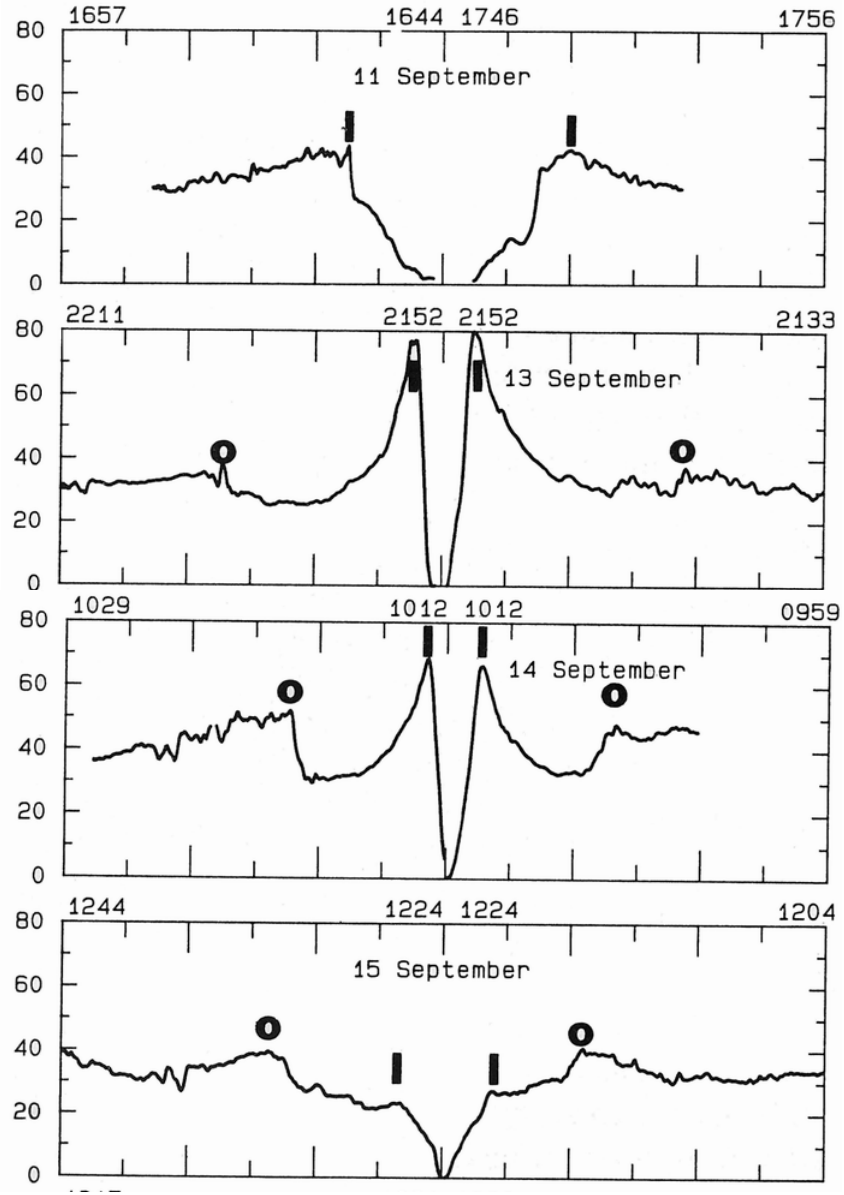


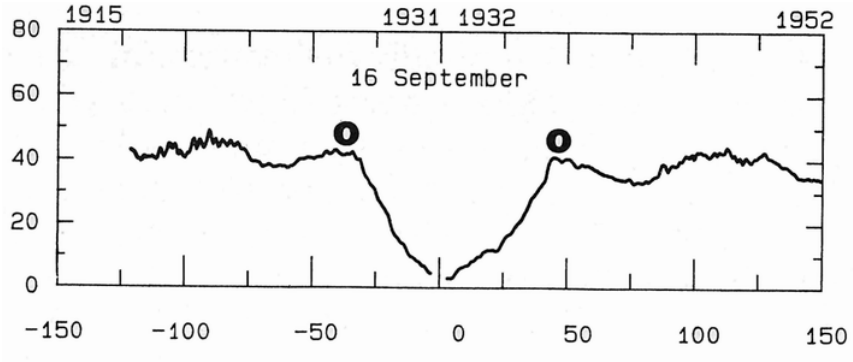


## Hurricane Gilbert (1988)

# A major issue in understanding changes in typhoon intensity

**Black and Willoughby (1992)**
**Hurricane Gilbert (1988)**

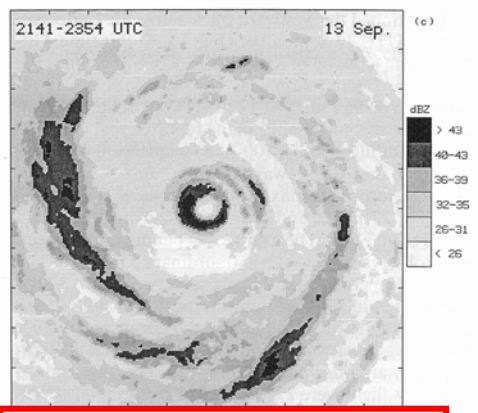


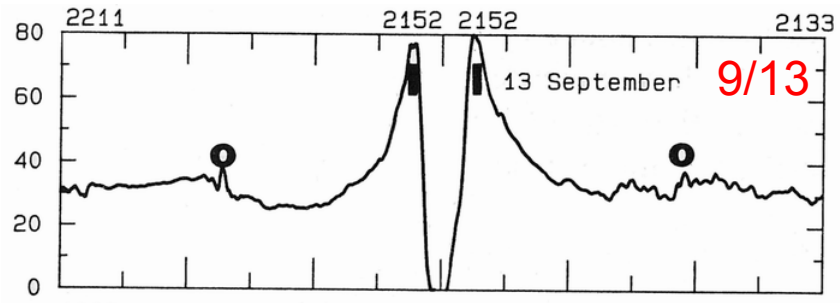


Development of symmetric structure from asymmetric convection in 12 hours

The contraction of the Outer tangential wind maximum

Core vortex intensity remains approximately the same during the contraction period

Inner core dissipate, TC weakens

# Black and Willoughby (1992)

Vertical cross sections of radar reflectivity of the concentric eyewall

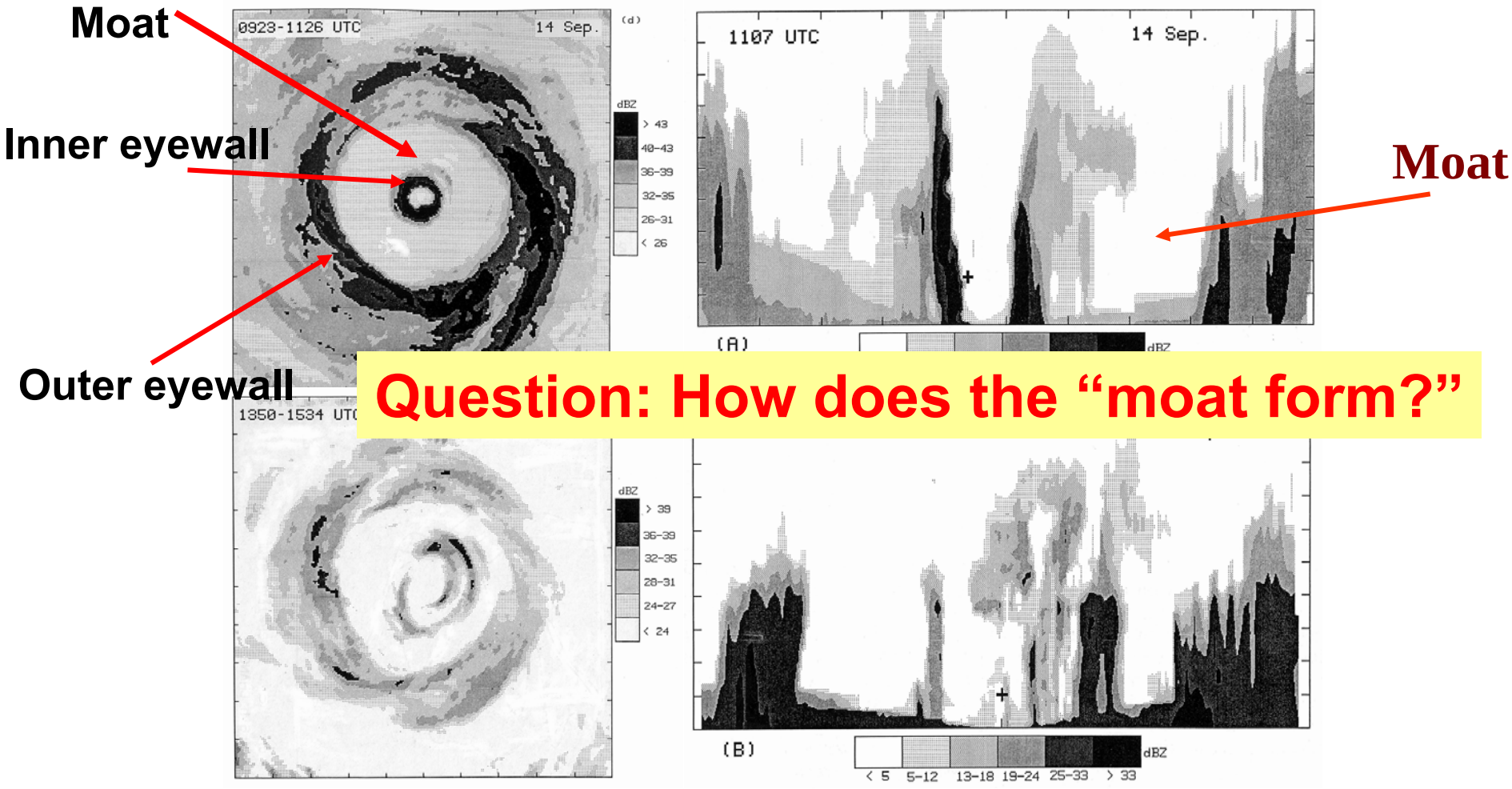


**Question: How does the "moat form?"**

# ELDORA data show downward motion between the two eyewalls

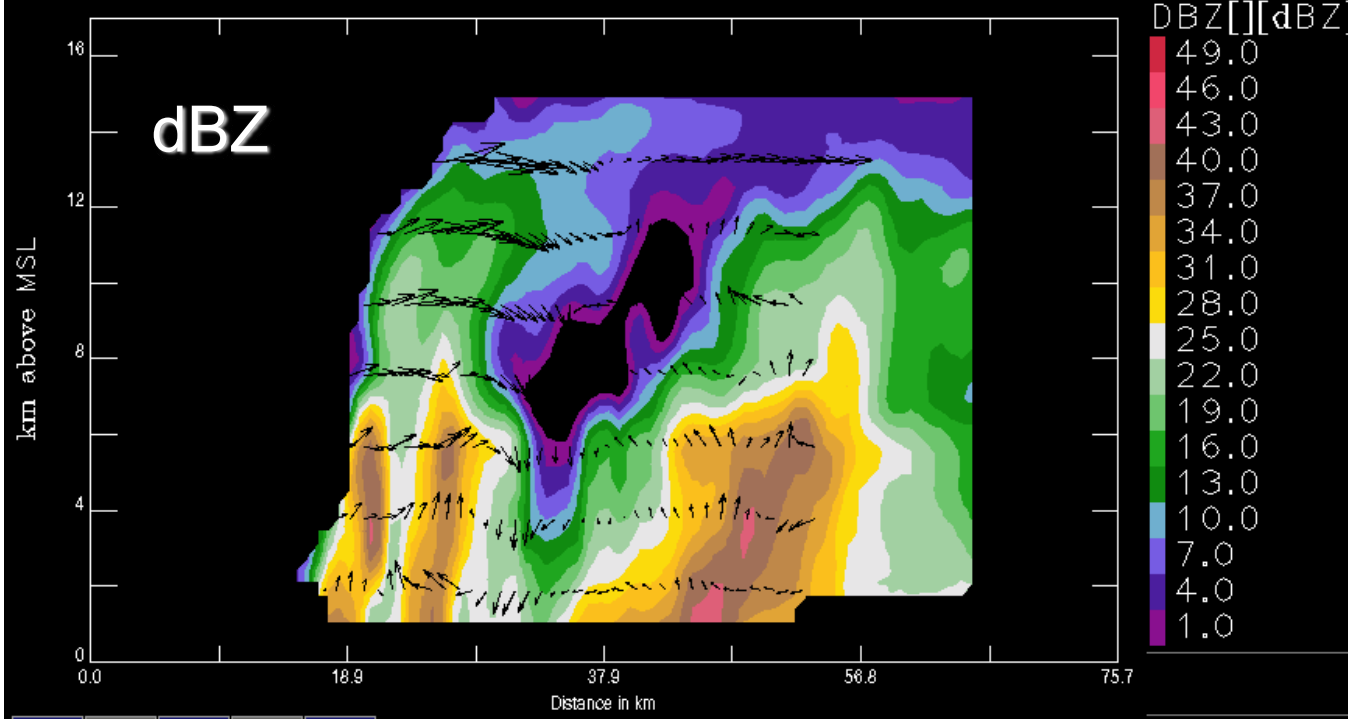


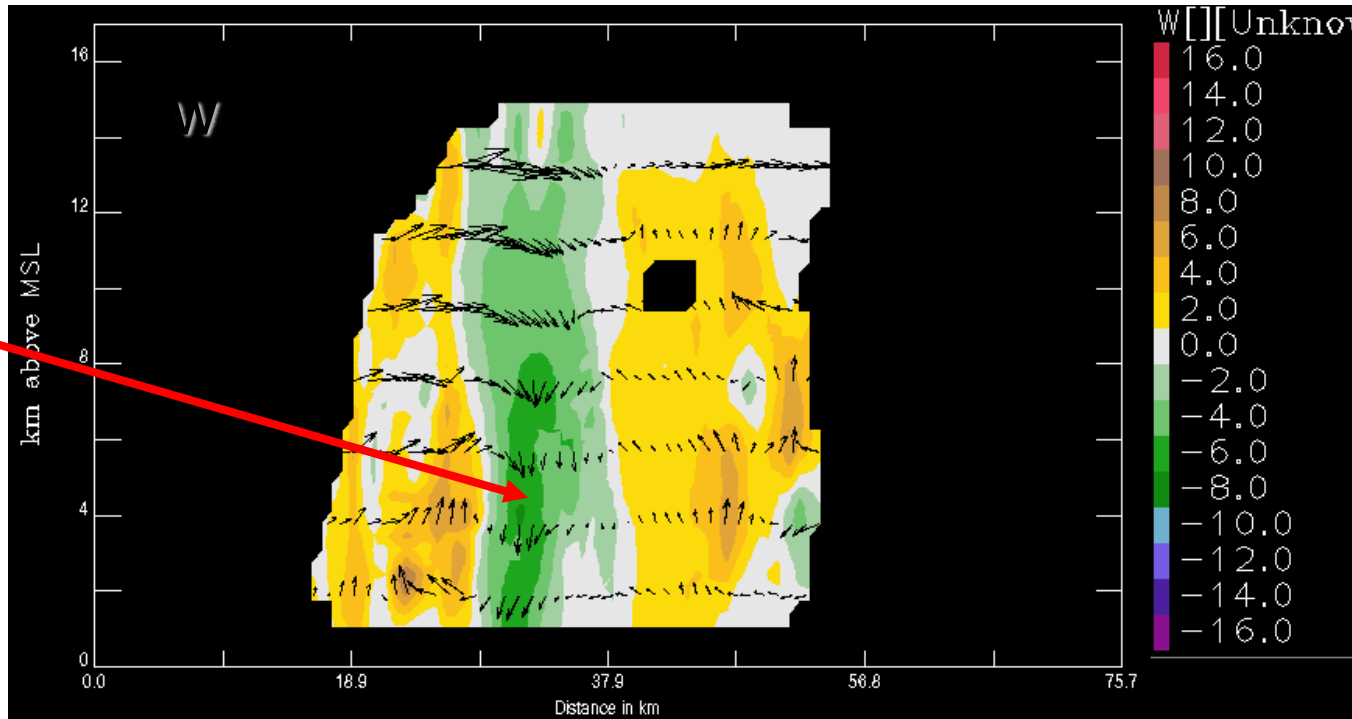


Subsidence

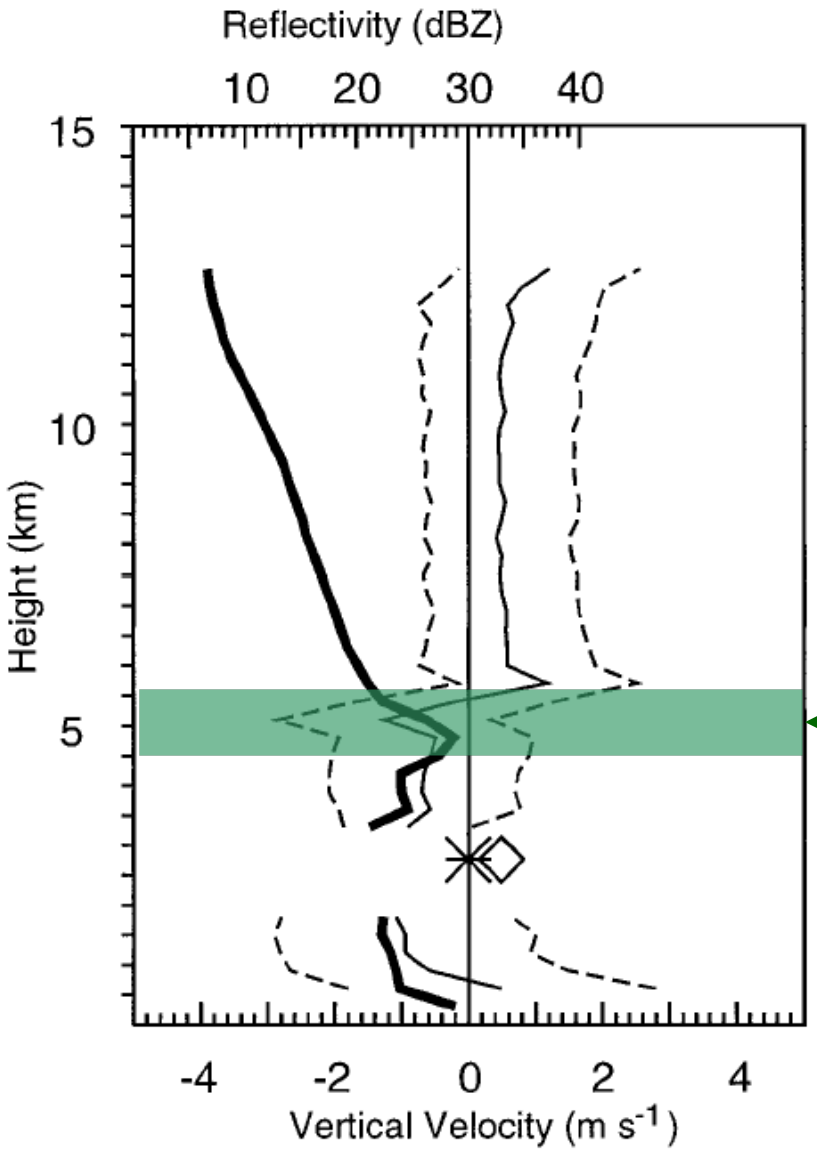


FIG. 12. Vertical profiles of average vertical velocity (thinner line) and reflectivity (thicker line), for the stratiform region from 30 to 55 km from the center of circulation. The average flight-level vertical velocity is denoted by a star and the diamond denotes the average of the absolute value of the vertical velocity. The dashed lines are plotted one standard deviation on each side of the vertical velocity plot.

# Hurricane Gilbert (1988)

**The strong subsidence induced by the intensified eyewall convection may also contribute to the formation of the moat.**

**bright band (4.5~5.5 km)**

**reflectivity**

**average vertical velocity**

**one standard deviation on each side of the vertical velocity**

*Dodge et al. (1999)*

## Thoughts from the 80's and 90's

Shapiro and Willoughby (1982) and Schubert and Hack (1982) proposed that heating-vorticity interaction can lead to convective-ring contraction.

$$d\zeta/dt \sim \zeta \bigtriangledown \cdot \mathbf{V}$$

Stronger$\zeta$ near the TC core favors the inward response

**Symmetrical Model**

Moat formation and eyewall replacement are related to the subsidence and the moisture cut-off.

# Typhoon Lekima (2001)

0935-1935 LST

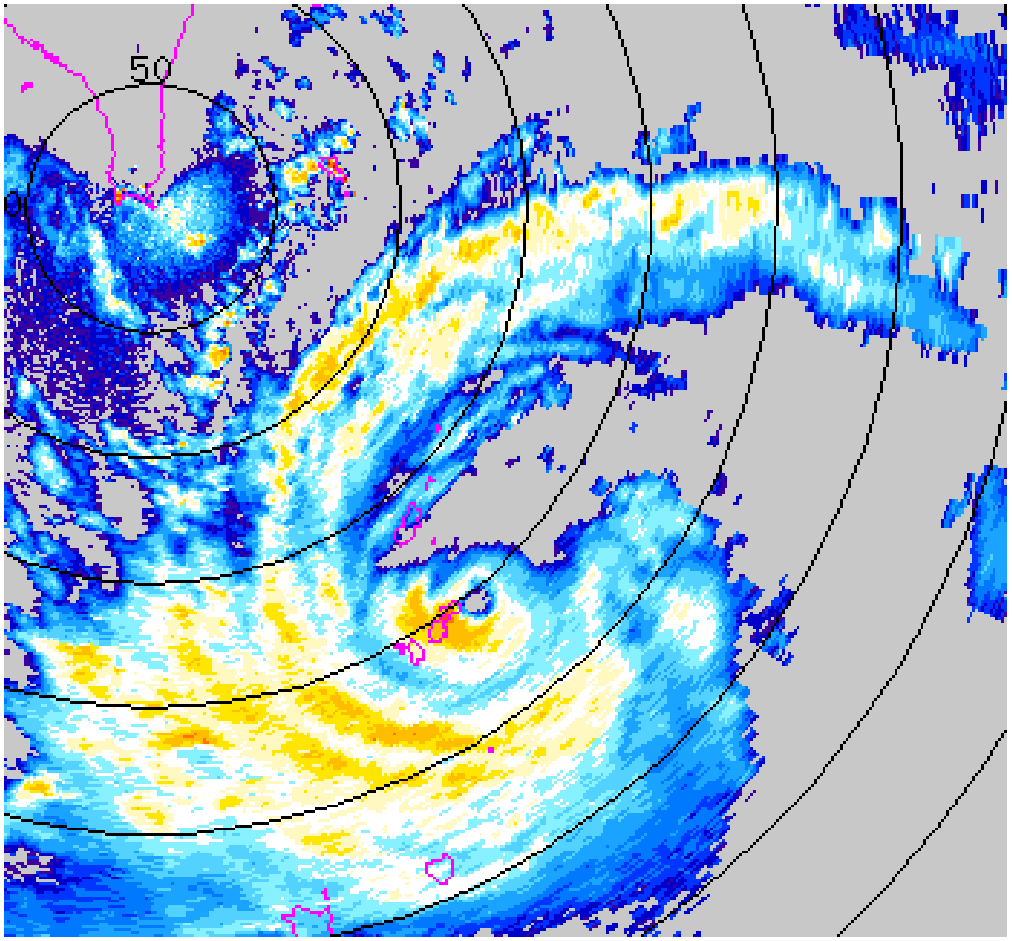


0925 1900LST

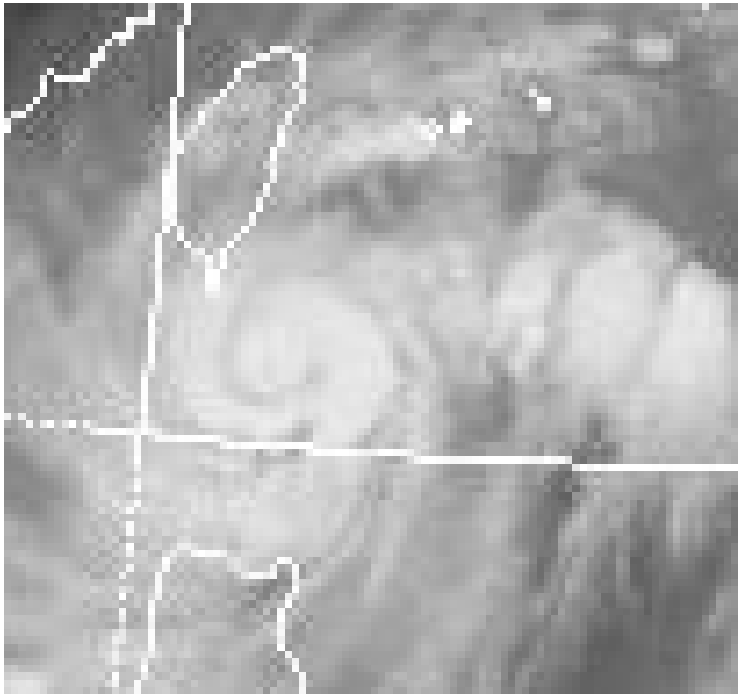

# Dritschel and Waugh (1992)

The same vorticity strength

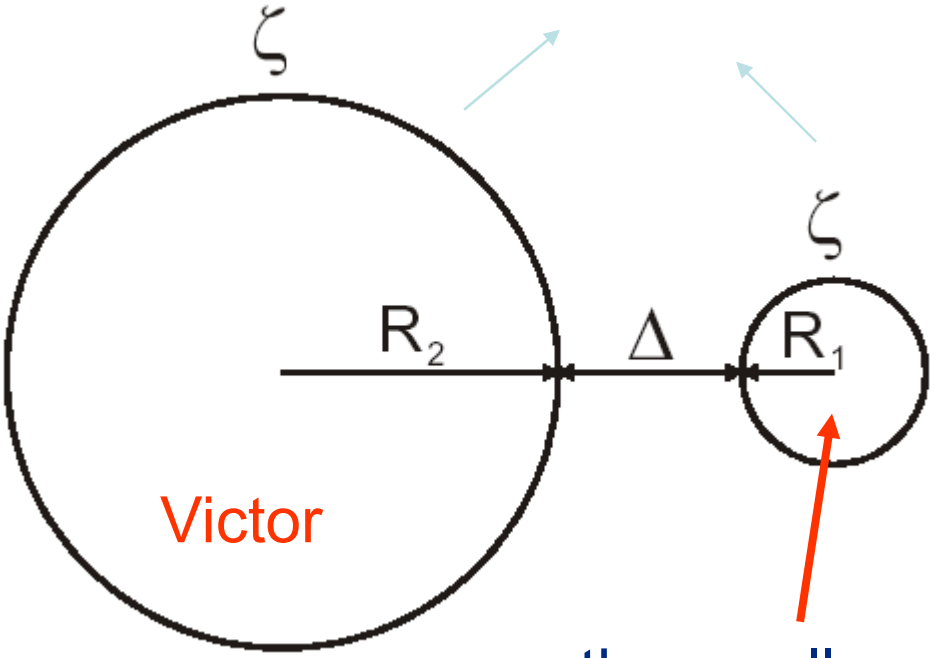


the smaller vortex was the one often being partially or totally destroyed

$$r = \frac{R_1}{R_2}$$ Vortex radius ratio

$$\Delta / R_1$$ Dimensionless gap

# Elastic interaction regime

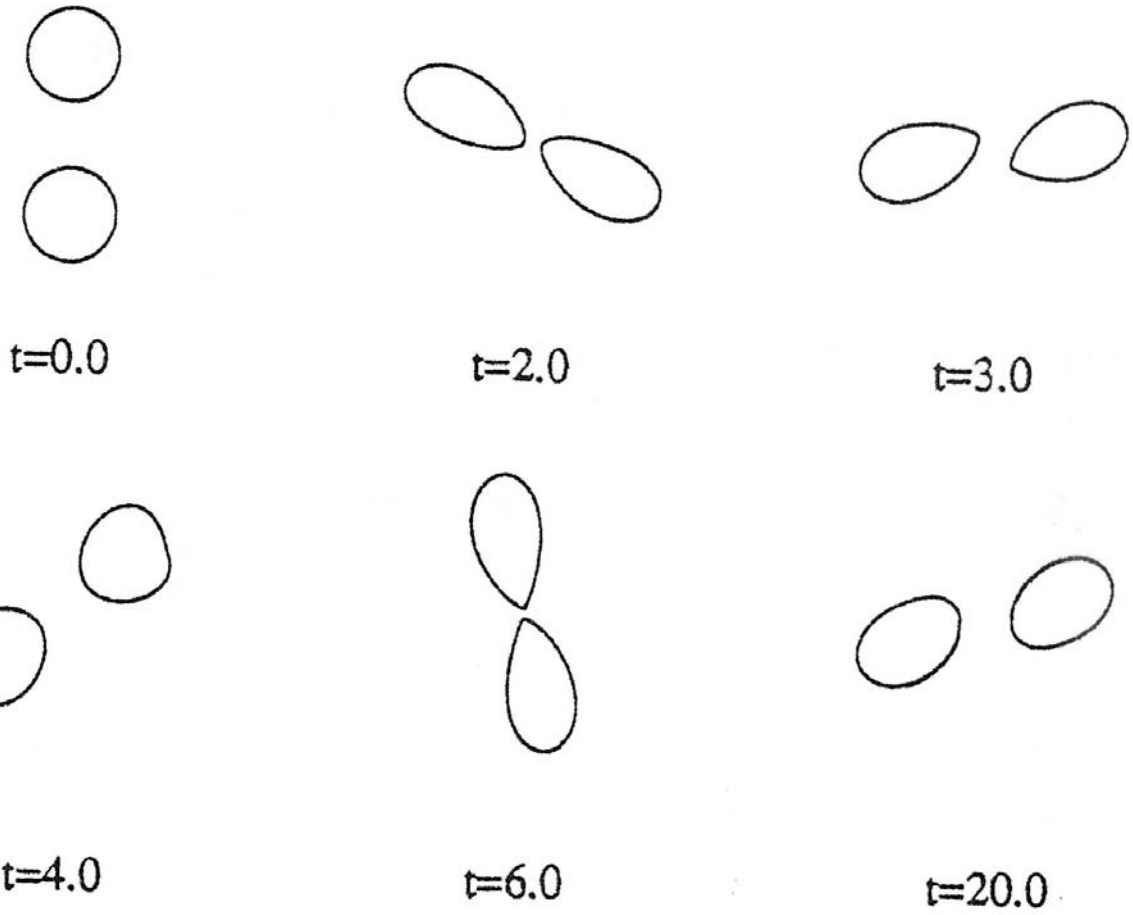

# 雙颱風的互繞 ----藤原效應

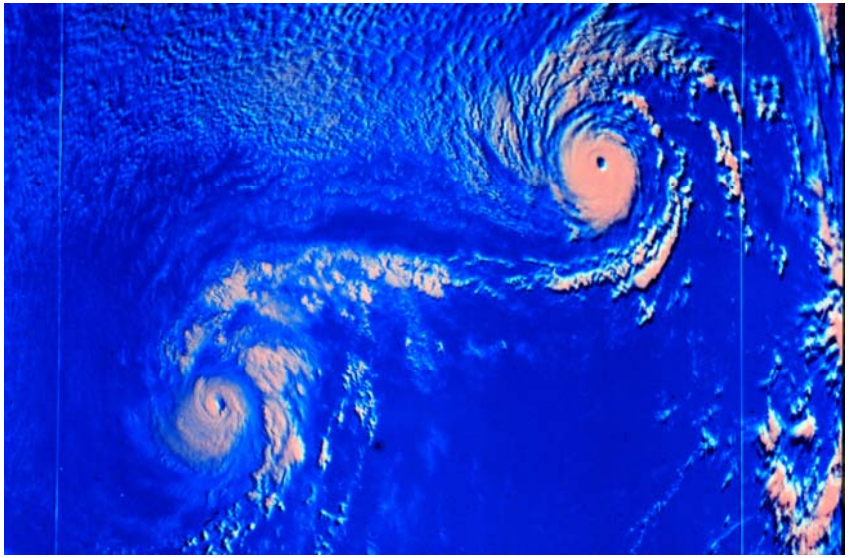

颱風 Ione 與 Kristen

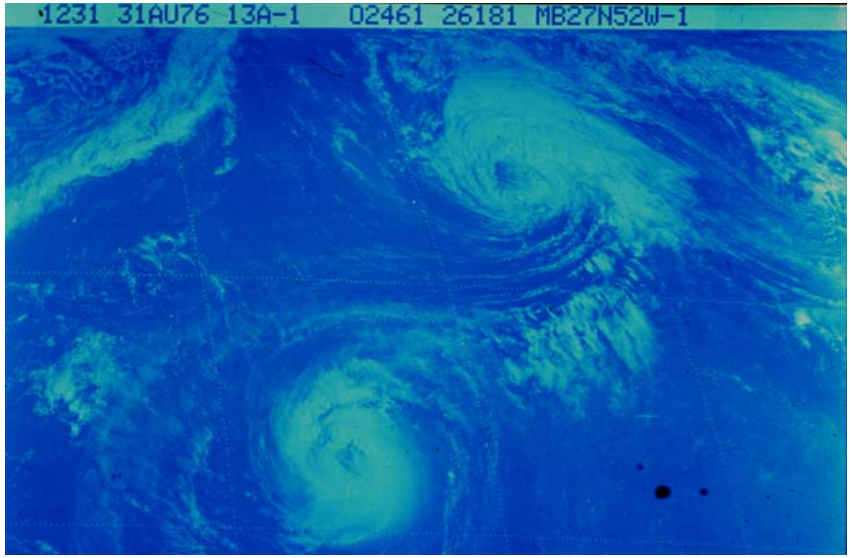


颱風 Emmy 與 Frances

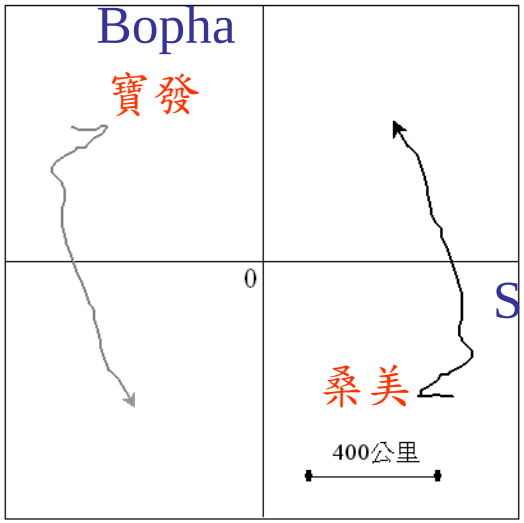


The unusual south movement of Typhoon Bopha

# Merger regime

partial merger (PM)

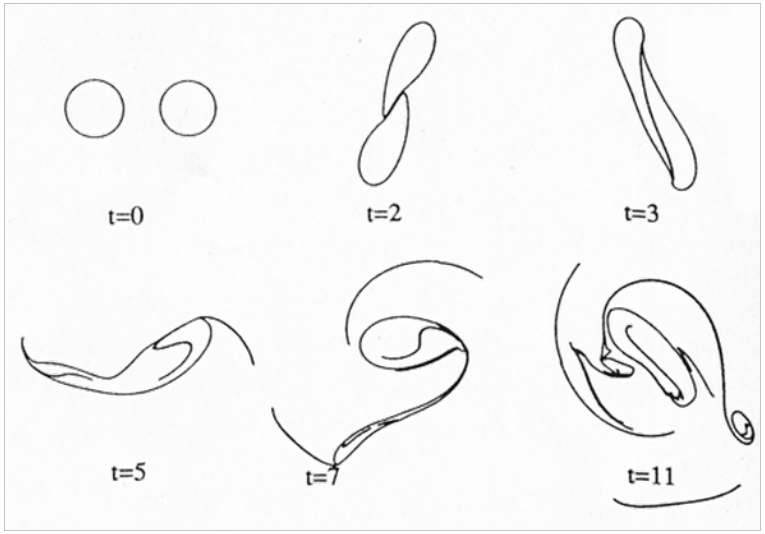


complete merger (CM)

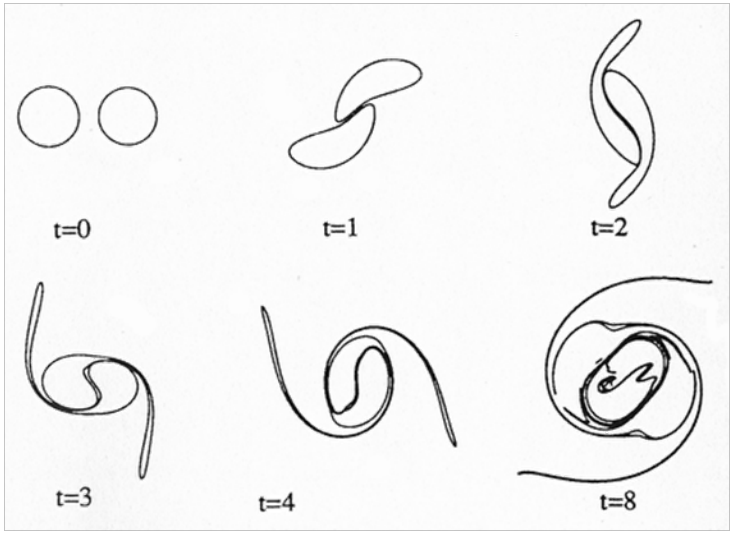

# Why ‘merger’ ?

- Chang (1983) – diabatic heating
- DeMaria & Chan (1984) – vortex vorticity gradient
- Dritschel and Waugh (1992)

  – advection + selective decay of 2D turbulence

# Chang (1983)

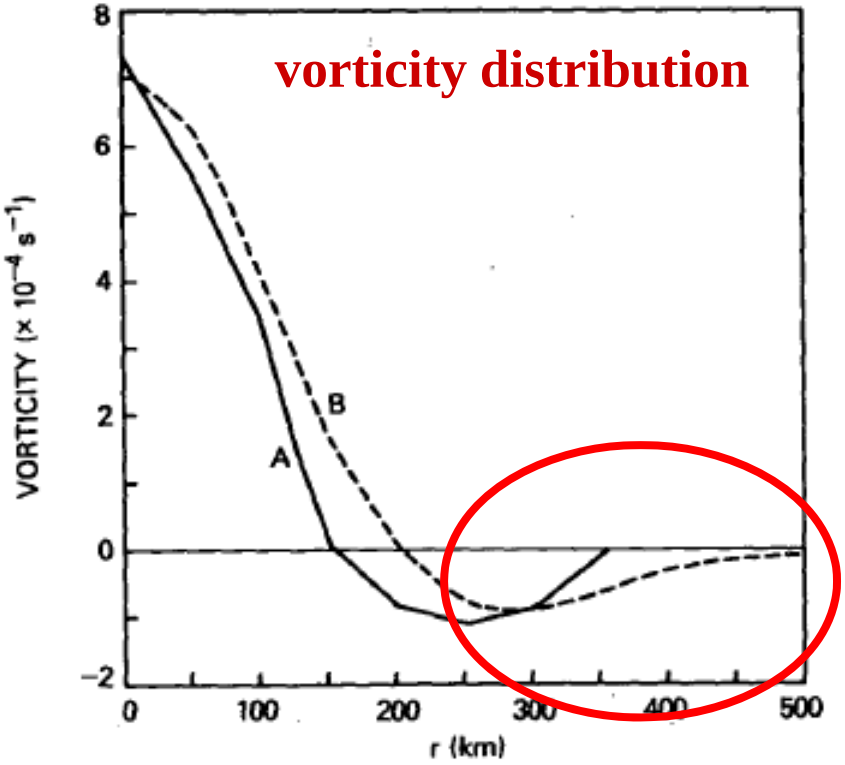


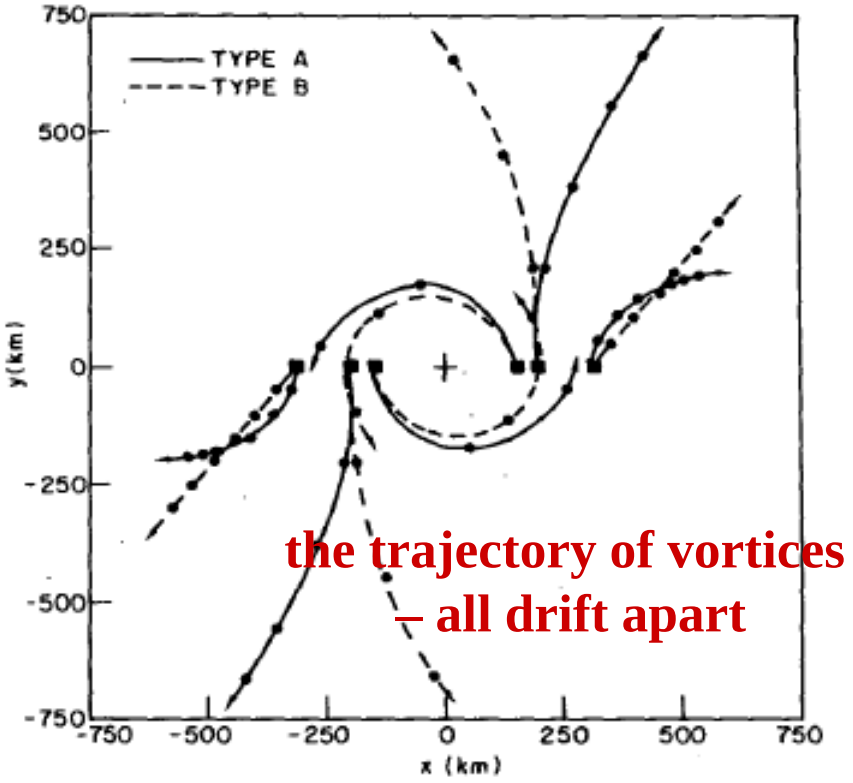


**non-diabatic heating**

# Chang (1983)

## diabatic heating

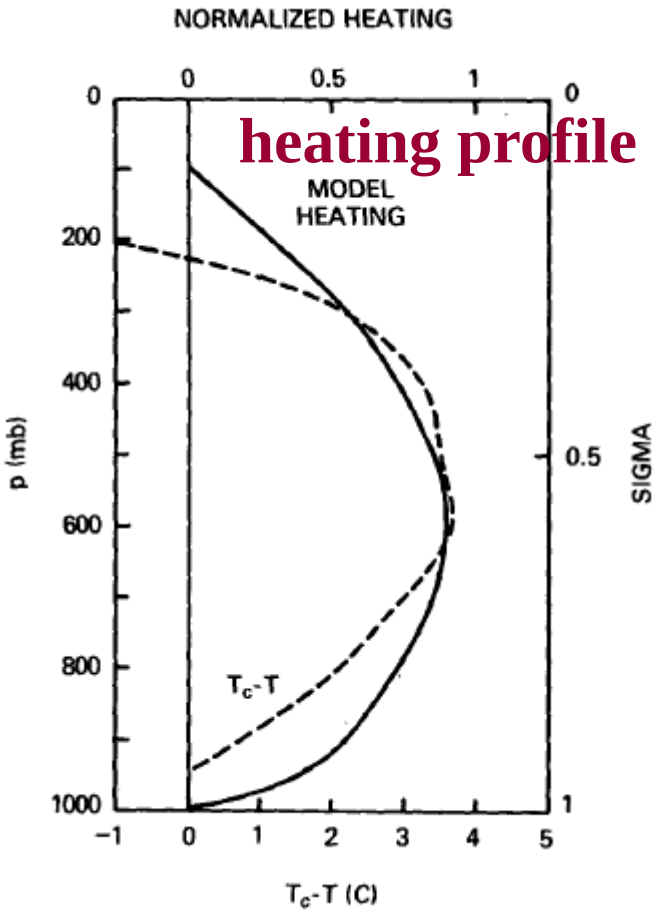


heating profile

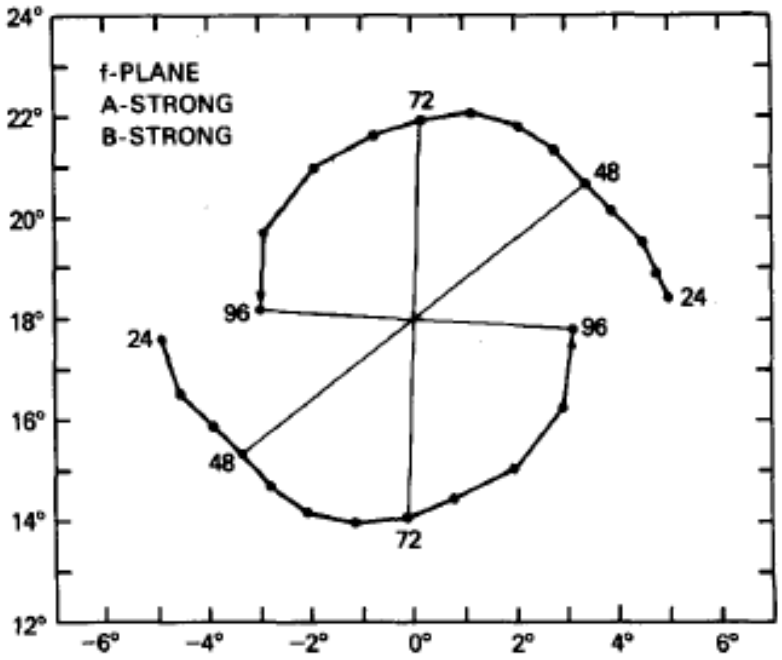


$$\frac{dQ}{dt} = 200\ (K\ day^{-1})$$

**The distance between two vortices decreases with time**

# DeMaria & Chan (1984)

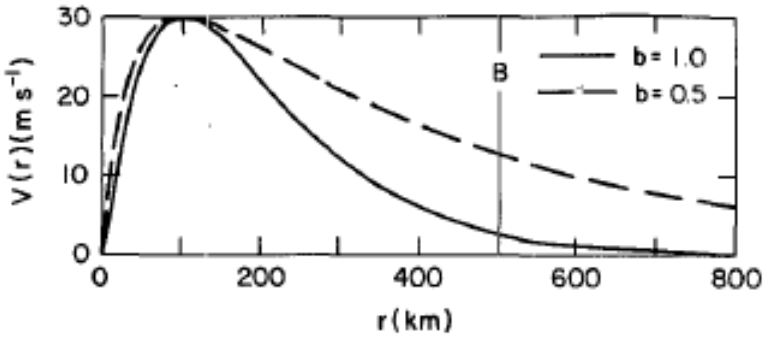


$$V(r) = V_m\left(\frac{r}{r_m}\right)\exp\left\{\frac{1}{b}\left[1-\left(\frac{r}{r_m}\right)^b\right]\right\},$$

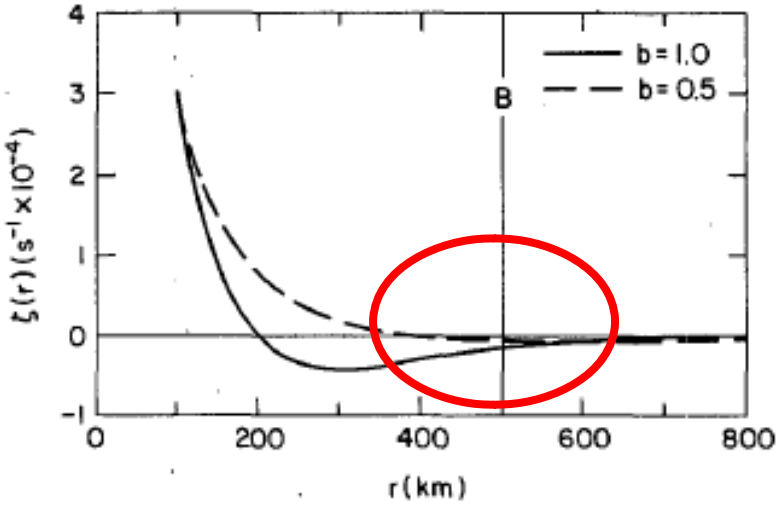


$$\zeta_{(r)} = \frac{2V_m}{r_m}\left[1-\frac{1}{2}\left(\frac{r}{r_m}\right)^b\right]\exp\left\{\frac{1}{b}\left[1-\left(\frac{r}{r_m}\right)^b\right]\right\}$$

**b : the factor determines the rate of tangential wind decays**

# DeMaria & Chan (1984)

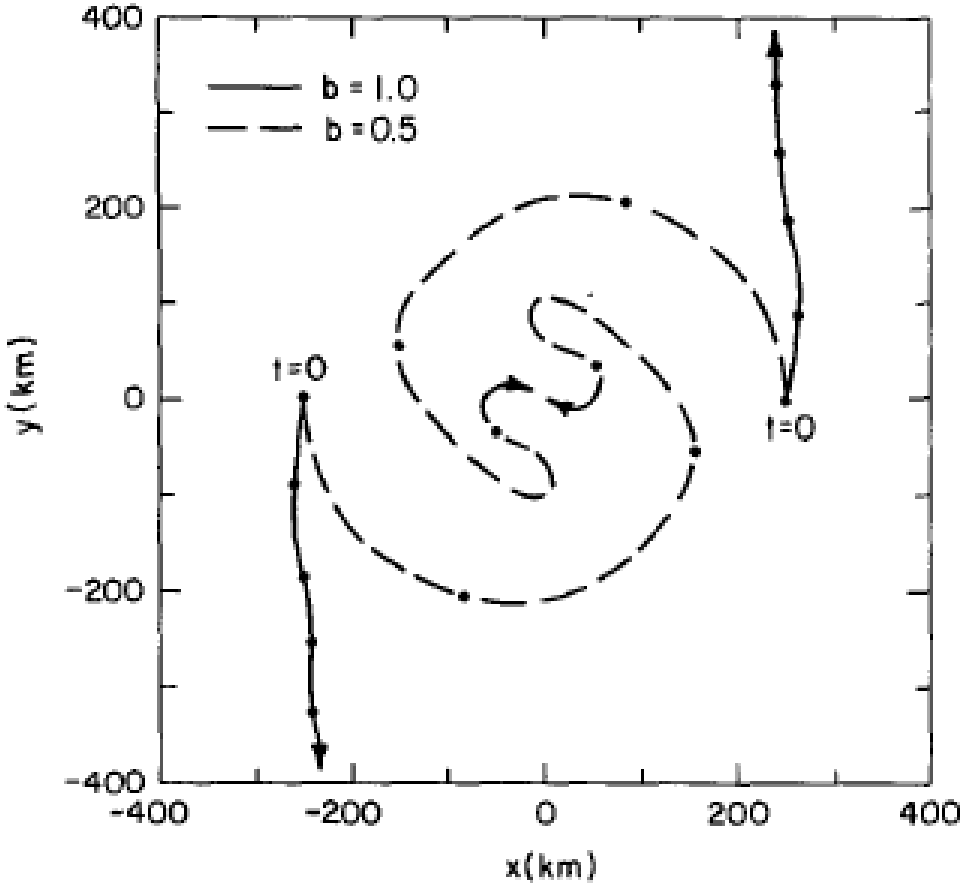


**b = 1.0 drift apart**

**b = 0.5 merge**

# Merger ---- 颱風 PAT 與 RUTH (1994)

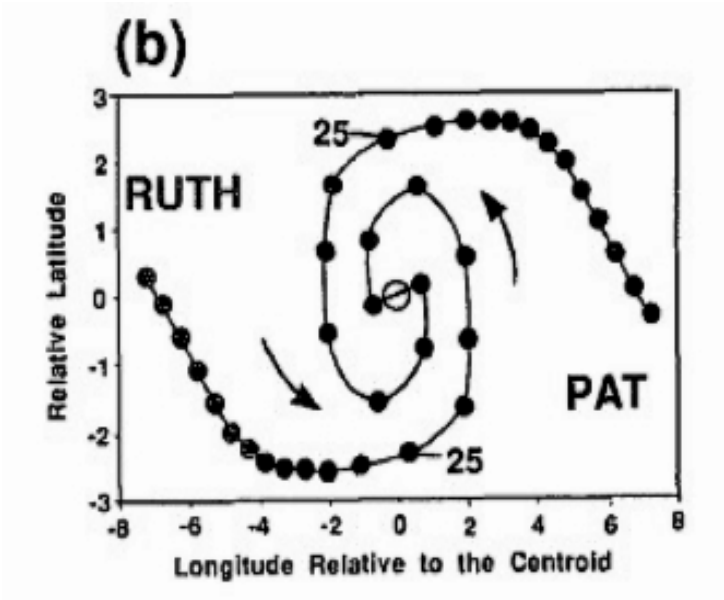


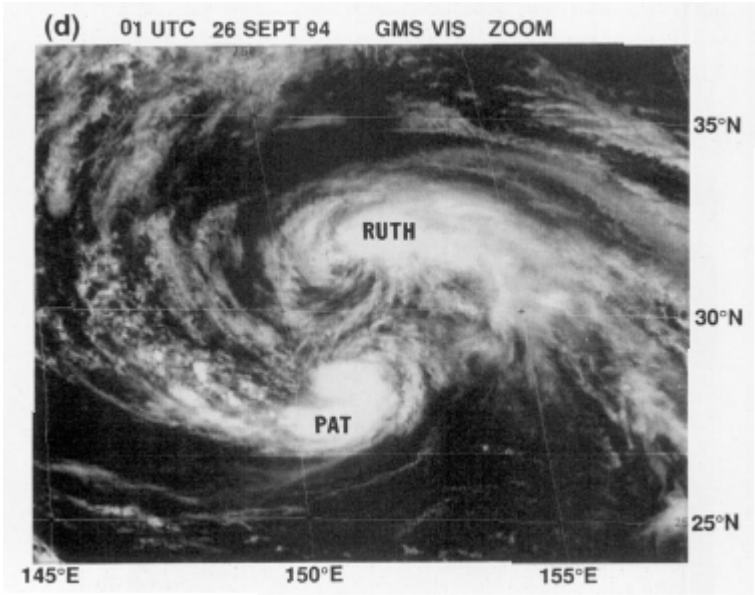


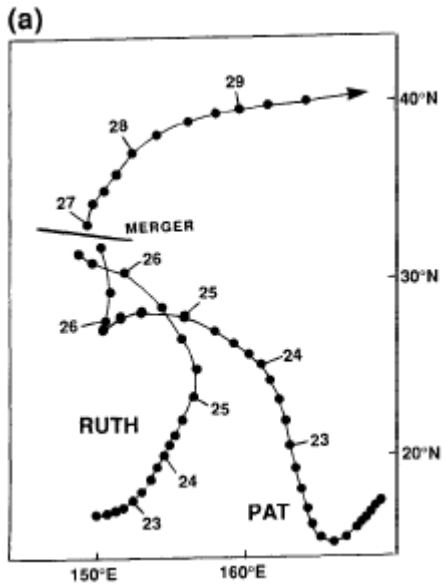


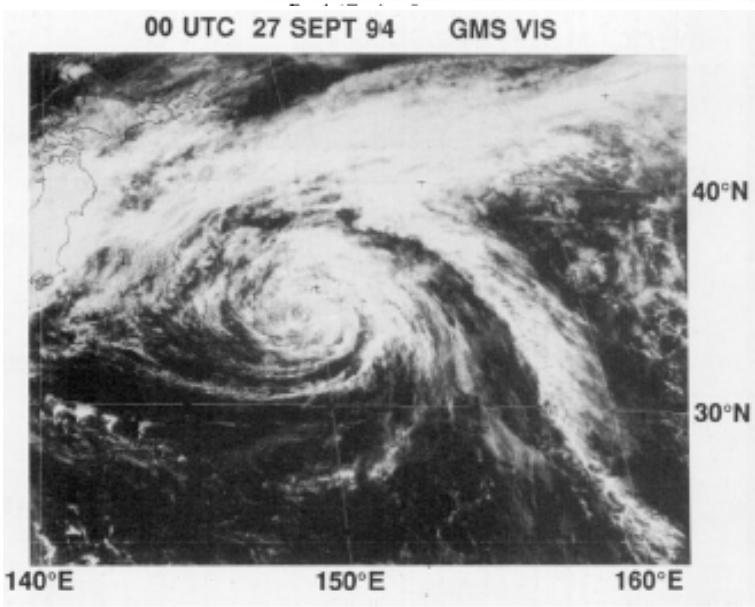


Lander 1995

# Lander and Holland (1993)

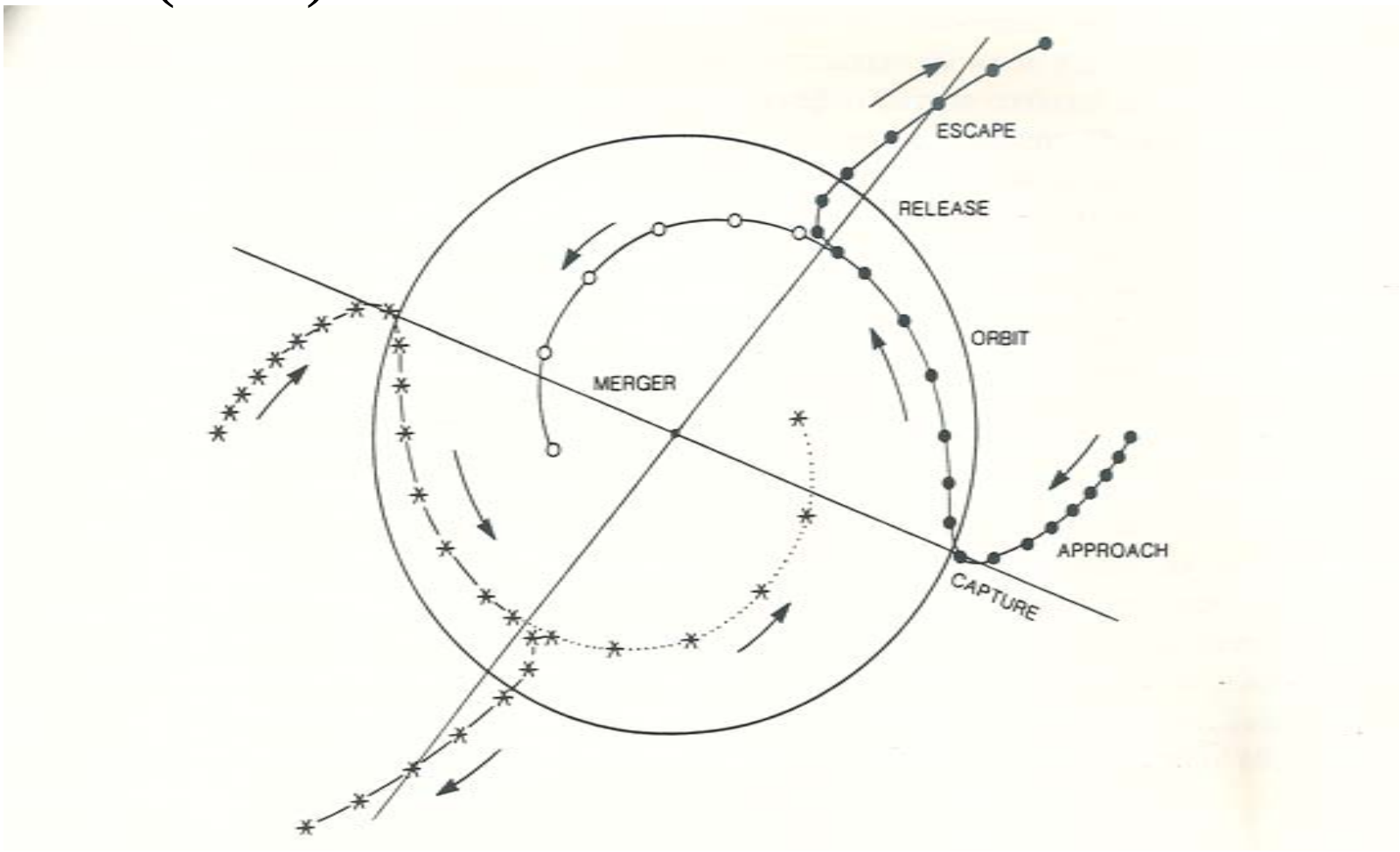


**Merger and Elastic Interaction** **Chaotic Behavior**

*Hendricks et al. (2004)*

# "Vortical" Hot Towers

- **The net effect of the hot towers is to produce strong small-scale (10km in diameter on average) lower-tropospheric ( below z ≈ 5km ) cyclonic PV towers.**

- **The strong updrafts in the hot towers converge and stretch existing low-level vertical vorticity into intense small-scale vortex tubes.**

- **Multiple mergers / axisymmetrization of these tubes in the lower troposphere.**

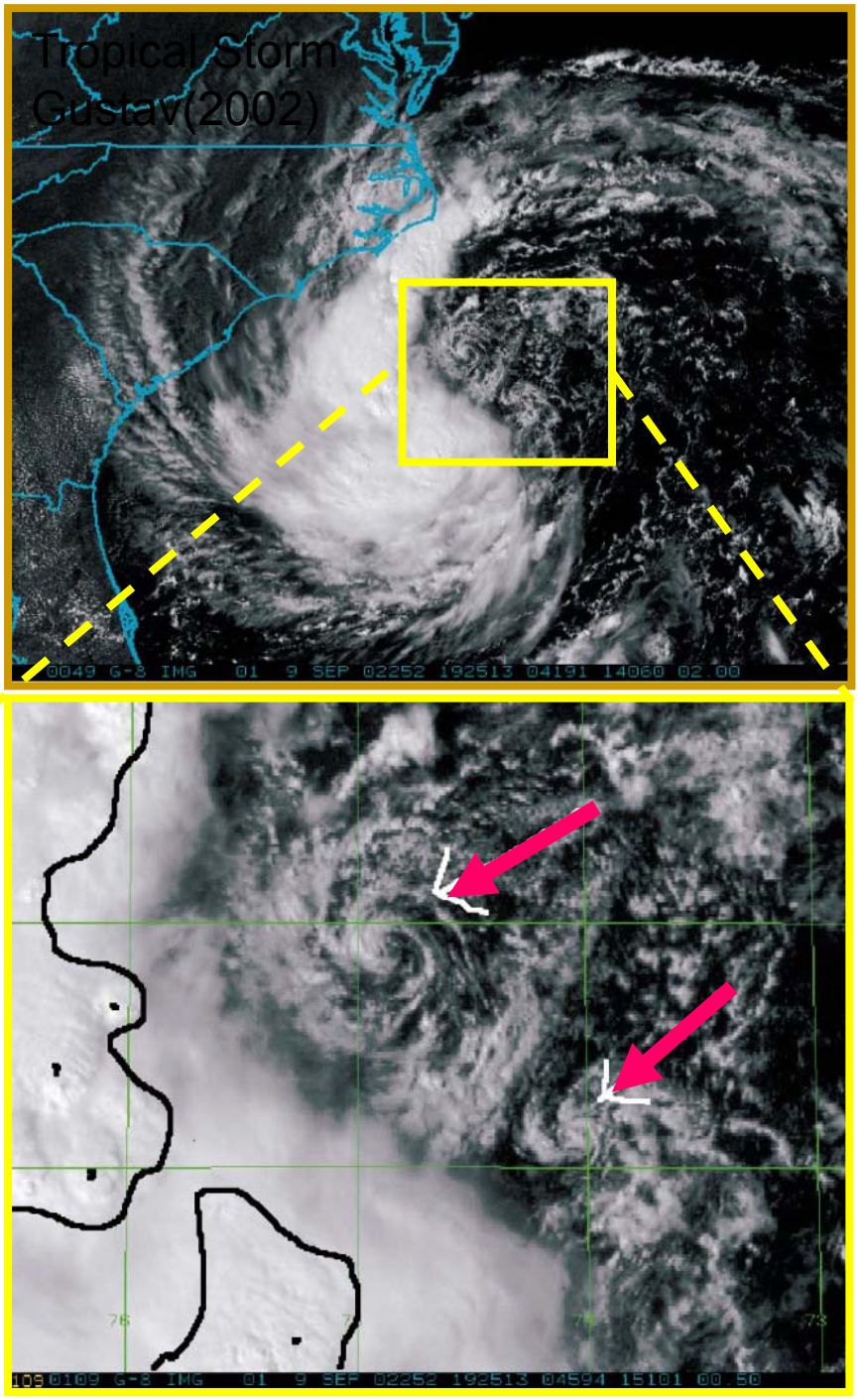

# "Vortical" Hot Towers

t=26.16 hr

$$\frac{D(PV)}{Dt} \approx \frac{f+\zeta}{\rho}\frac{\partial \dot{\theta}}{\partial z}$$

$$\left|\frac{\partial \dot{\theta}}{\partial z}\right| \approx 45\ K\ h^{-1} km^{-1}$$

$$\approx \frac{10^{-3}\ s^{-1}}{0.7\ kg\ m^{-3}}\left(1.25\times10^{-5}\ K\ s^{-1}\ m^{-1}\right)$$

$$\approx 64\ PVU\ h^{-1}$$

$$\left(\begin{array}{l} 1\,PVU \\ =1\times10^{-6}\ m^2 s^{-1} K\ kg^{-1} \end{array}\right)$$

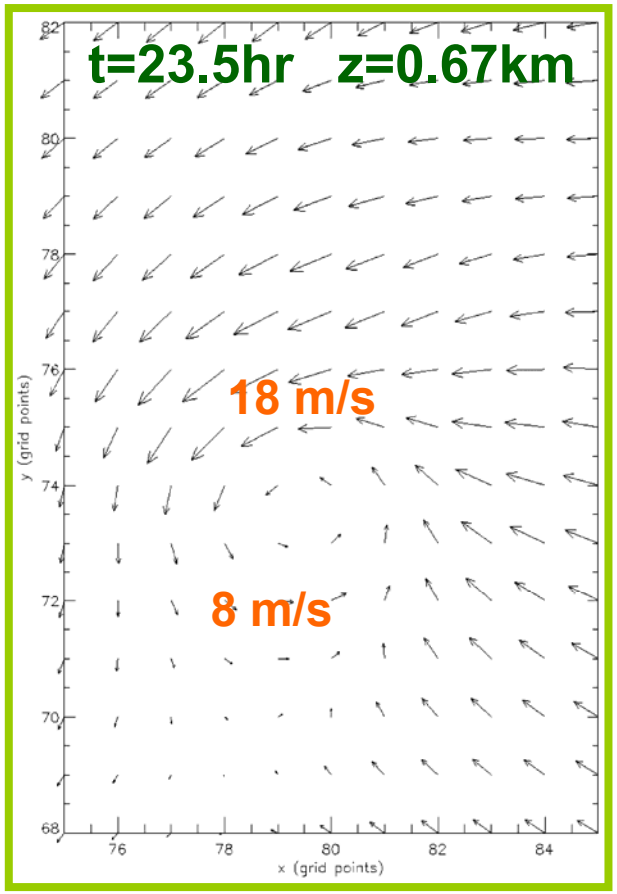


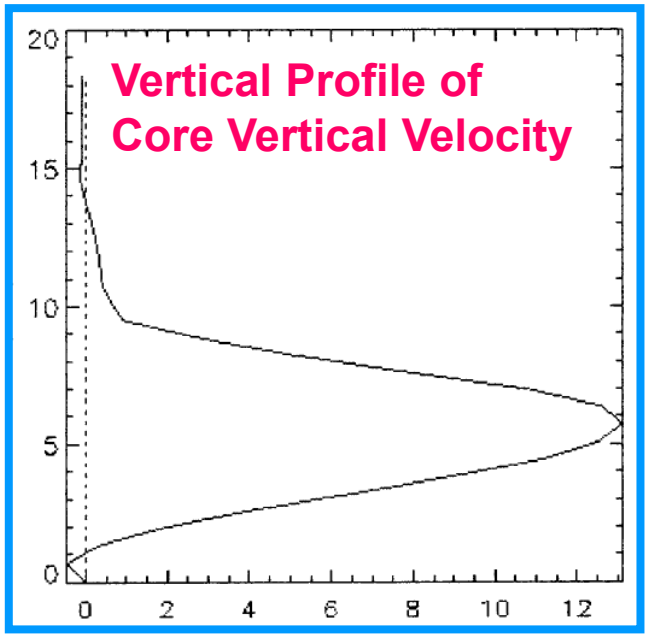


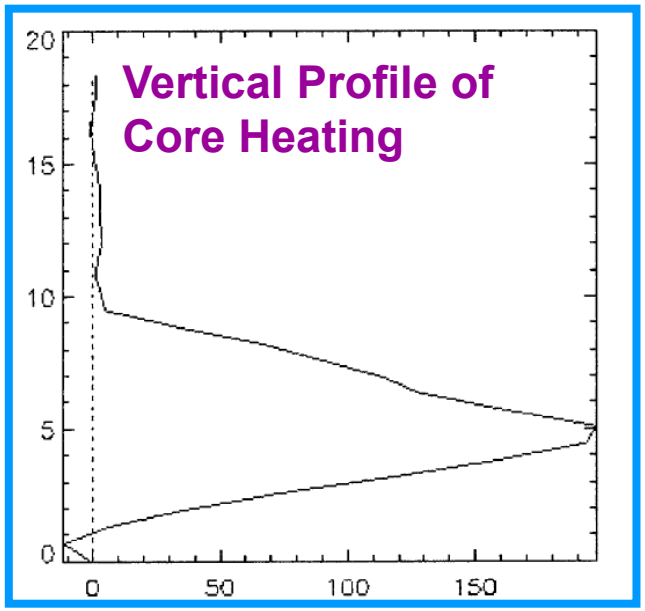


*Hendricks et al. (2004)*

# *Lander and Holland (1993)*

**Tracks of mesoscale vortices**

**Centroid-relative motion of Alpha and Bravo**

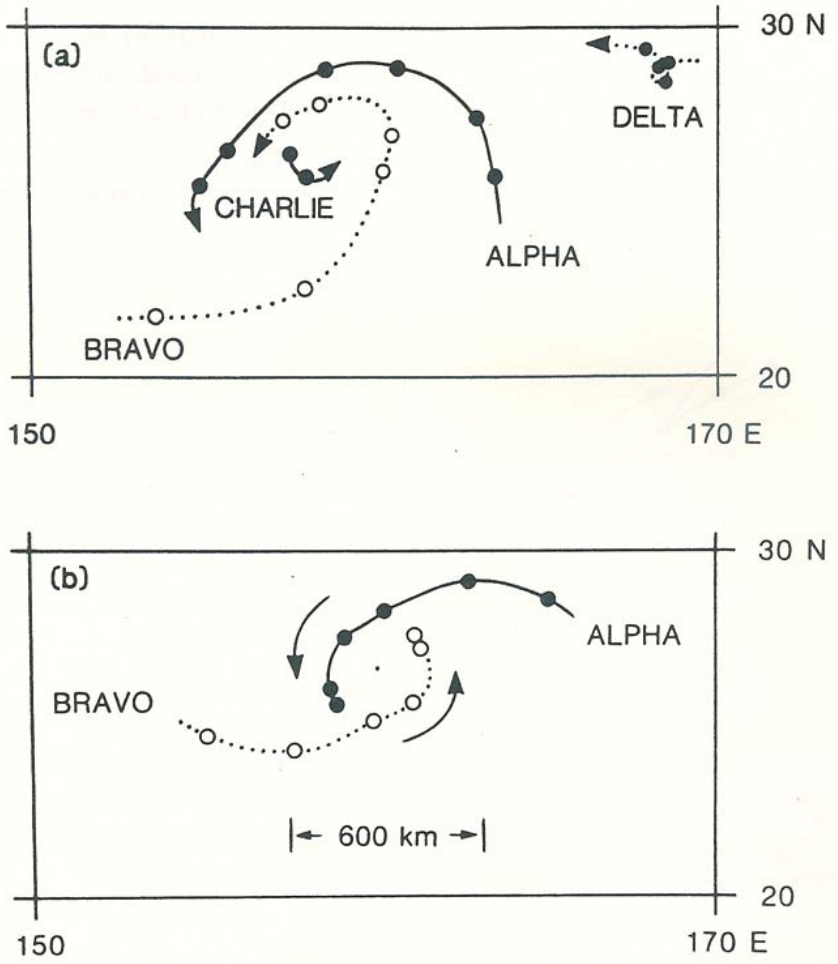


Figure 6. (a) Tracks of mesoscale vortices Alpha, Bravo, Charlie and Delta and (b) centroid-relative motion of Alpha and Bravo. Dots on the tracks are at irregular time intervals and show fixes obtained from visible satellite imagery.

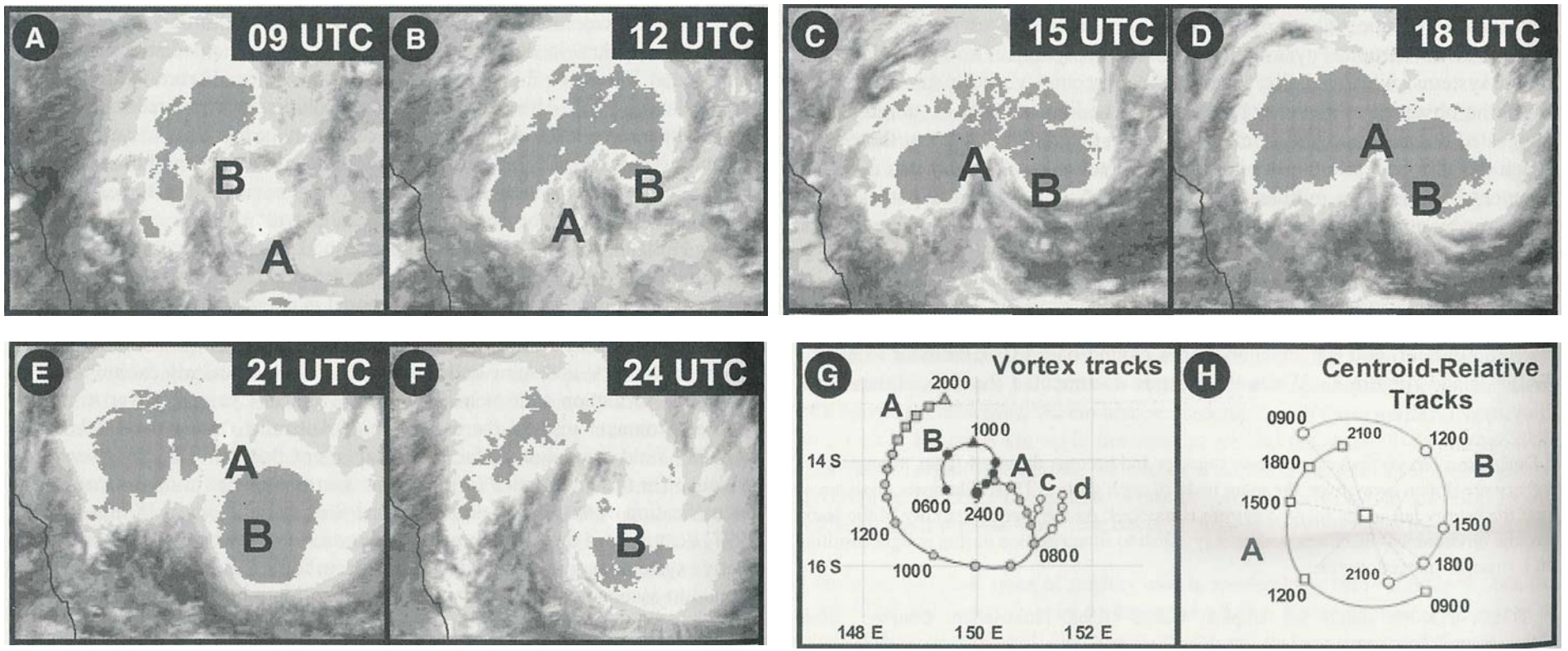


(A)-(F) The locations of the two mesovortices A and B during the development of Tropical Cyclone Oliver superposed on three-hourly satellite imagery for the period 0900 UTC February 4 to 0000 UTC February 5, 1993; (G) Tracks of four of the vortices obtained from radar data. The positions are not evenly spaced and so times (in UTC) of some of the vortex positions are marked; (H) three-hourly centroid-relative tracks of mesovortices A and B from 0900 UTC to 2100 UTC February 4[Simpson et al., 1997].

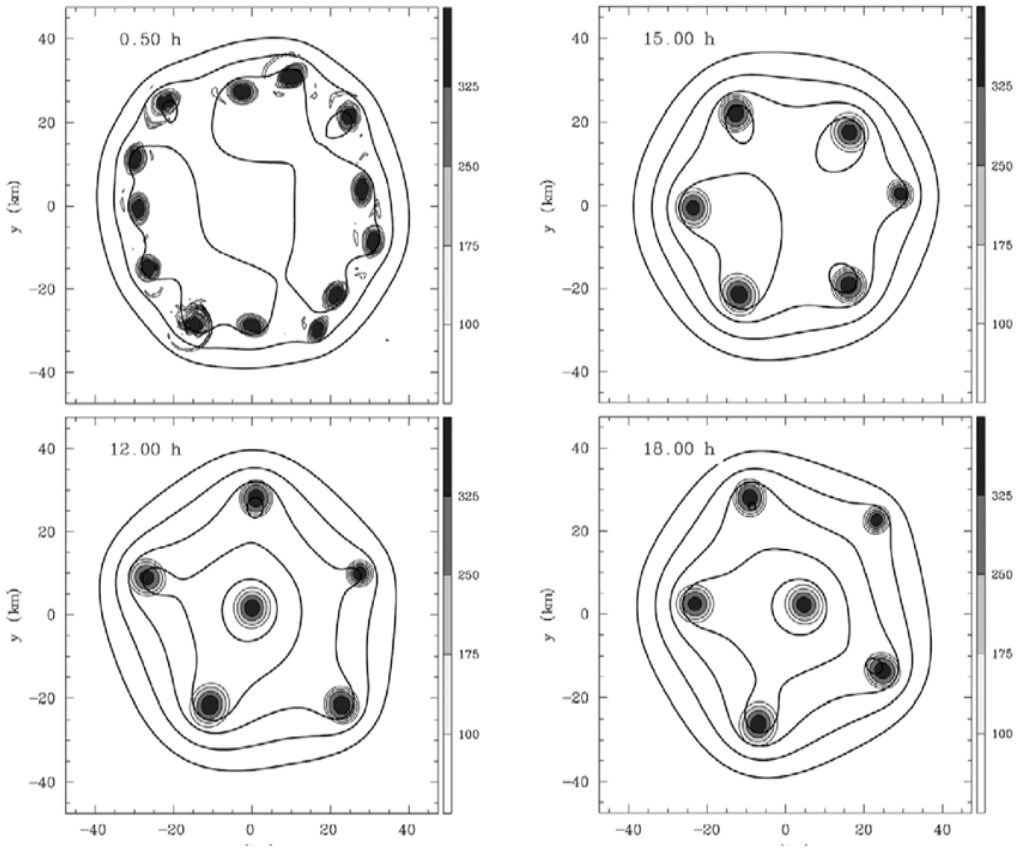


FIG. 2. Evolution of vorticity (shaded) and streamfunction contours (bold) for the numerical experiment of Kossin and Schubert (2001). Values along the label bar are in units of $10^{-4}$ $s^{-1}$. The shape of the streamlines transitions from a pentagon to a hexagon and back to a pentagon over 6 h.

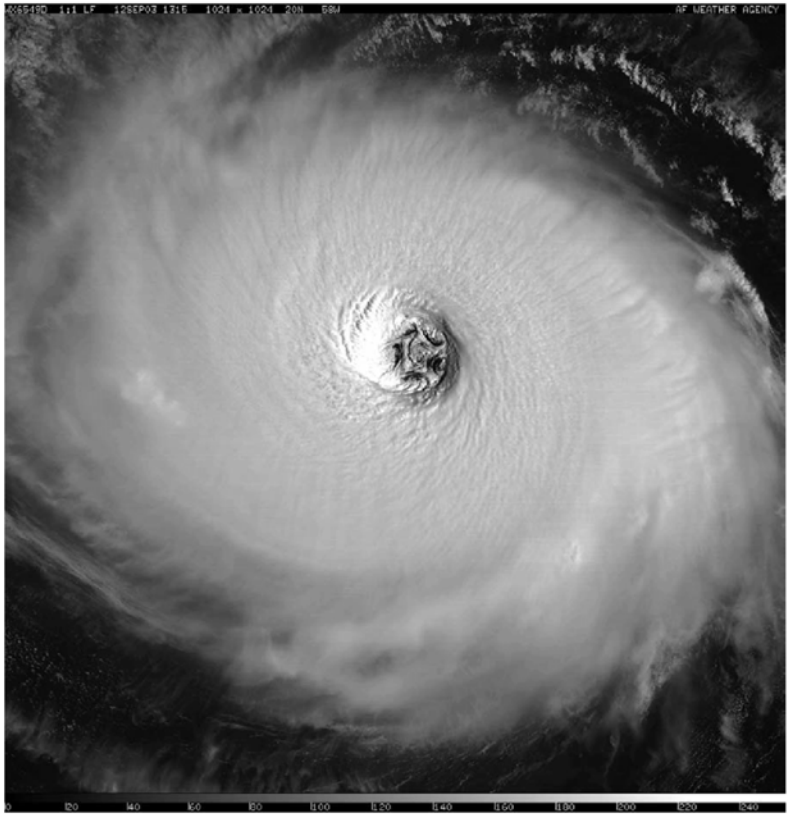

FIG. 1. Defense Meteorological Satellite Program (DMSP) image of Hurricane Isabel at 1315 UTC 12 Sep 2003. The starfish pattern is caused by the presence of six mesovortices in the eye—one at the eye center and five surrounding it.

MESOVORTICES IN HURRICANE ISABEL

BY JAMES P. KOSSIN AND WAYNE H. SCHUBERT

**Importance of Asymmetric Vorticity Dynamics**

# 納莉颱風眼附近的中尺度渦旋

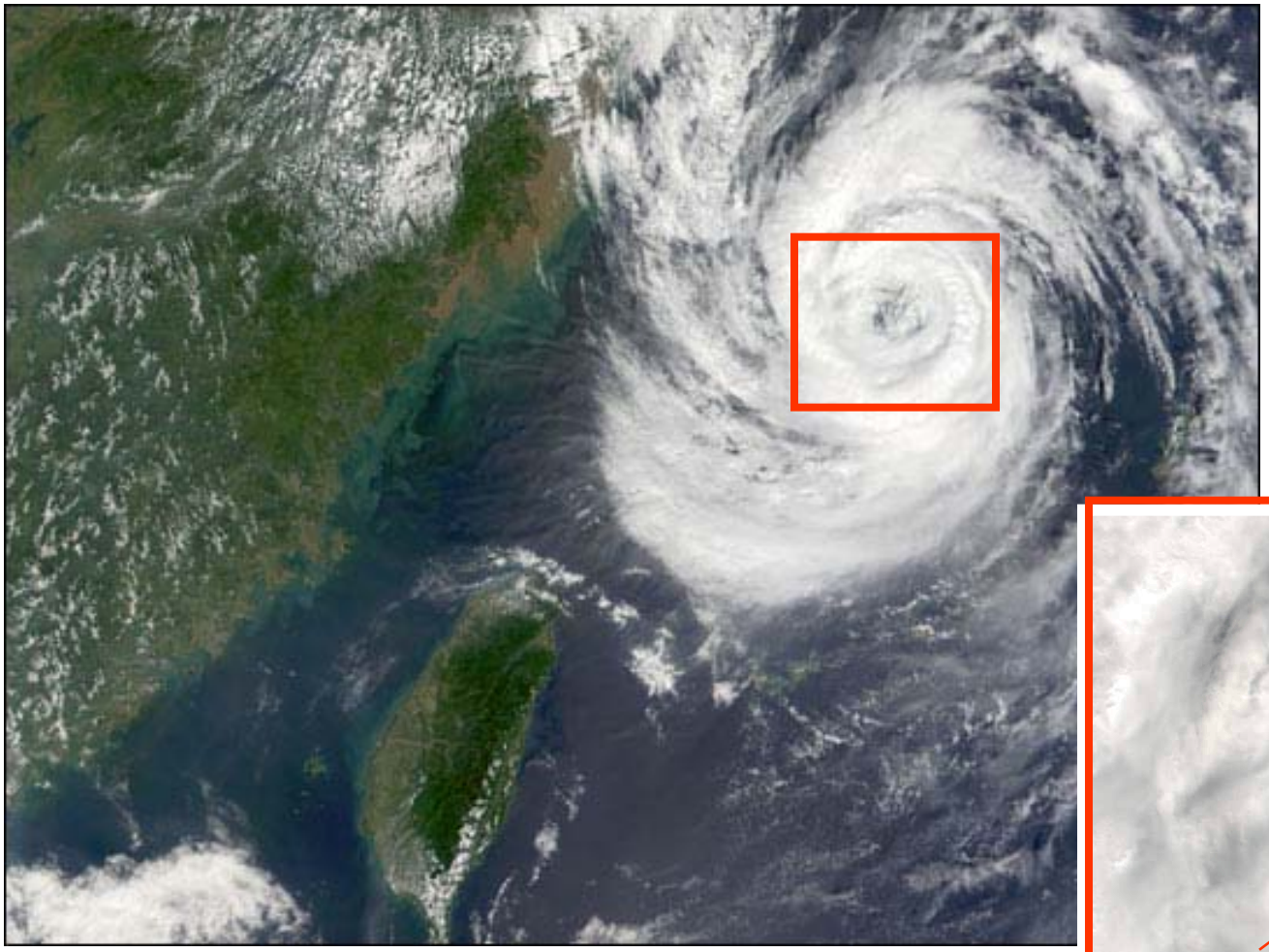

侵台納莉颱風登陸前颱風眼附近觀測到3 個中尺度渦旋

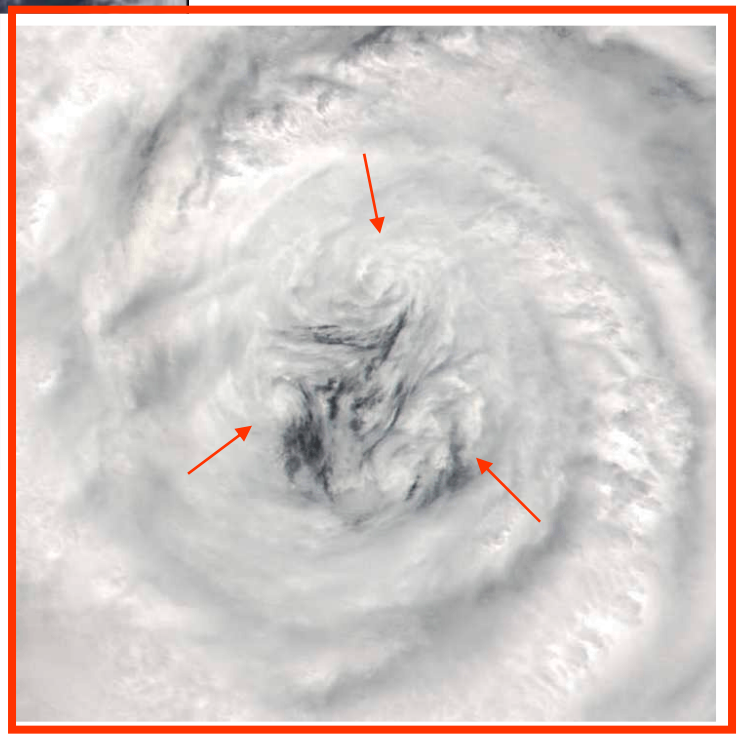

# Kossin and Schubert (2002)
# Mixing due to Barotropic Instability

20X20 km

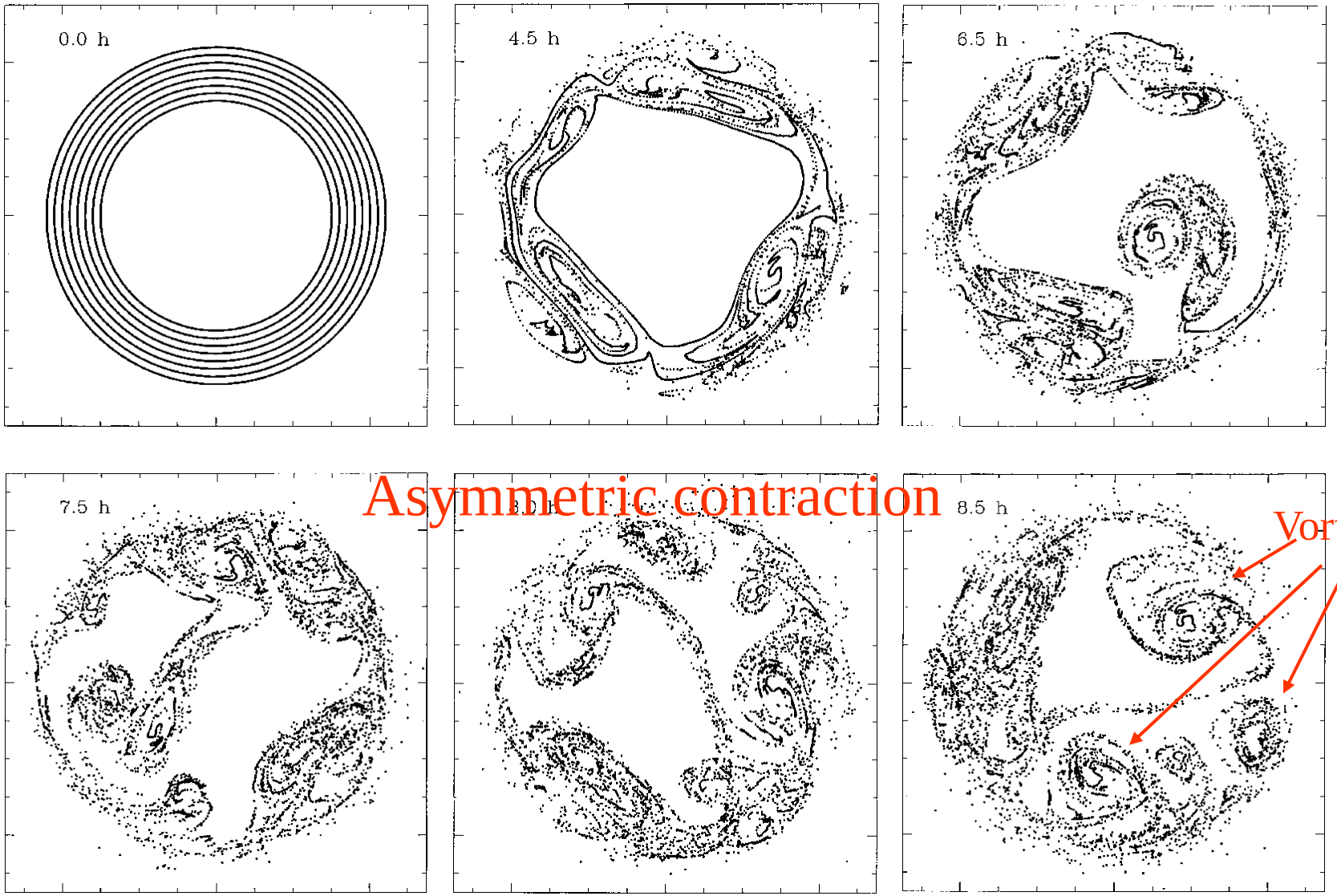


Advective rearrangement is different from the down-gradient diffusion

# Straining out regime

partial straining - out (PSO)

complete straining - out (CSO)

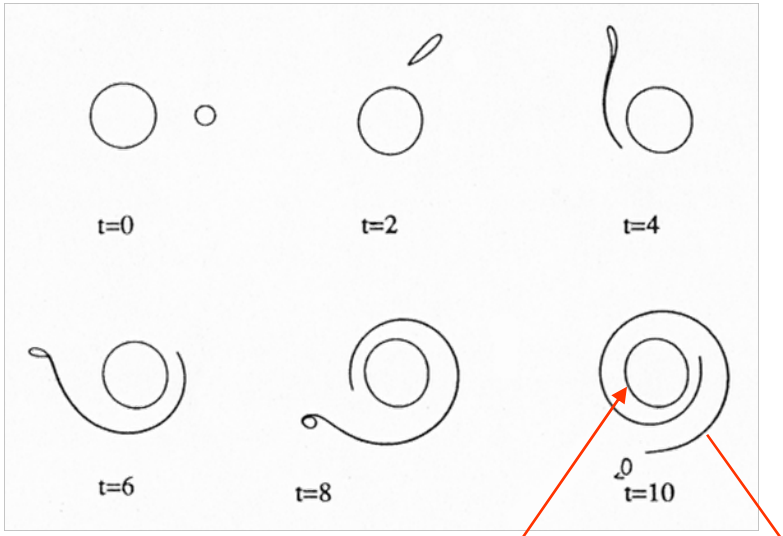


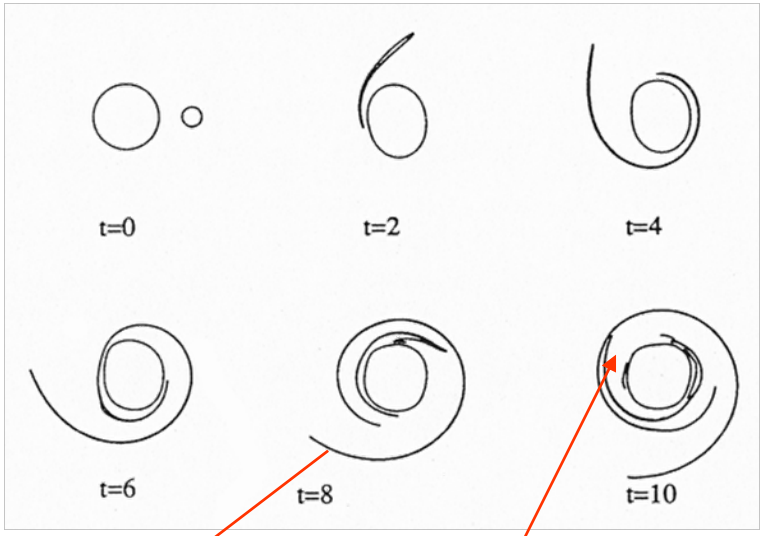


Clear gap

Clear gap

Adverse shear effect

The bands are too thin to be called concentric eyewalls.

# Kuo et al. ( 2000 ) MWR

## Typhoons Zeb and Alex ; straining – out regime

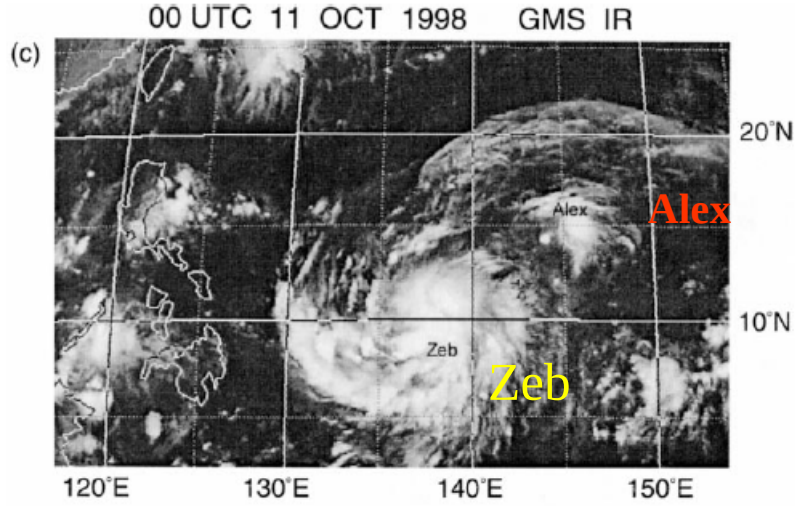


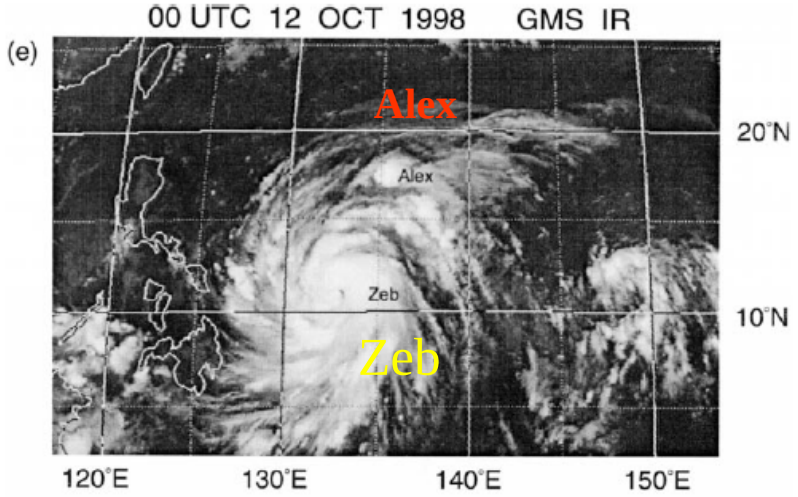


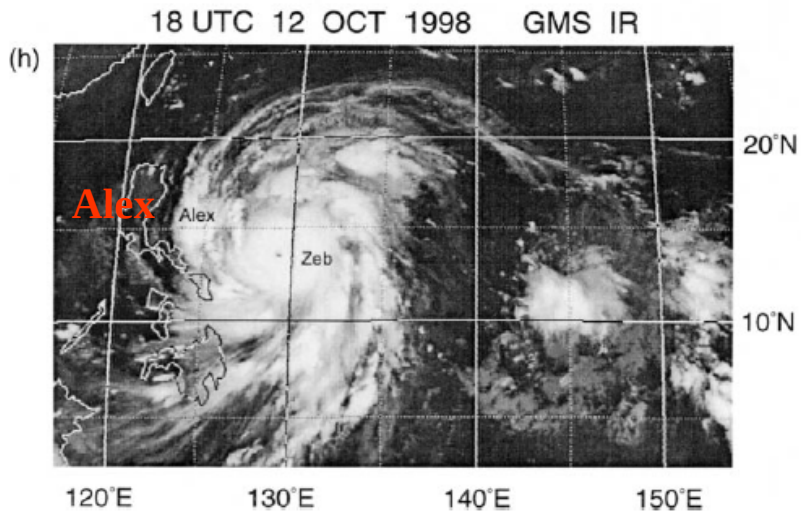


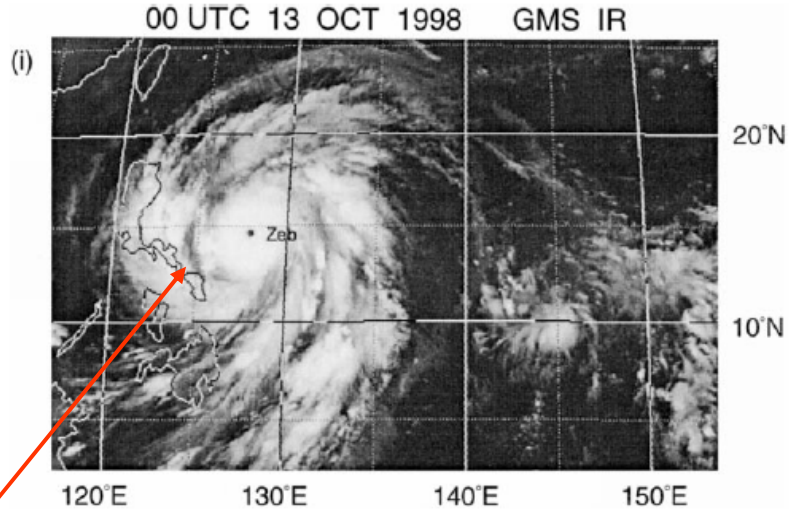


Clear gap between the Zeb and the remains of Alex

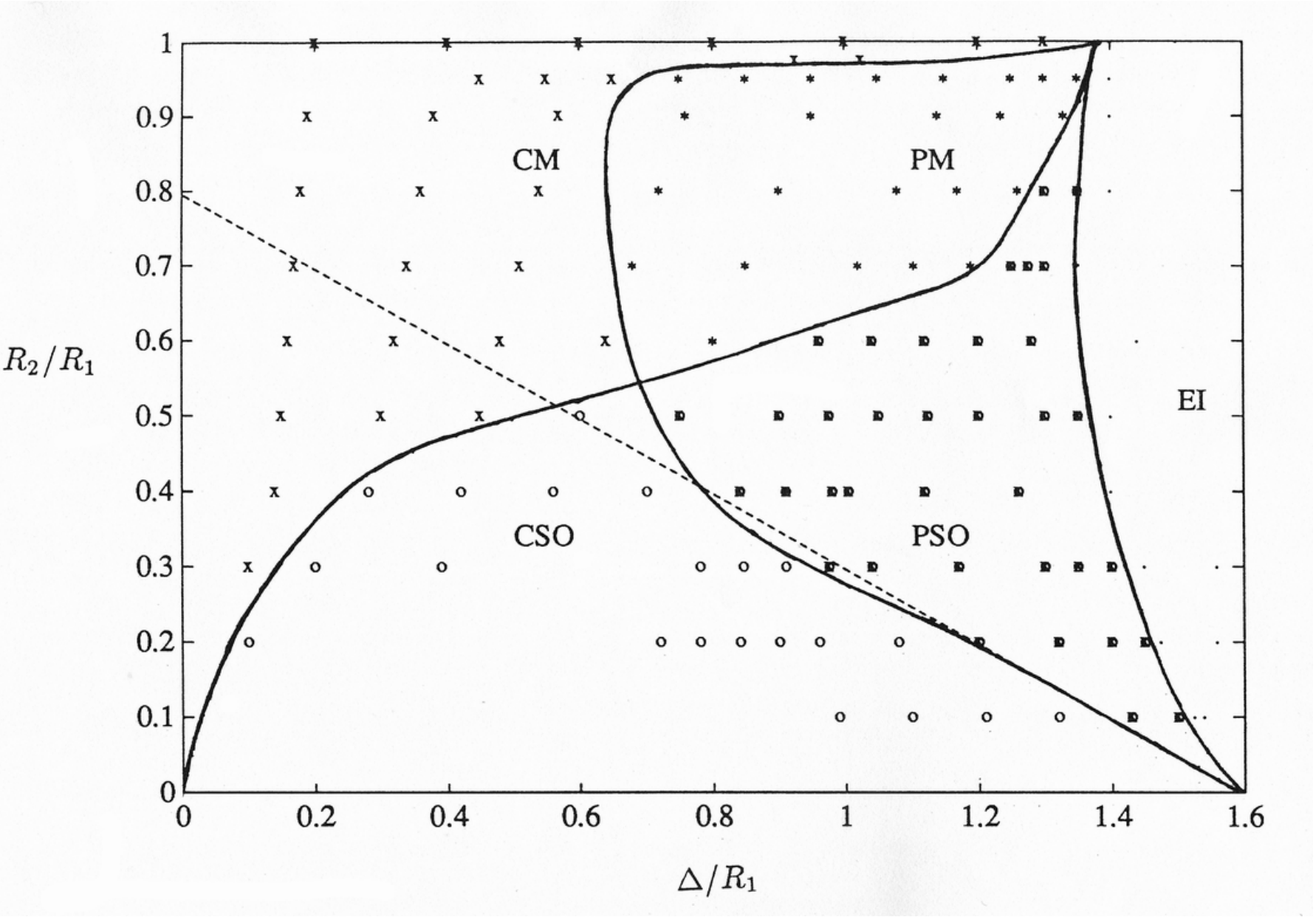


Dritschel and Waugh 1992

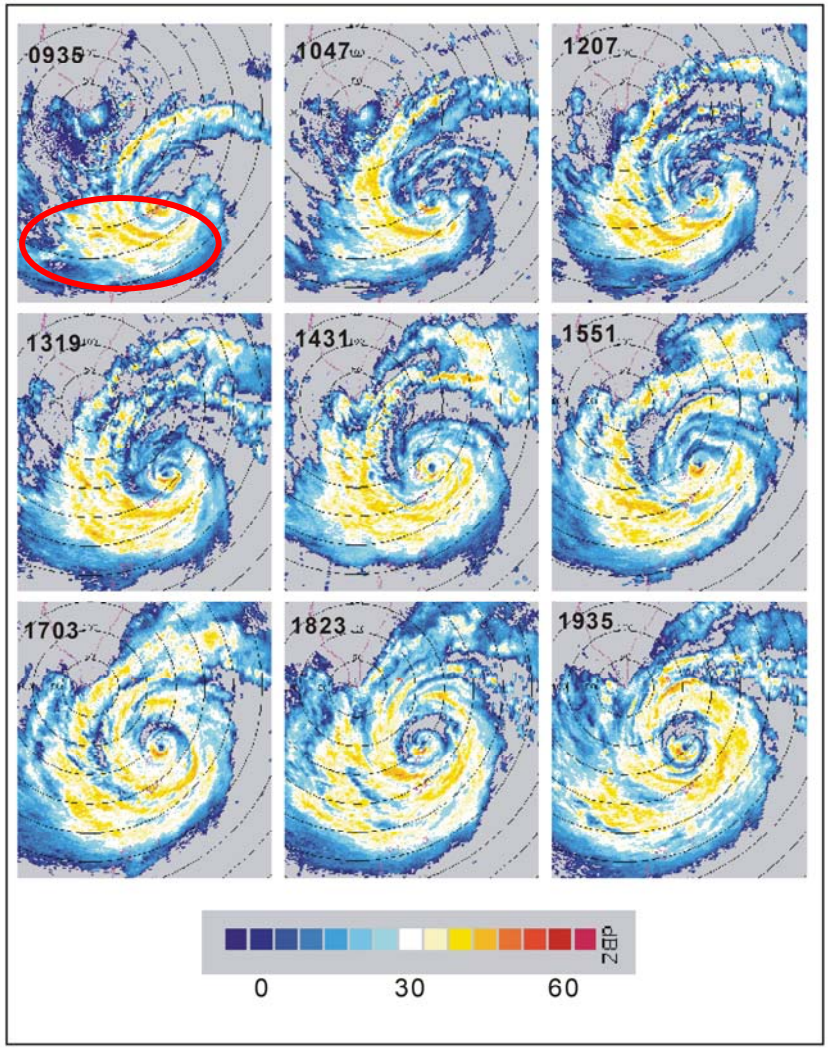


Figure 1a: Reflectivity at 0.5 elevation angle for Typhoon Lekima (2001) from the Central Weather Bureau WSR-88D (10 cm) radar at Kung-Ting for the period 0935 to 1935 September 25. The sequence of the images is from left to right and from top to bottom. The time interval between each image is approximately 75 min. The local time of observation is indicated on top of each image. The radial increment of the circles centered at radar station is 50 km. The nine images illustrate the formation of a concentric eyewall.

**Concentric eyewalls formation in Typhoon Lekima (2001) near Taiwan**

**A huge area of convection outside the core vortex that wraps around the inner eyewall to form the concentric eyewalls in about 12 hours.**

**Kuo et al. (2004)**

# Binary vortex interaction

$$r = \frac{R_1}{R_2}$$

$$\Delta / R_1$$

$$\gamma = \frac{\zeta_1}{\zeta_2}$$

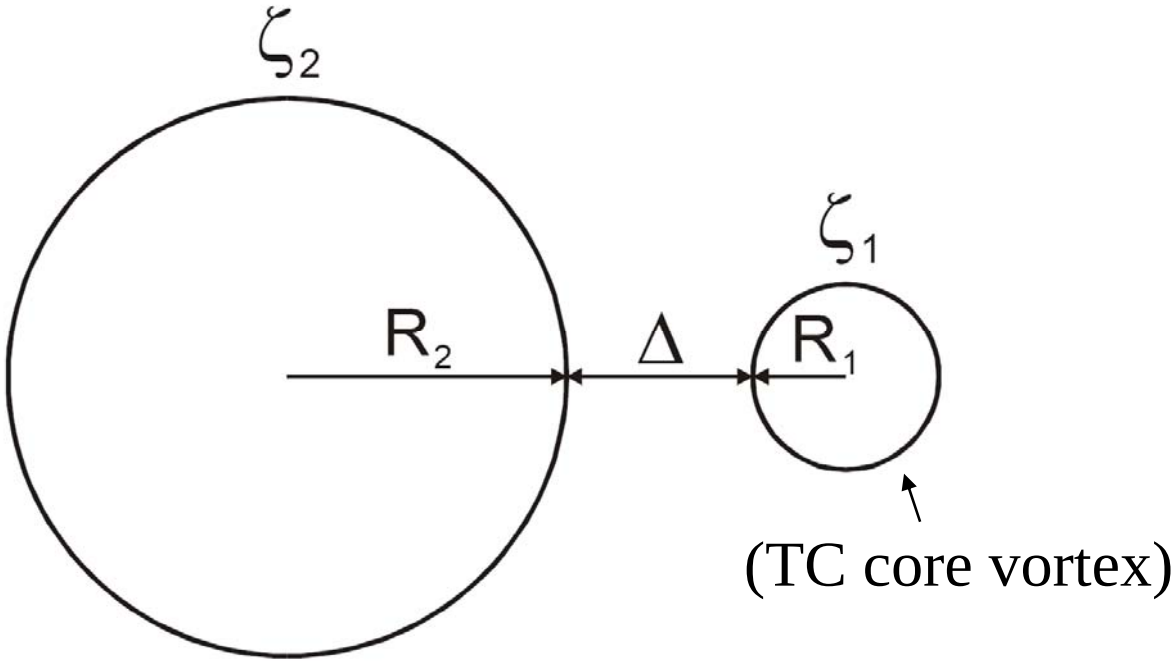


An extension of Dritschel and Waugh's (1992) work.

In addition to the radii ratio and the normalized distance between the two vortices, the vorticity ratio is added as a third external parameters.

Interaction of a small and strong vortex (representing TC core) with a large and weak vortex (representing vorticity induced by convection outside the TC core)

$$\gamma = \frac{\zeta_1}{\zeta_2}$$

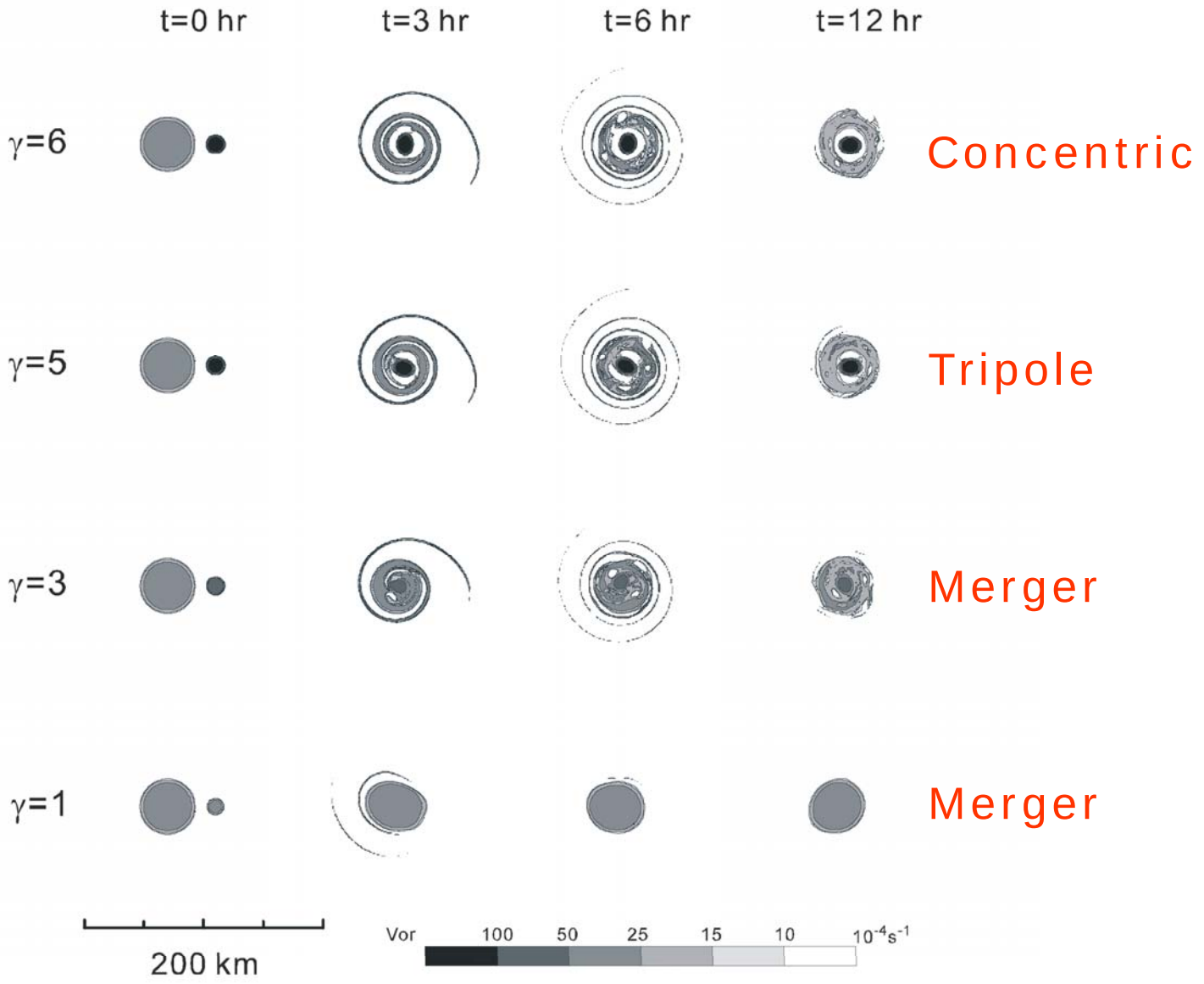


Figure 3: The sensitivity of the vorticity field in the binary vortex experiments with respect to the vorticity strength ratio ($\gamma$) at hour 0, 3, 6 and 12 with the dimensionless gap $\Delta/R_1=1$, and the vortex radius ratio r=1/3.

# Vortex radius ratio

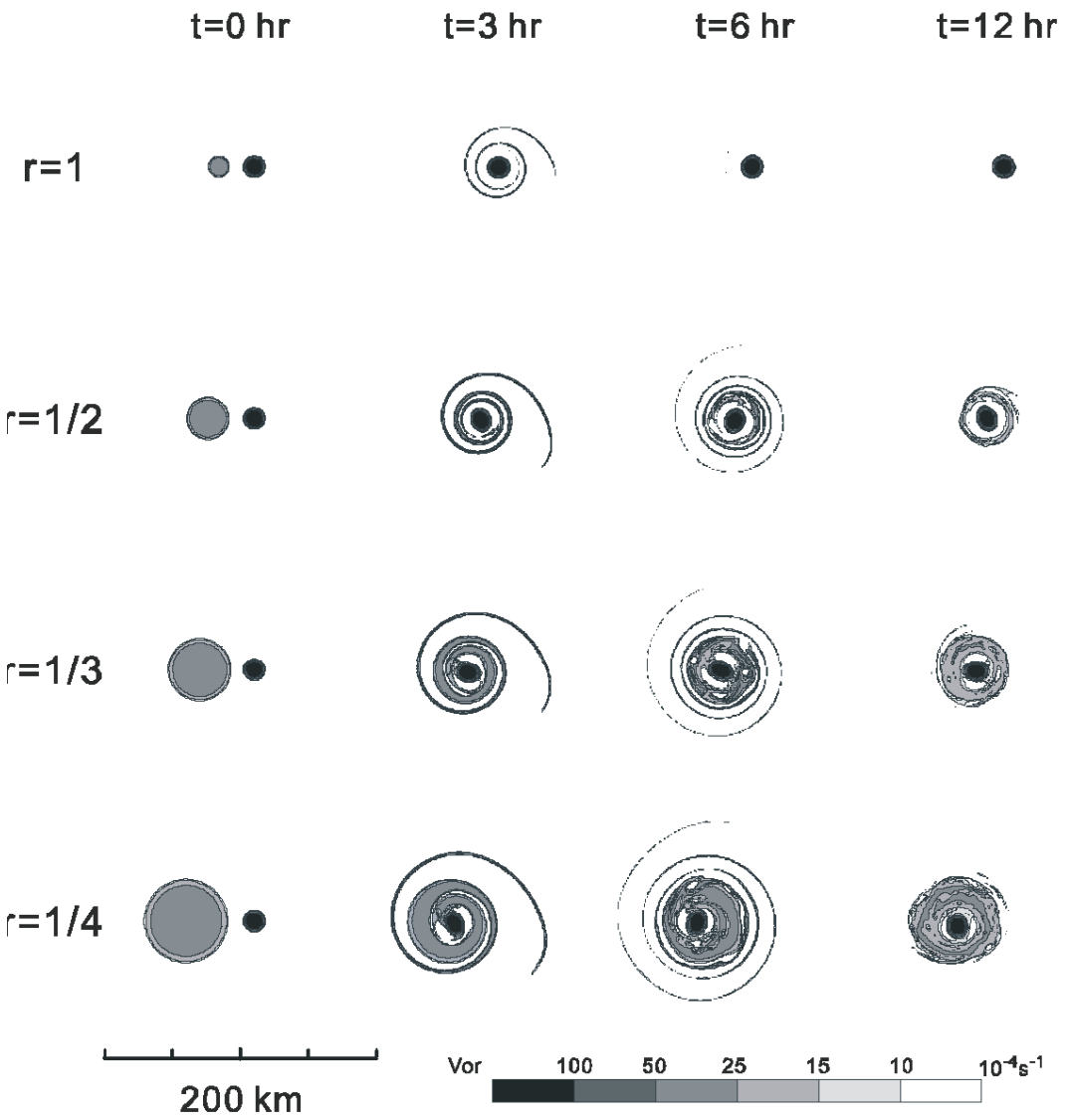


Figure 5: The sensitivity of the vorticity field in the binary vortex experiments with respect to the vortex radius ratio r at hour 0, 3, 6 and 12 with the vorticity strength ratio $\gamma$=5, and the dimensionless gap $\Delta/R_1$=1.

$\gamma = 10$

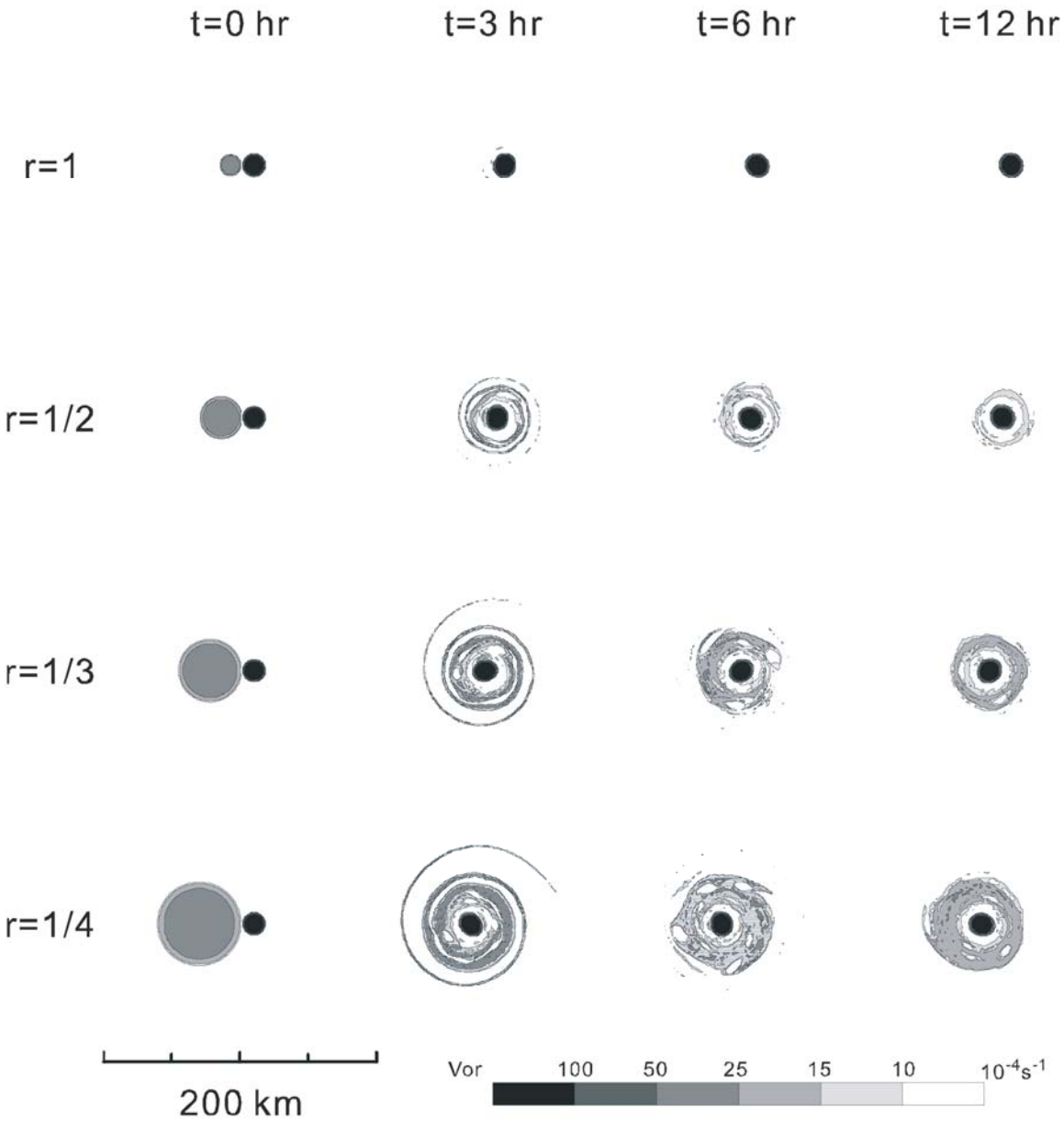


Figure 6: Similar to Figure 5 except that the dimensionless gap $\Delta/R_1=0$ and the vorticity strength ratio $\gamma=10$.

Same strain outside the RMW but different core vortex strength

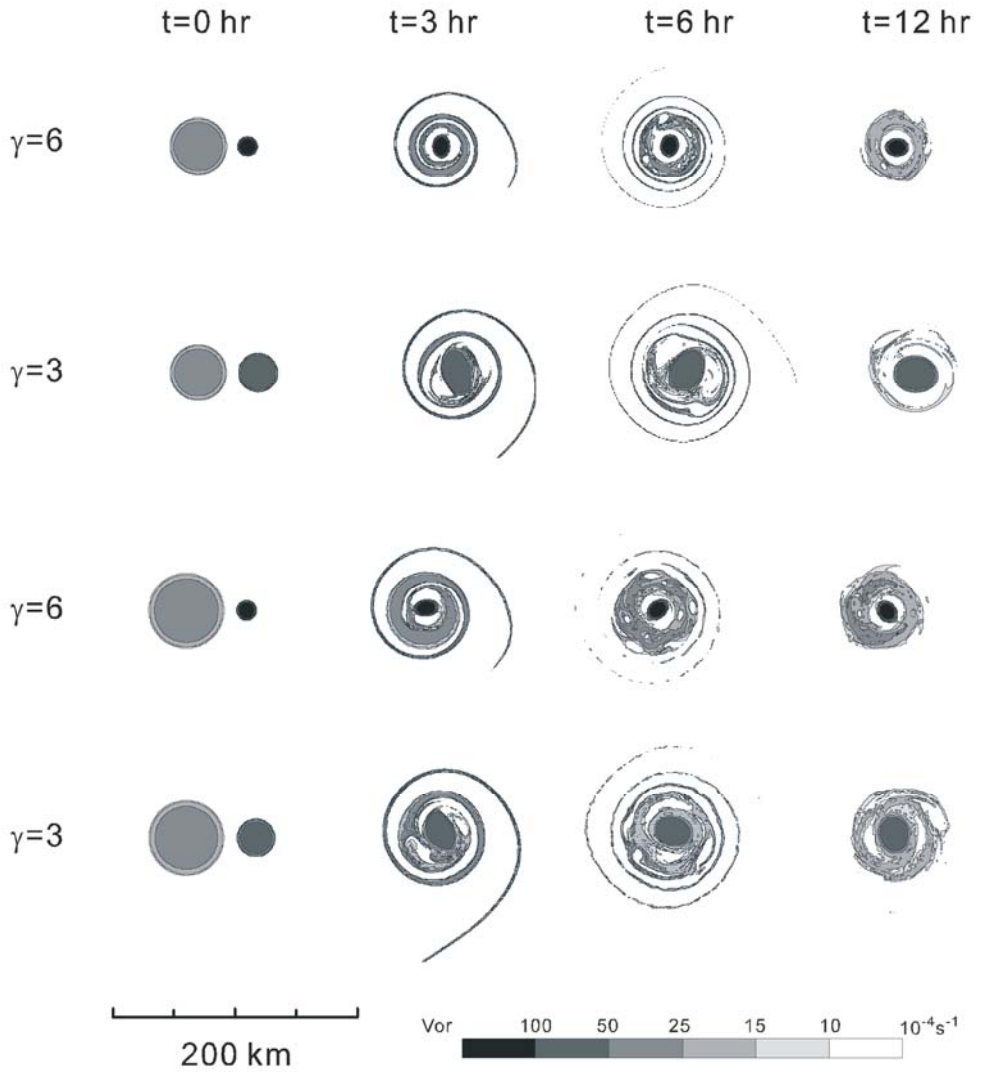


Figure 9: The sensitivity of the vorticity field in the binary vortex experiments with the core vortices process the same maximum wind but different radius of vorticity field. Two core vortices considered have the vorticity and radius of ($1.8 \times 10^{-2}s^{-1}$, 10 km) and ($0.9 \times 10^{-2}s^{-1}$, 20 km) respectively. The dimensionless gap is 1 in the experiments. The outer vortices considered have the radius of 30 km and 40 km respectively.

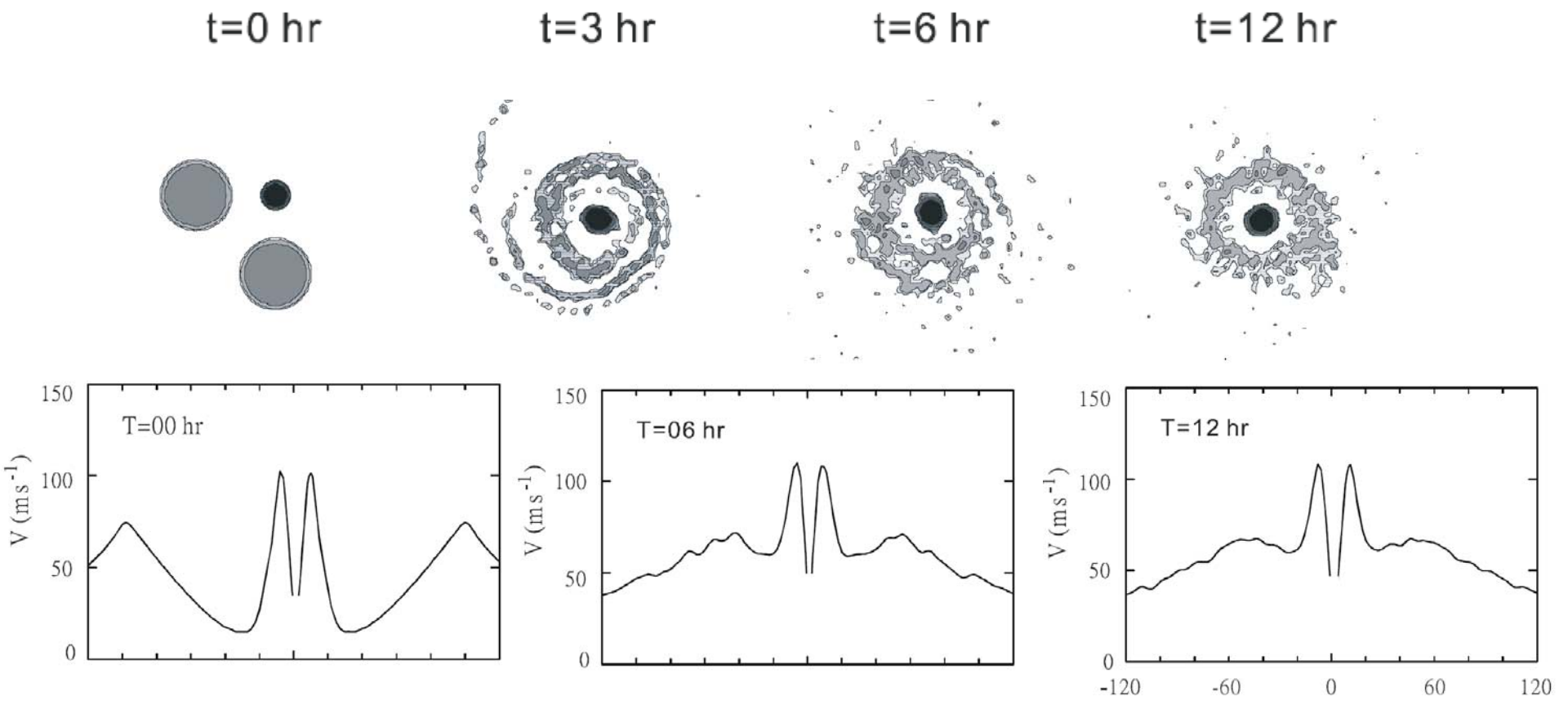


Figure 13: The tangential wind speed for radial arms toward the west (left portion) and the south (right portion) that emanate from the vortex center at various times for the experiment in the second row of Figure11.

The contraction of the secondary wind maximum by nonlinear advective dynamics.

Kuo et al. (2004)

- A very strong core vortex at least six times stronger than the neighboring vorticity
- A relative larger neighboring vorticity area
- A separation distance within three to four times the core vortex radius

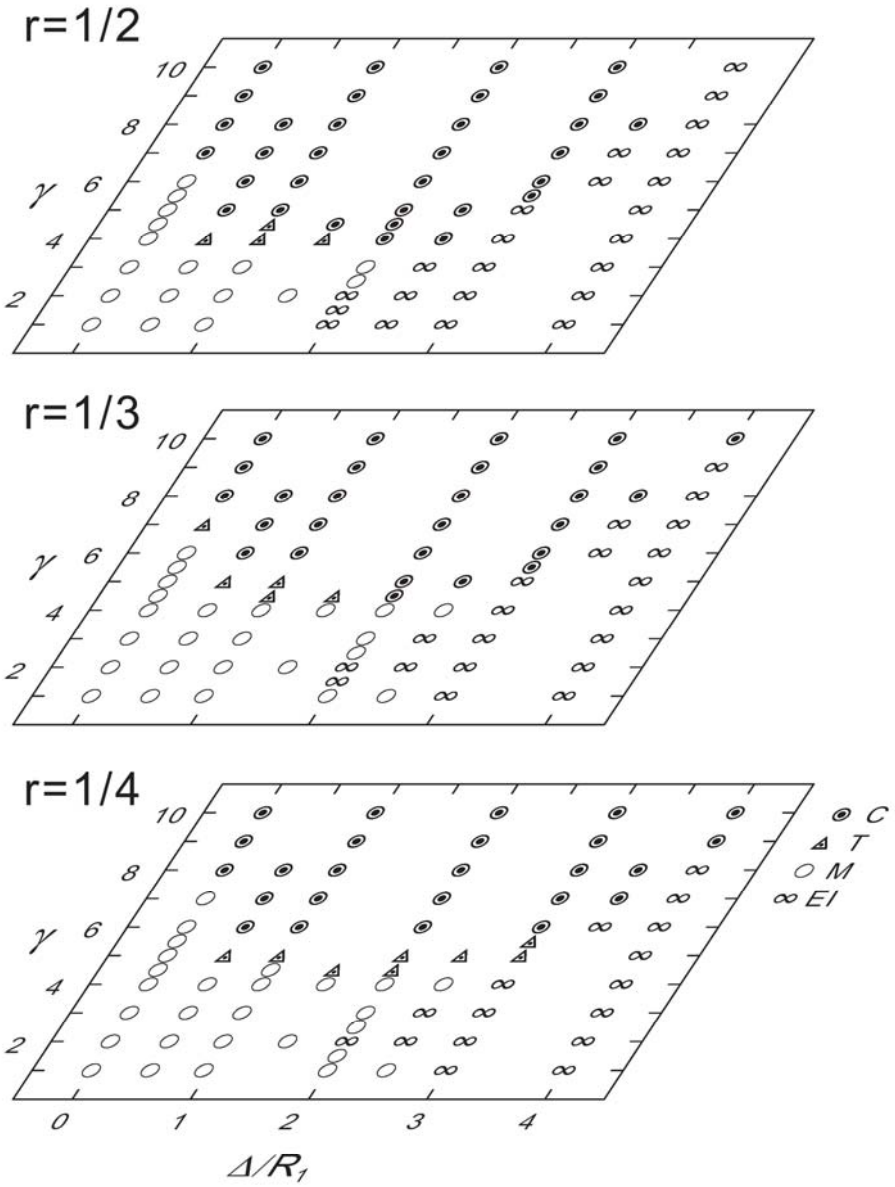


Fig 10. Summary of numerical experiments with the parameters of the vorticity strength ratio ( γ ), the dimensionless gap $\Delta/R_1$, and the vortex radius ratio r. We have classified the resulting structures into the C (concentric), T (tripole), M (complete or partial merger), and EI (elastic interaction) regimes.

2003-09W
IMBUDO

072012Z-130kts
**0720-0942Z**

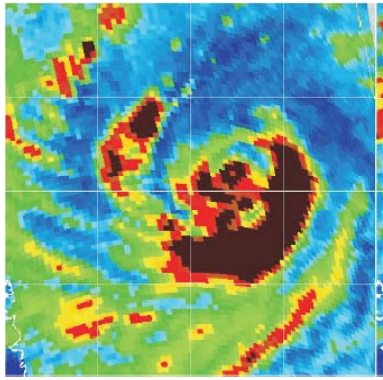

072012Z-130kts
**0720-1244Z**

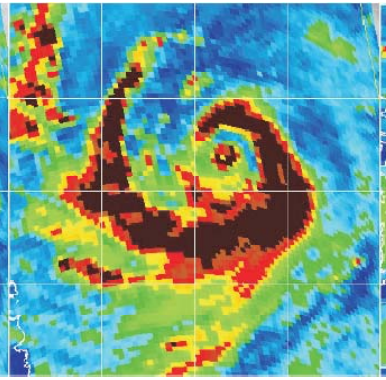

072100Z-130kts
**0720-2219Z**

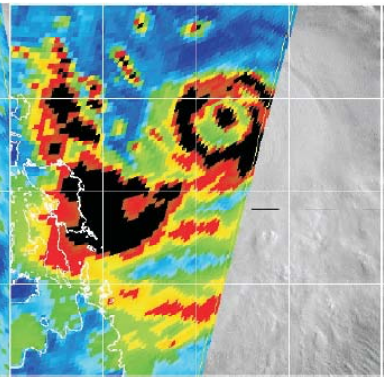

2003-14W
DUJUAN

083112Z-95kts
**0831-1214Z**

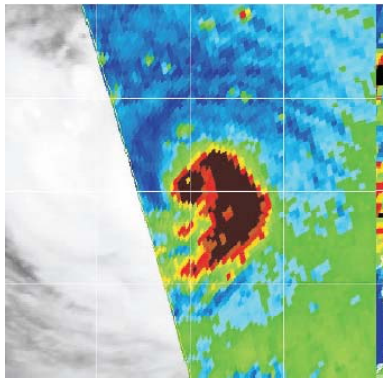

090100Z-120kts
**0831-2235Z**

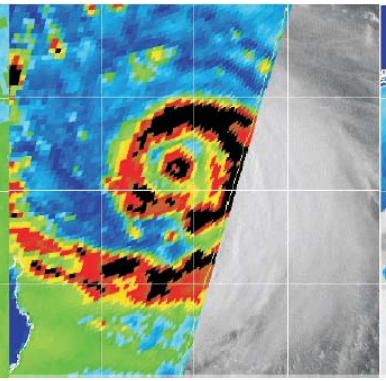

090112Z-125kts
**0901-0949Z**

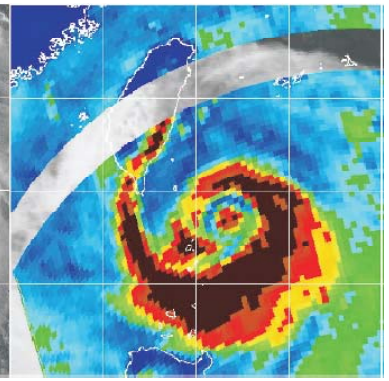

2003-15W
MAEMI

091000Z-150kts
**0909-2209Z**

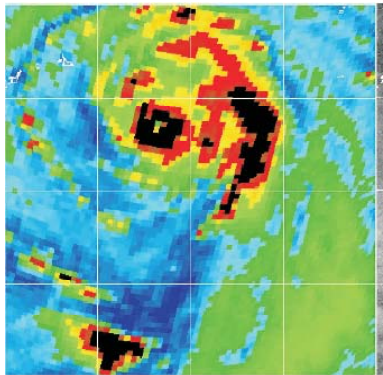

091000Z-150kts
**0909-2239Z**

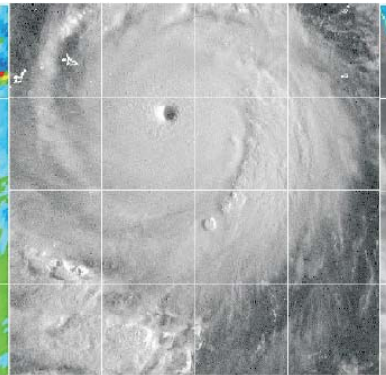

091012Z-150kts
**0910-0925Z**

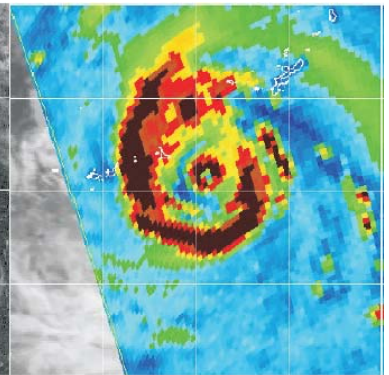

2004-09W
DIANMU

061800Z-120kts
**0618-0049Z**

061812Z-130kts
**0618-1202Z**

061900Z-120kts
**0619-0033Z**

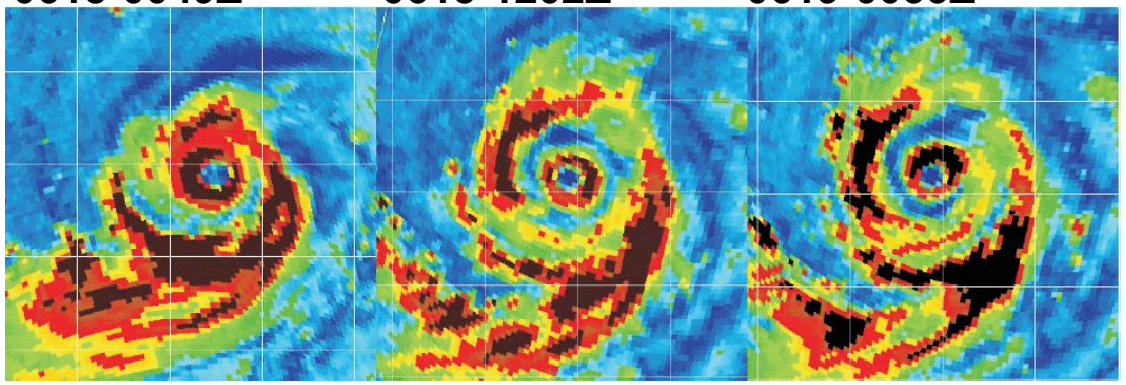

2003-20W
KETSANA

102100Z-95kts
**1020-2302Z**

102112Z-125kts
**1021-0954Z**

102112Z-125kts
**1021-1246Z**

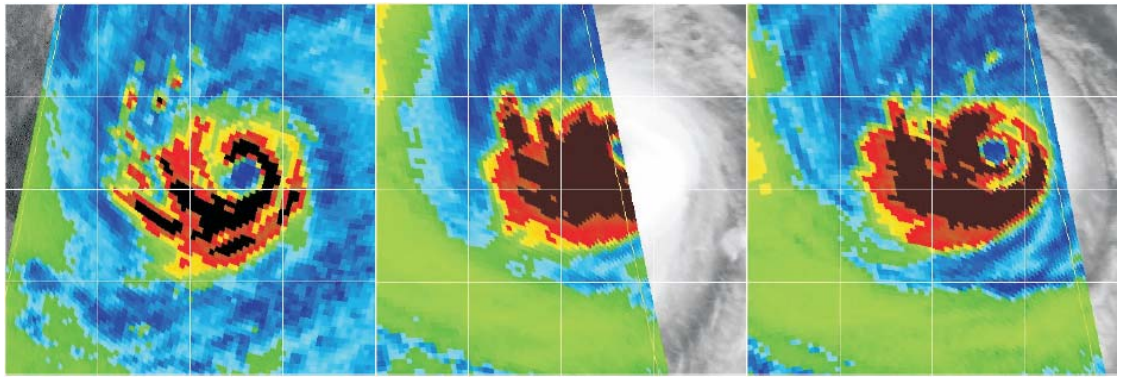

1997-14W
WINNIE

081412Z-110kts
**0814-1031Z**

081500Z-105kts
**0814-2316Z**

081600Z-85kts
**0816-0154Z**

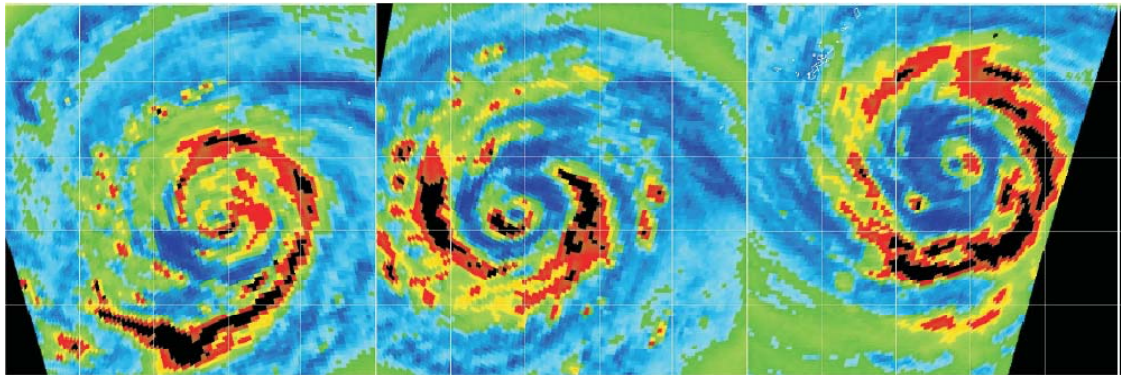

2000-18W
BILIS

082112Z-135kts
**0821-1214Z**

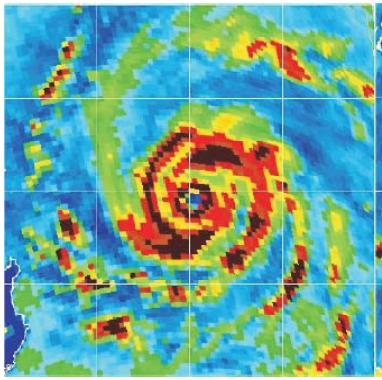

082200Z-140kts
**0821-2152Z**

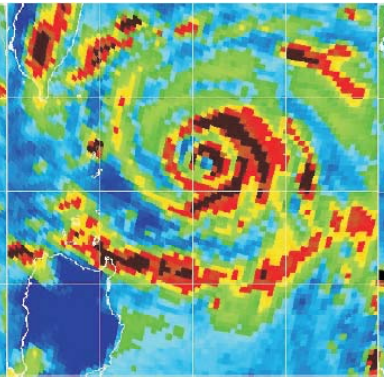

082200Z-140kts
**0822-0047Z**

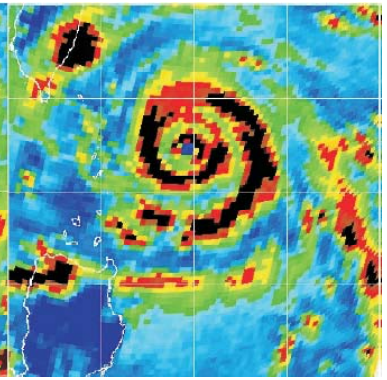

2000-22W
SAOMAI

091000Z-120kts
**0909-2109Z**

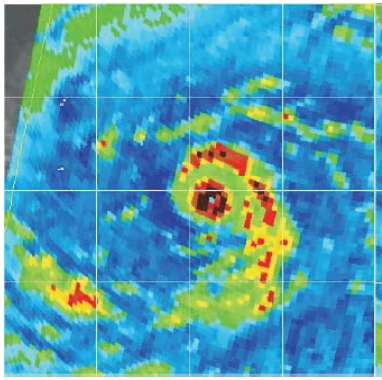

090100Z-120kts
**0831-2235Z**

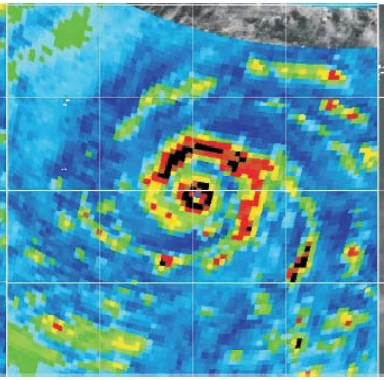

090112Z-125kts
**0901-0949Z**

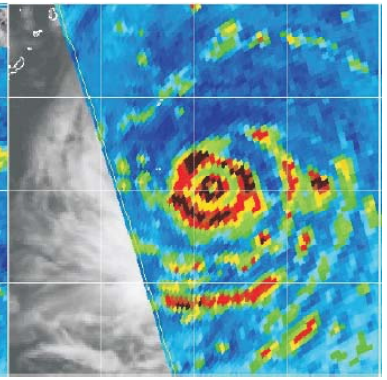

2001-26W
PODUL

102112Z-140kts
**1024-1049Z**

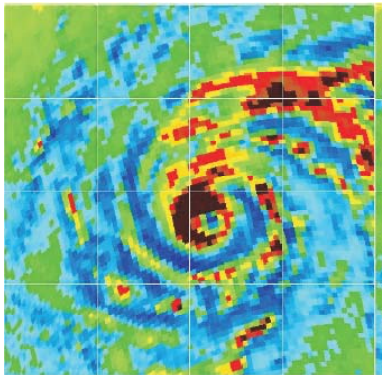

102500Z-130kts
**1024-2228Z**

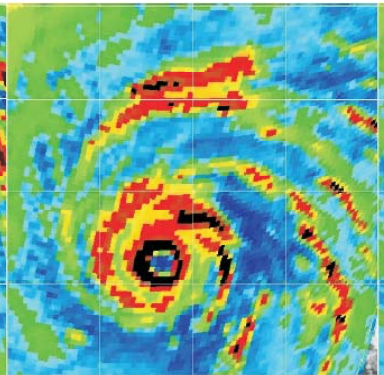

102500-130kts
**1024-2323Z**

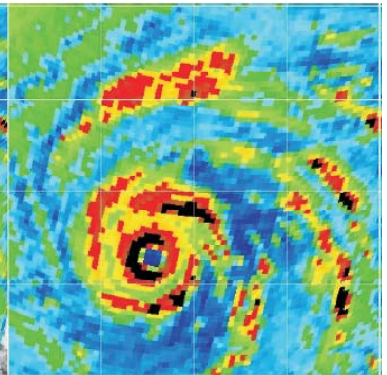

## Advective dynamics: Core structure important

TC structure is characterized by a relatively slow tangential wind decrease outside the radius of maximum wind (RMW) and a corresponding skirt of significant cyclonic relative vorticity.(Mallen et al. 2005)

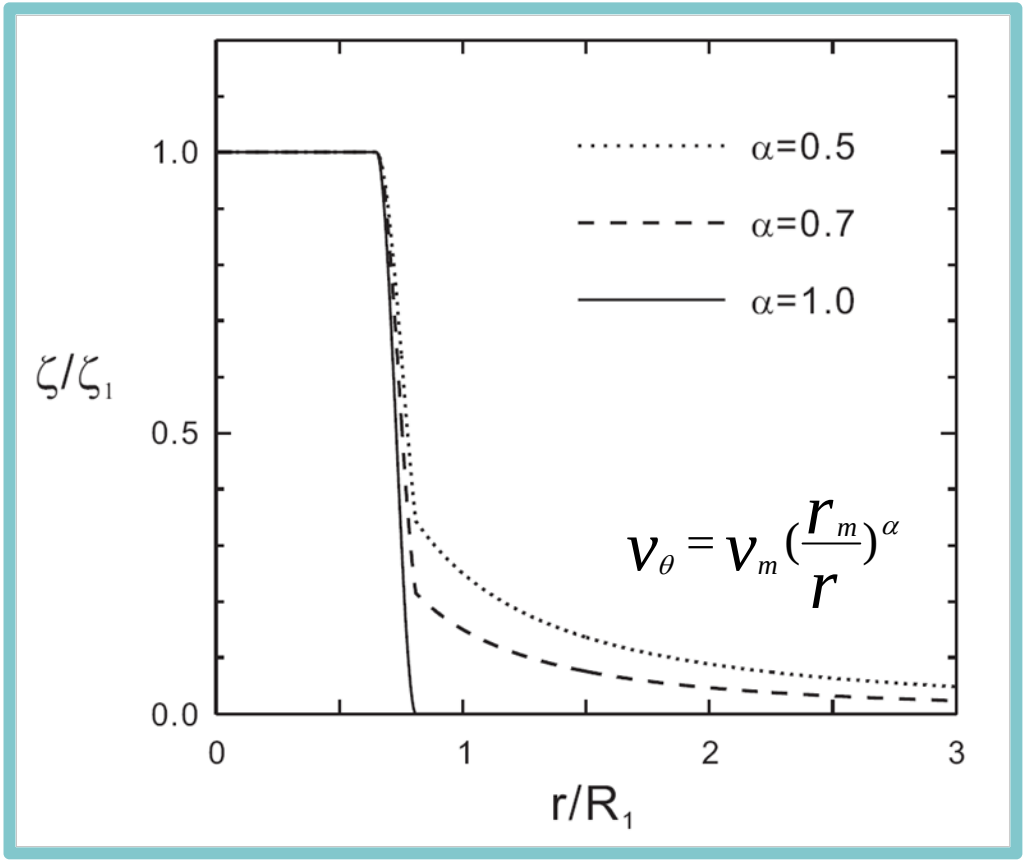


**Radial profiles of the vorticity for the strong core vortex**

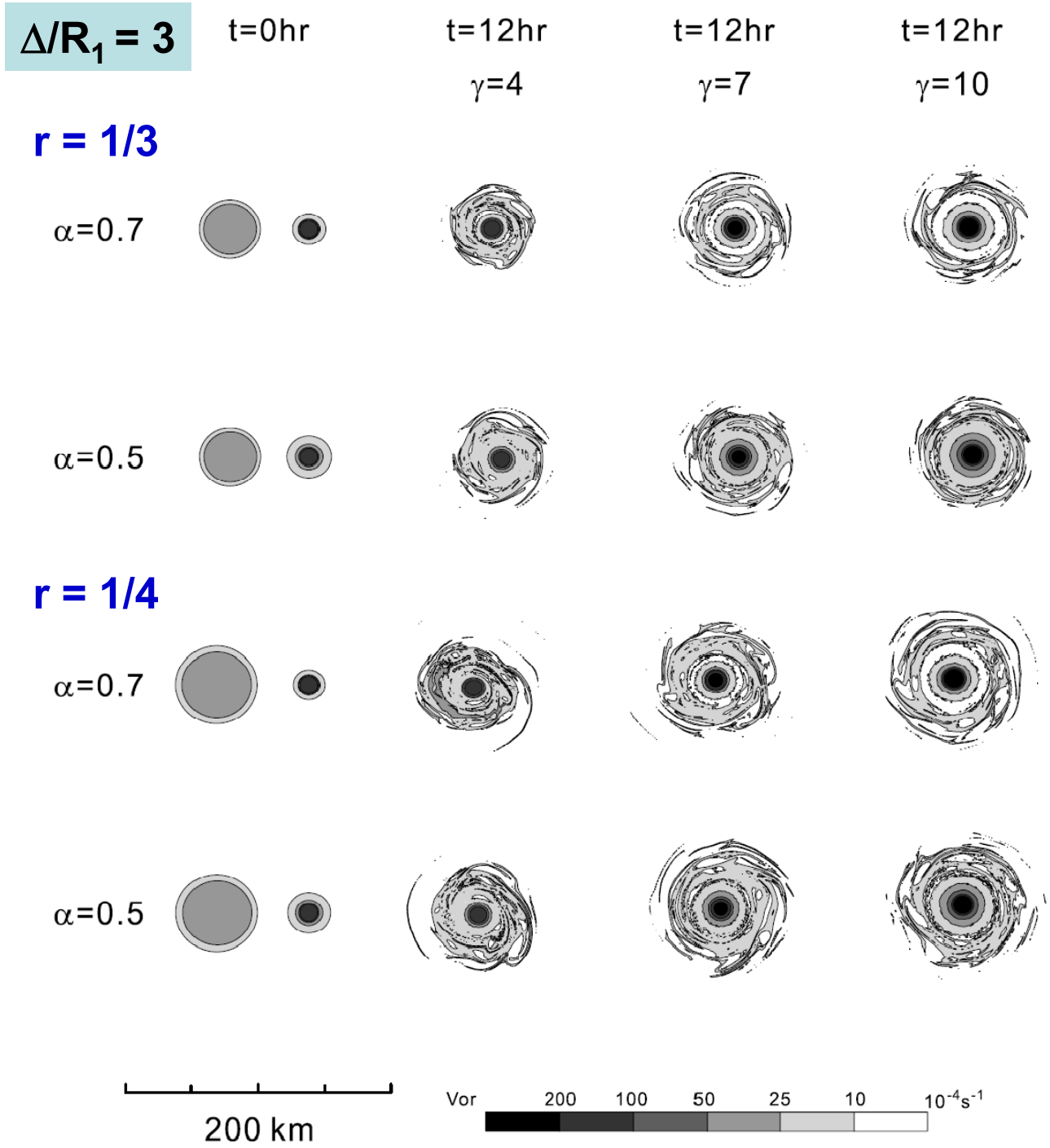
Δ/R1 = 3
t=0hr
t=12hr
γ=4
t=12hr
γ=7
t=12hr
γ=10
r = 1/3
α=0.7
α=0.5
r = 1/4
α=0.7
α=0.5
200 km
Vor
200
100
50
25
10
10-4s-1

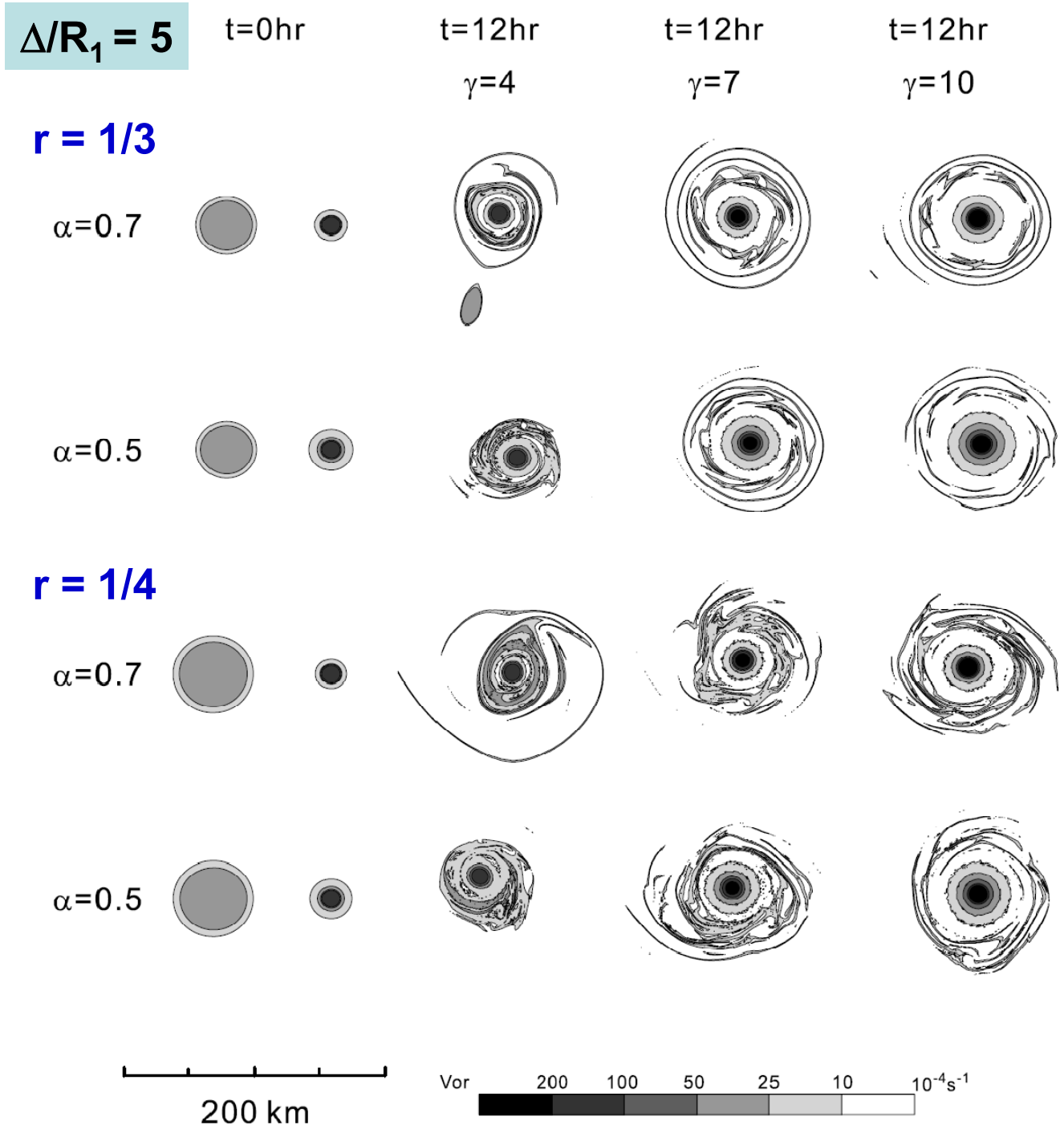
Δ/R1 = 5
t=0hr
t=12hr
γ=4
t=12hr
γ=7
t=12hr
γ=10
r = 1/3
α=0.7
α=0.5
r = 1/4
α=0.7
α=0.5
200 km
Vor
200
100
50
25
10
10-4s-1

**Examples of the vorticity field at hour 12, showing different classifications of binary vortex interactions involving a skirted core vortex.**

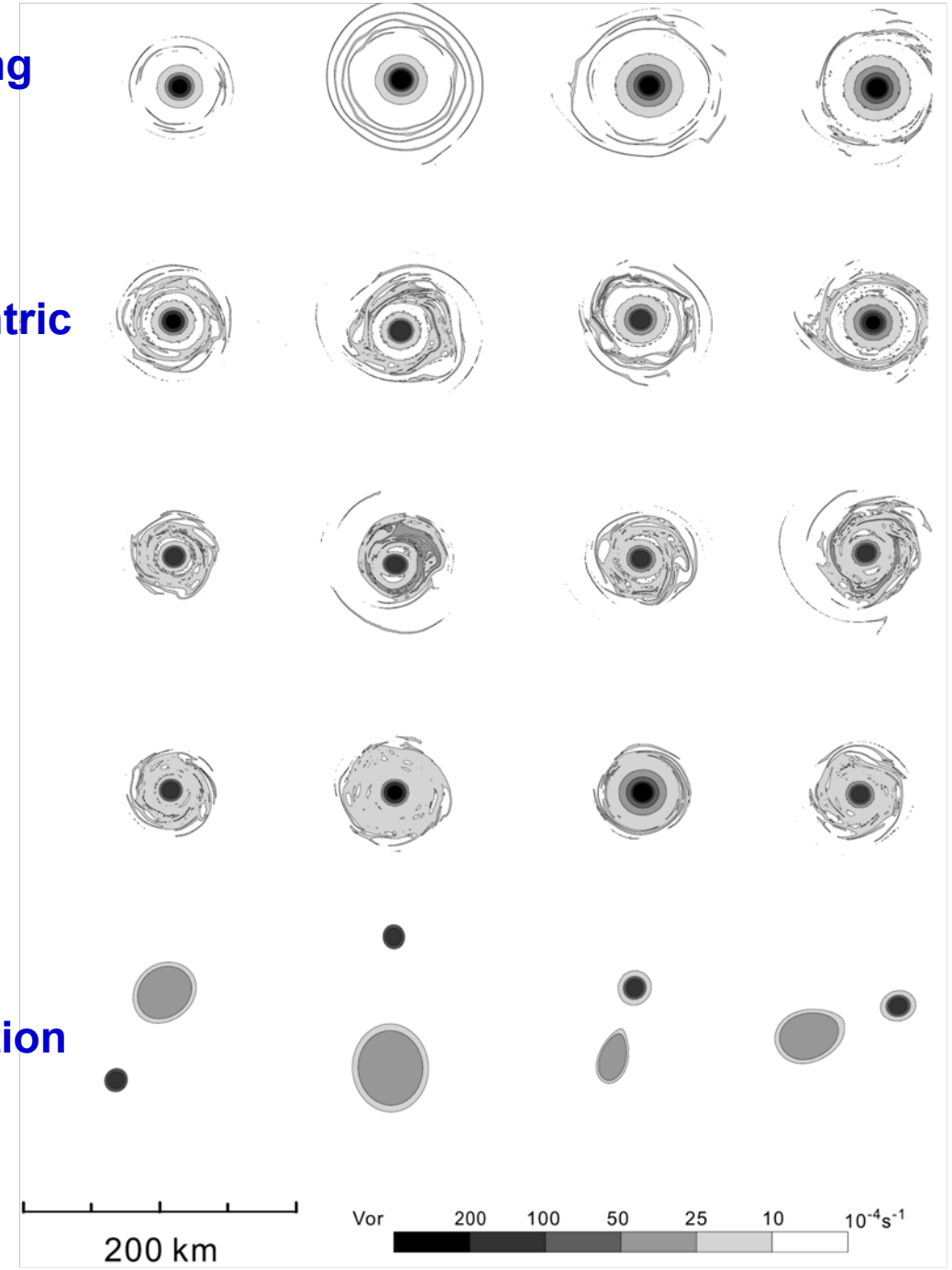

$\alpha = 0.7 \quad \gamma = 7 \quad r = 1/4 \quad \Delta/R_1 = 5$

**The formation of concentric eyewalls**

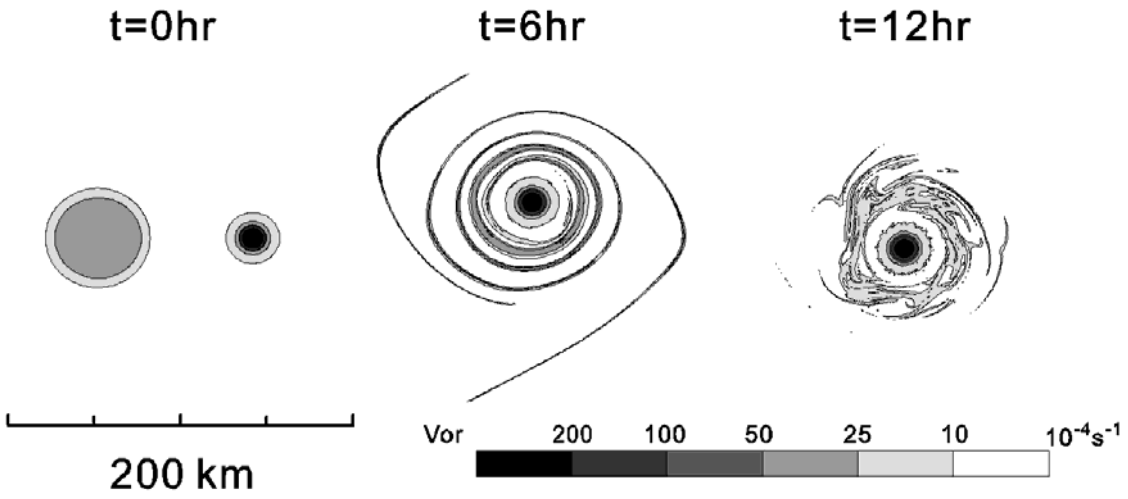


**The contraction of the secondary wind maximum by nonlinear advection dynamics.**

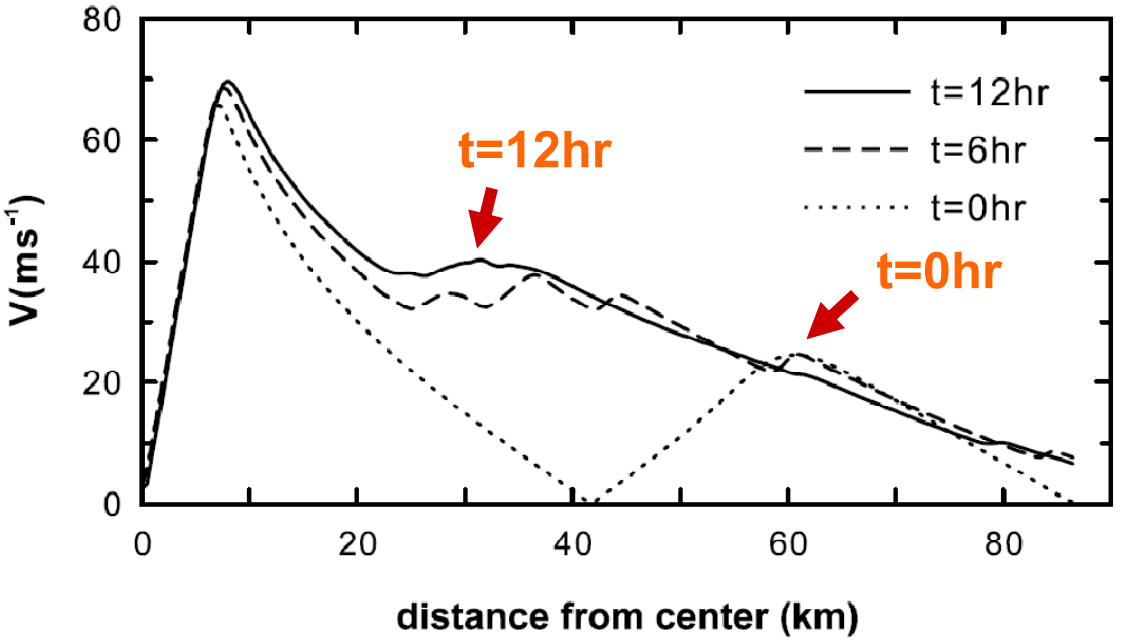

# Binary vortex interaction

**Dritschel and Waugh (1992)**

【Variables】

$R_1, R_2$

$\Delta$

$\zeta$

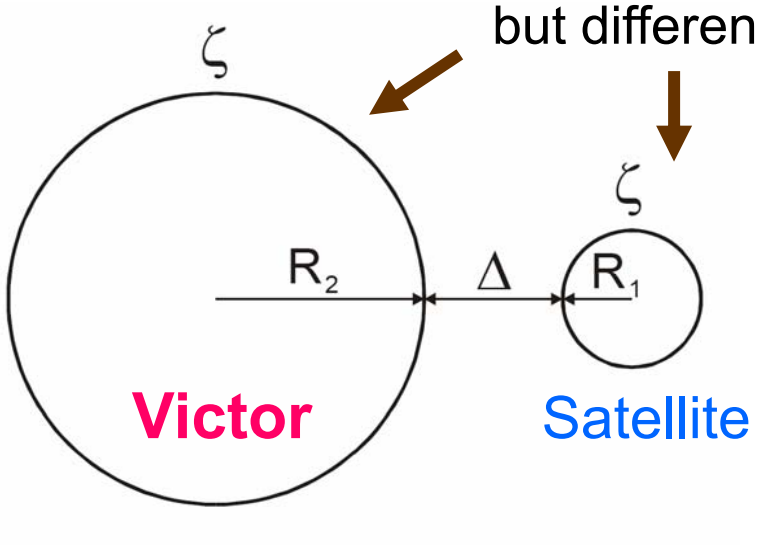


【Parameters】

- Vortex radius ratio $(r) = \dfrac{R_1}{R_2}$
- Dimensionl ess gap $(\dfrac{\Delta}{R_1})$

【Conclusion】

- Elastic Interaction (EI)
- Partial straining-out (PSO)
- Complete straining-out (CSO)
- Partial merger (PM)
- Complete merger (CM)

# Binary vortex interaction

Kuo et al. (2004)

【Variables】

$$R_1, R_2; \Delta; \zeta_1, \zeta_2$$

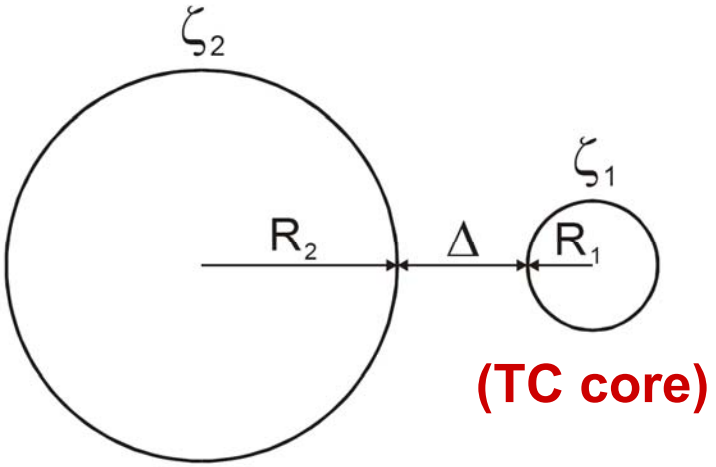


【Parameters】

- Vortex radius ratio $(r) = \dfrac{R_1}{R_2}$
- Dimensionl ess gap $(\dfrac{\Delta}{R_1})$
- Vortex strength ratio $(\gamma) = \dfrac{\zeta_1}{\zeta_2}$

- **An extension of Dritschel and Waugh's (1992) work.**
- **In addition to the radii ratio and the normalized distance between the two vortices, the vorticity ratio is added as a third external parameters.**

**Dritschel and Waugh (1992)**

$$R_1,\ R_2,\ \Delta,\ \zeta$$

$$r = \frac{R_1}{R_2},\ \Delta/R_1$$

**Kuo et al. (2004)**

$$R_1,\ R_2,\ \Delta,\ \zeta_1,\ \zeta_2$$

$$r = \frac{R_1}{R_2},\ \Delta/R_1,\ \gamma = \frac{\zeta_1}{\zeta_2}$$

**Kuo et al. (2006)**

$$R_1,\ R_2,\ \Delta,\ \zeta_1,\ \zeta_2,\ \alpha$$

$$r = \frac{R_1}{R_2},\ \Delta/R_1,\ \gamma = \frac{\zeta_1}{\zeta_2},\ \alpha$$

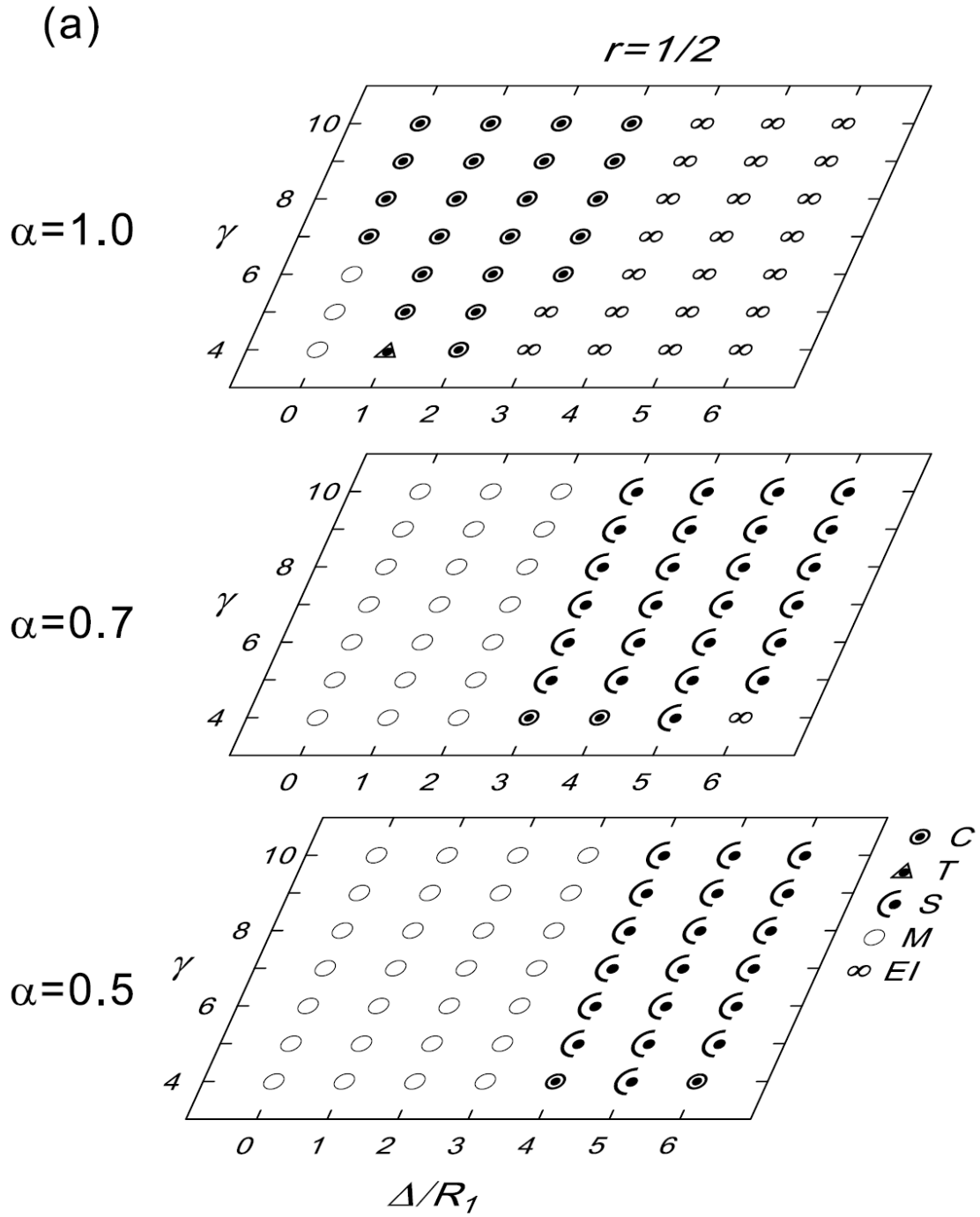
(a)
r=1/2
α=1.0
α=0.7
α=0.5
γ
10
8
6
4
0
1
2
3
4
5
6
∞
C
T
S
M
∞ EI
Δ/R1

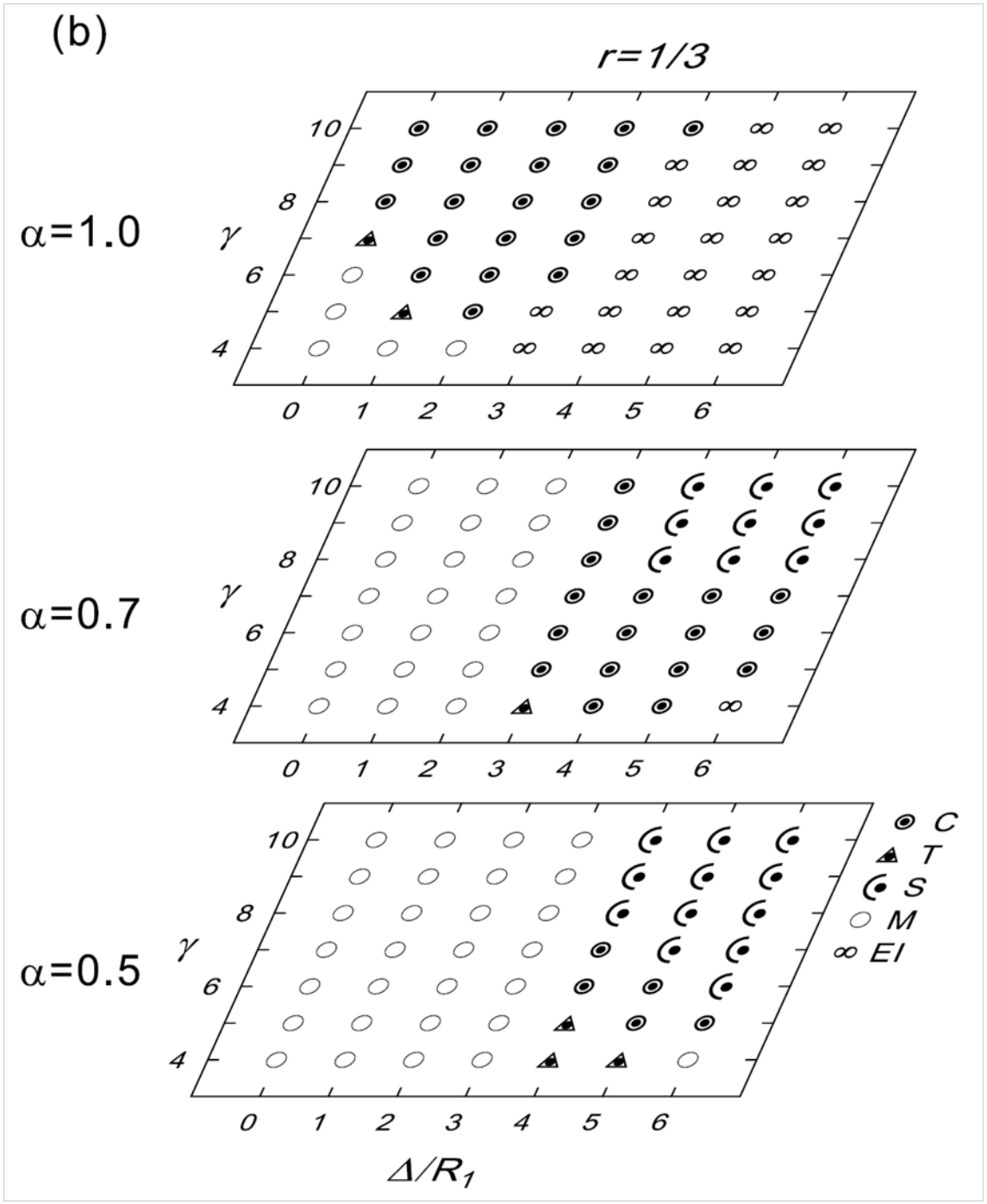
(b)
r=1/3
α=1.0
α=0.7
α=0.5
γ
10
8
6
4
0
1
2
3
4
5
6
∞
C
T
S
M
∞ EI
Δ/R1

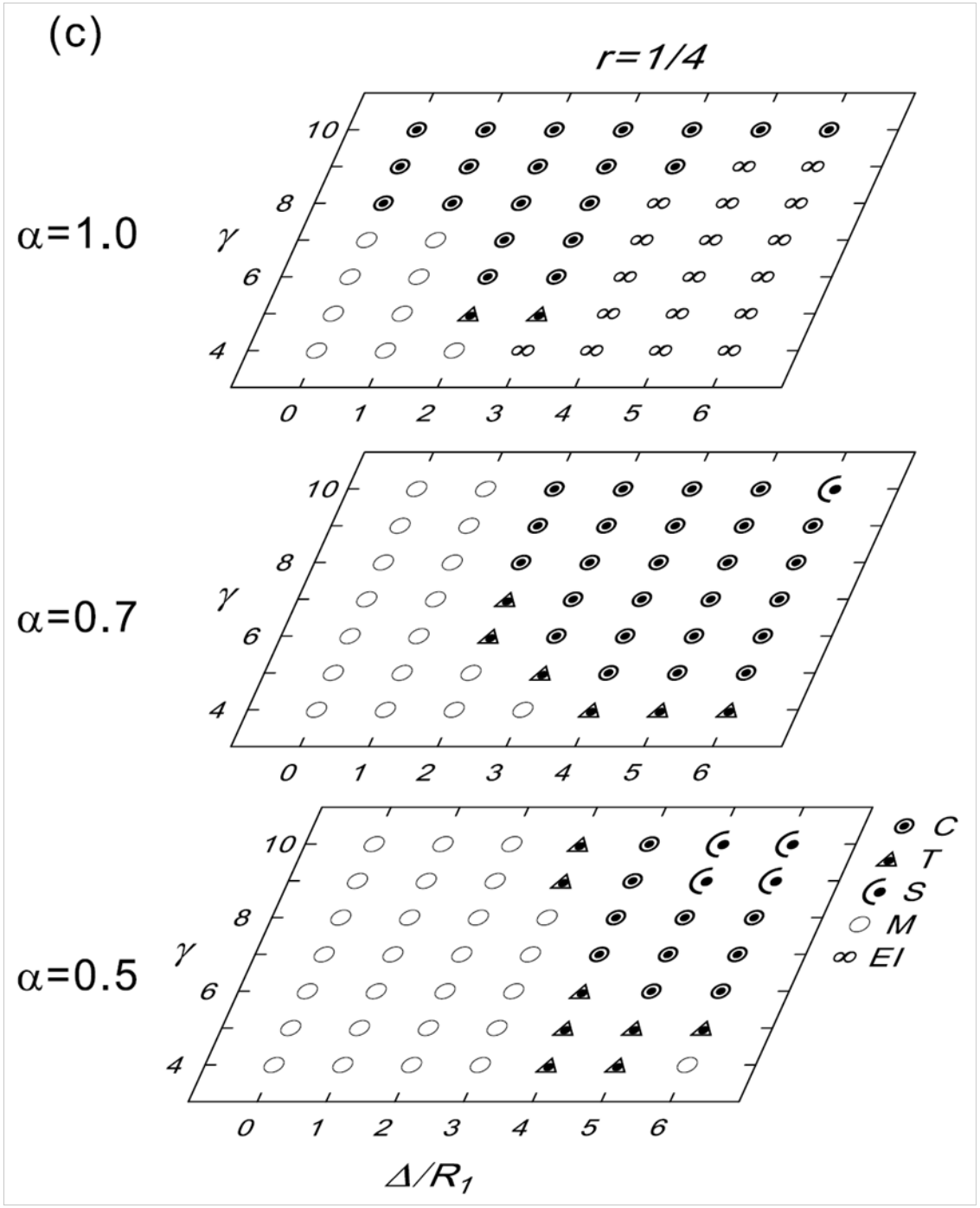
(c)
r=1/4
α=1.0
α=0.7
α=0.5
γ
10
8
6
4
0
1
2
3
4
5
6
∞
C
T
S
M
EI
Δ/R1

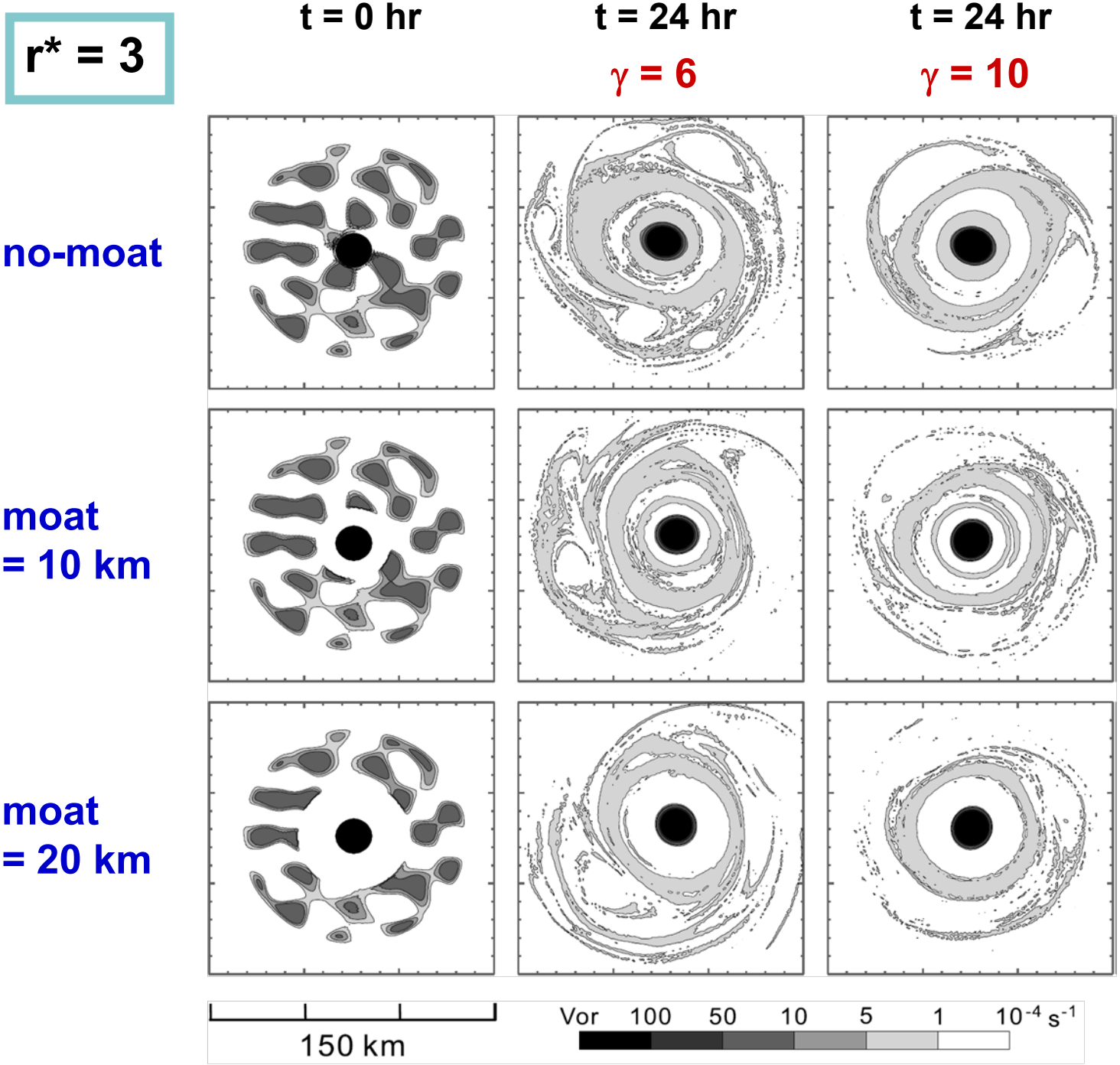
r* = 3
t = 0 hr
t = 24 hr
γ = 6
t = 24 hr
γ = 10
no-moat
moat
= 10 km
moat
= 20 km
150 km
Vor 100 50 10 5 1 10-4 s-1

# Hurricane Juliette (2001)

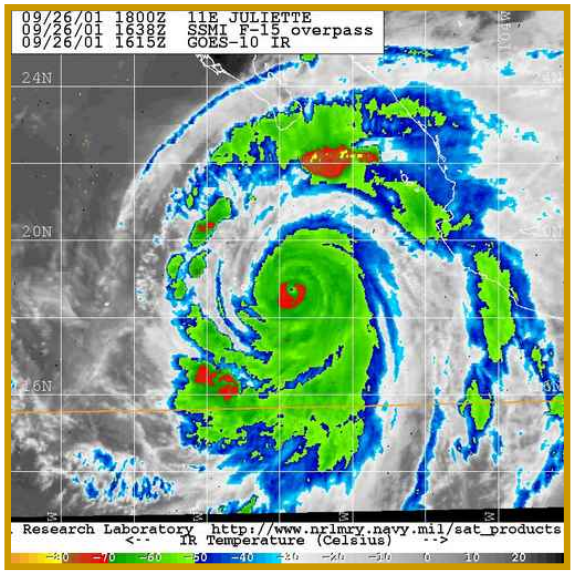


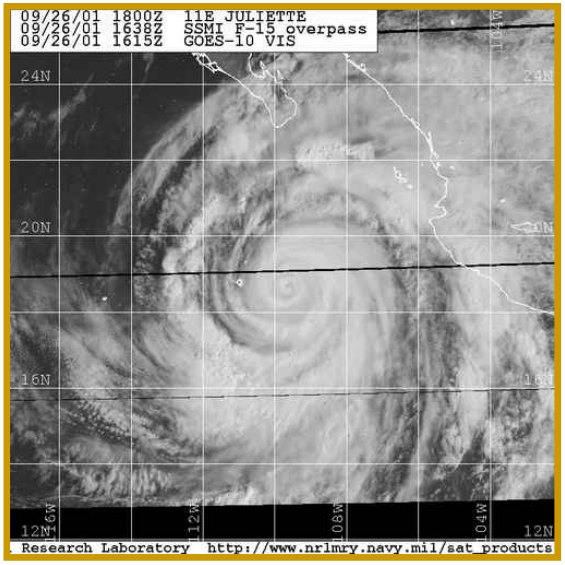


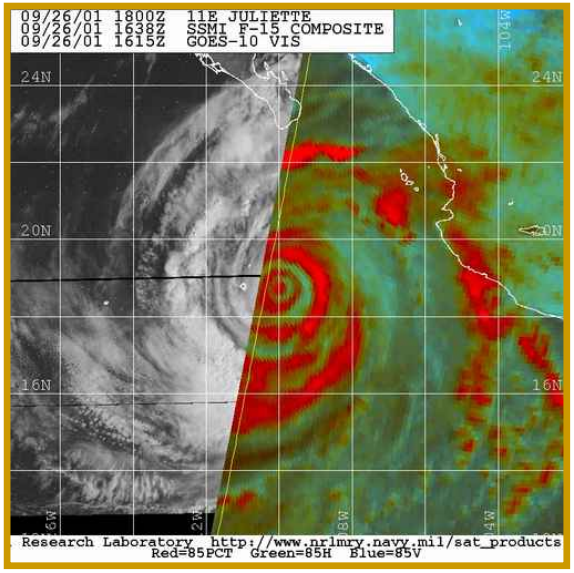


"the crew found three concentirc eyewalls, defined by three peaks in tangential wind in each of the radial legs and by three complete rings of enhanced radar reflectivity with radii of 11, 56, and 90 km."

*McNoldy (2004)*

## Observation

## Juliette (2001)

### 0112Z

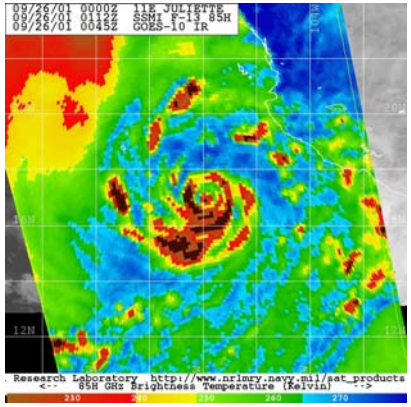

### 0405Z

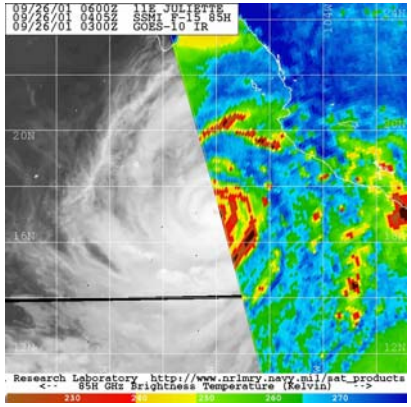

### 1346Z

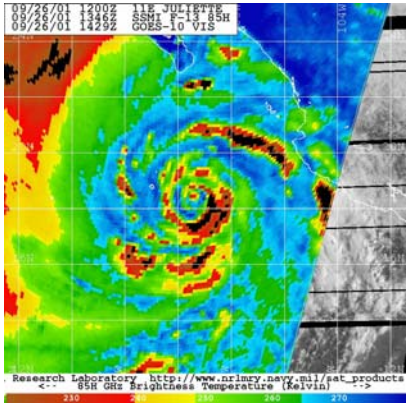

### 1638Z

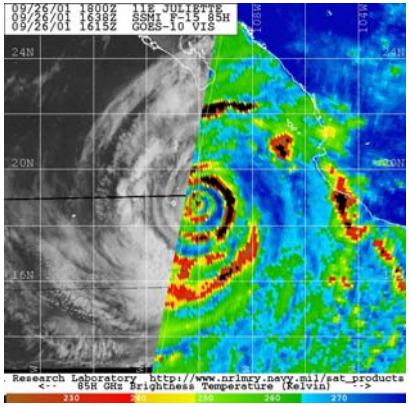

## Simulation

### t=0hr

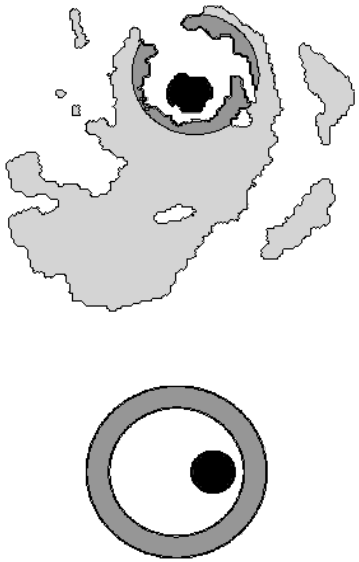

### t=3hr

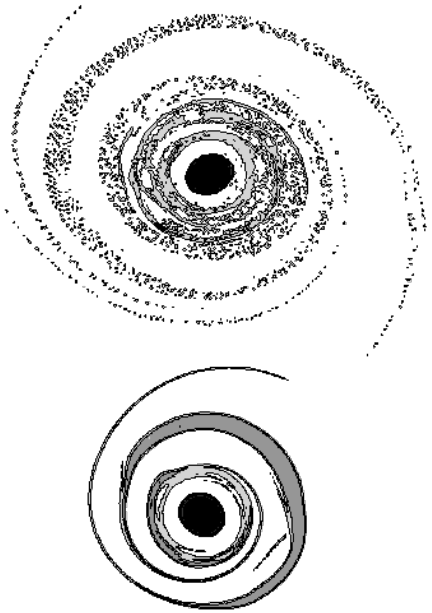

### t=12hr

### t=15hr

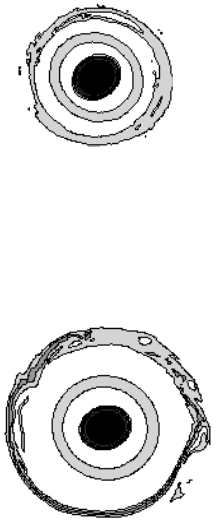

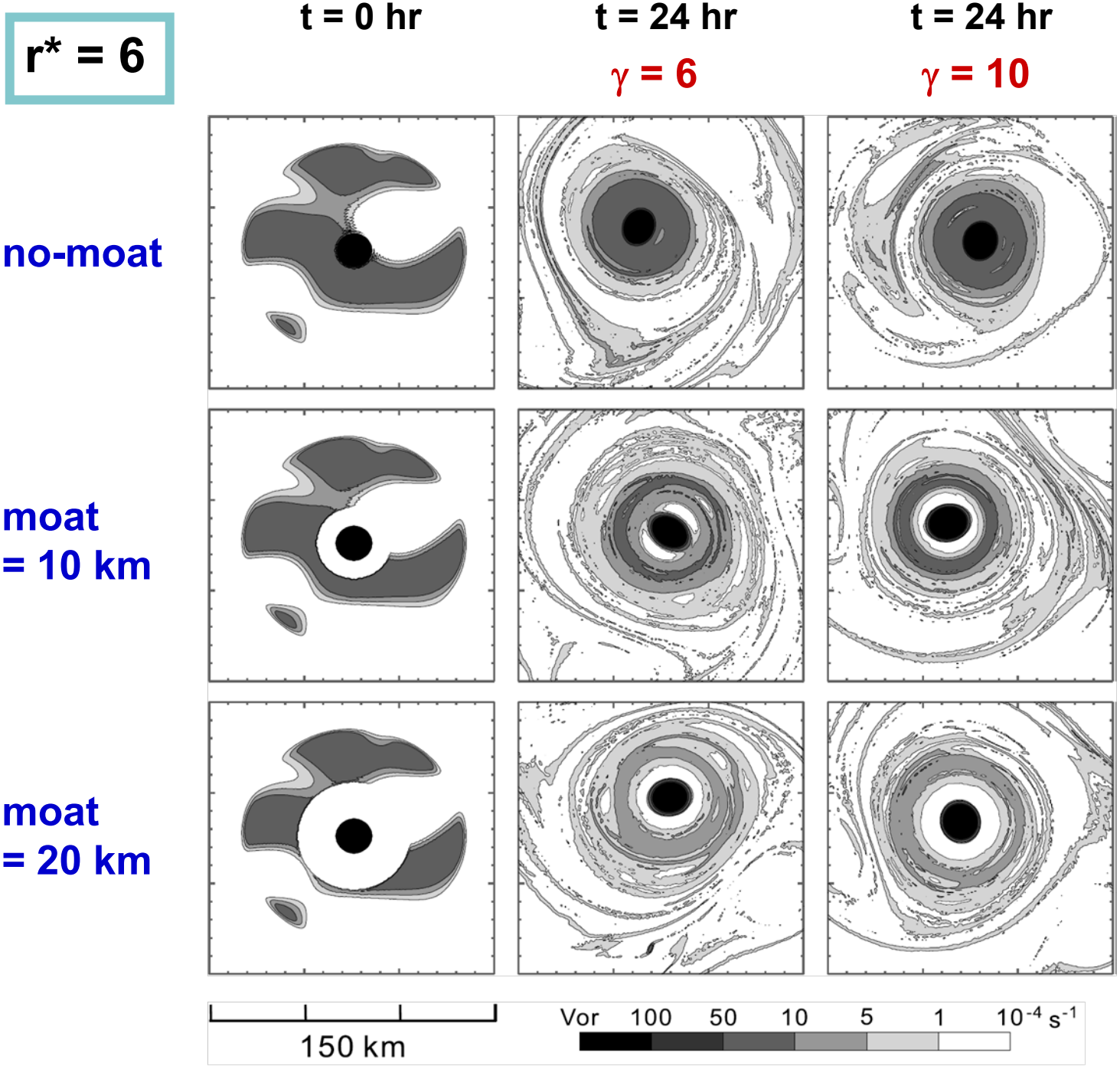
r* = 6
t = 0 hr
t = 24 hr
γ = 6
t = 24 hr
γ = 10
no-moat
moat
= 10 km
moat
= 20 km
150 km
Vor 100 50 10 5 1 10-4 s-1

**r* = 4**

| t = 0 hr | t = 24 hr<br>γ = 6 | t = 24 hr<br>γ = 10 |
|---|---|---|

**Isotropic distribution**

**Anisotropic distribution**

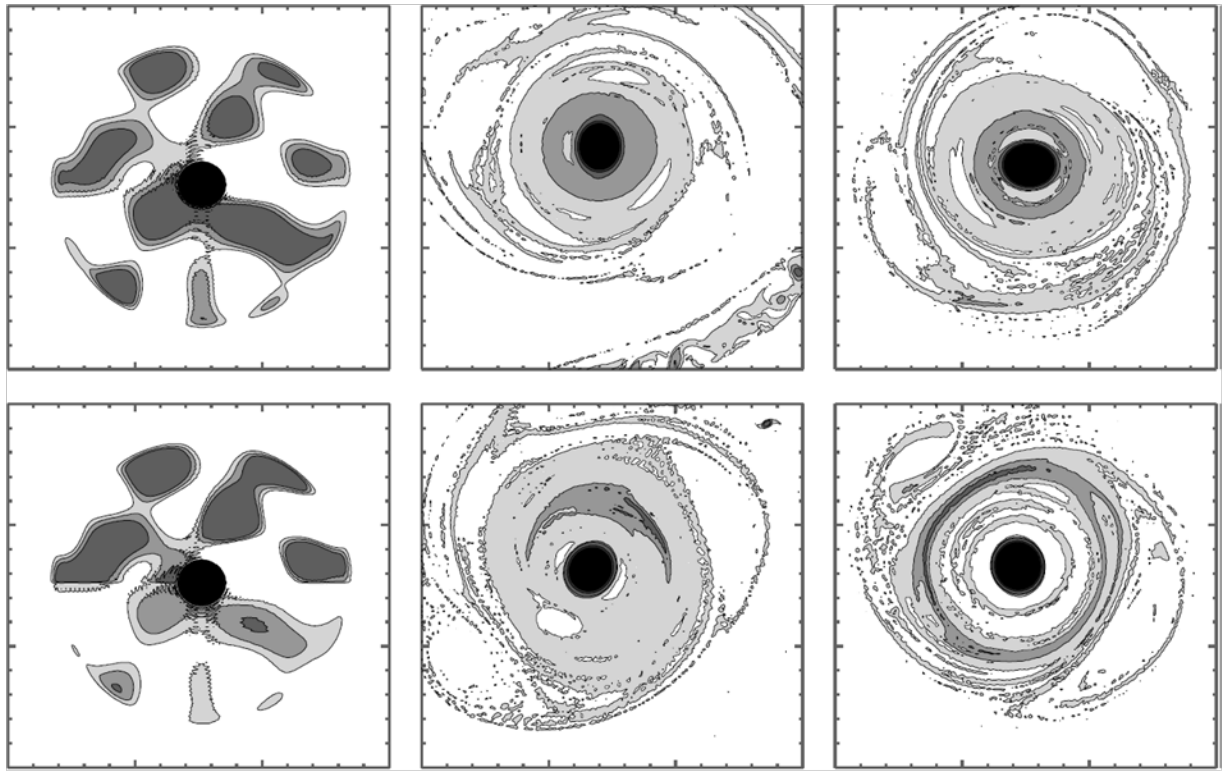

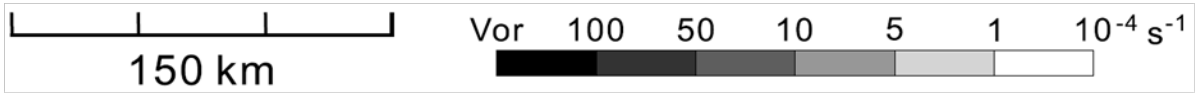

# Weiss(1981,1991), Rozoff et al. (2006)

$$\frac{D}{Dt}(\nabla\zeta) = -J(\nabla\psi, \zeta)$$

$$\rightarrow \nabla\zeta(t) \propto \exp(\lambda t) \quad \lambda = \pm\frac{1}{2}\sqrt{Q} = \pm\frac{1}{2}\sqrt{S_1{}^2 + S_2{}^2 - \zeta^2}$$

$$S_1 = \frac{\partial u}{\partial x} - \frac{\partial v}{\partial y} \text{ (stretch deformatio n)}$$

$$S_2 = \frac{\partial v}{\partial x} + \frac{\partial u}{\partial y} \text{ (shear deformatio n)}$$

Q > 0 (strain dominates)

→vorticity gradient will be stretched

Q < 0 (vorticity dominates)

→vortex is stable (survival of eyewall meso-vortices)

**Rozoff et al. (2006)**

**The strong differential rotation outside the radius of maximum wind of the core vortex may also contribute to the formation and maintenance of the moat.**

**The Rapid Filamentation Zone: A zone with the filamentation time smaller than the 30 min convective turnover time.**

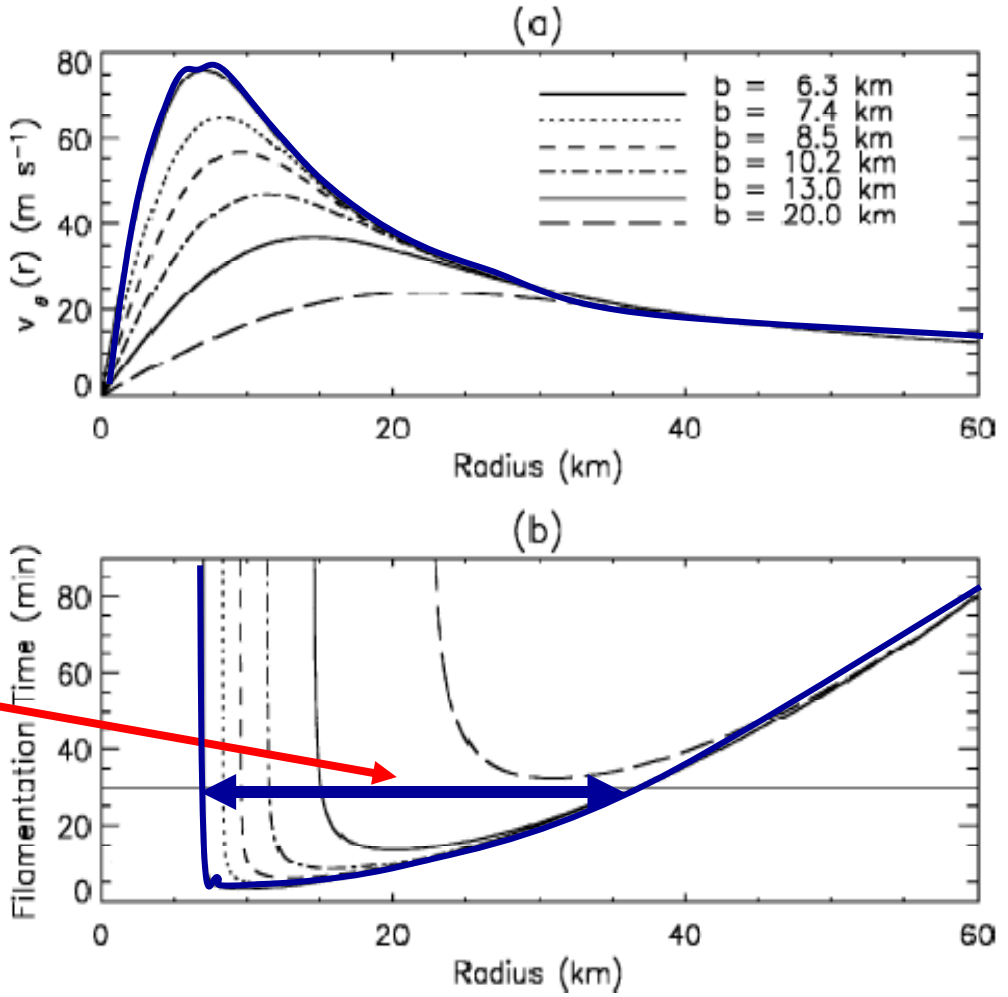


FIG. 2. (a) Radial profiles of $v_\theta$ $(r)$ as given by (15) for six different values of the parameter $b$. (b) Corresponding radial profiles of $\tau_{fil}(r)$ as given by (16). The filamentation times $\tau_{fil}(r)$ are plotted only in the strain-dominated regions, where $S_1^2 + S_2^2 - \zeta^2 > 0$.

# Moat size ($r_0$) estimated from filamentation time

$$\tau_{fil} = 2 \Big/ \sqrt{\left(\frac{\partial v_\theta}{\partial r} - \frac{v_\theta}{r}\right)^2 - \left(\frac{\partial v_\theta}{\partial r} + \frac{v_\theta}{r}\right)^2}$$

$$\tau_{fil} = \frac{r}{v_\theta \sqrt{\alpha}} = \frac{2}{\zeta}\left(\frac{r}{r_m}\right)^{\alpha+1} \alpha^{-\frac{1}{2}} = \tau_0$$

$$\frac{r}{r_m} = \left(\frac{\zeta}{2}\tau_0 \alpha^{\frac{1}{2}}\right)^{\frac{1}{\alpha+1}}$$

$$r_0 = r - r_m = \left(\frac{\zeta}{2}\tau_0 \alpha^{\frac{1}{2}}\right)^{\frac{1}{\alpha+1}} r_m - r_m$$

$v_m$ : best track data

$r_m$ : inner eyewall radius

$$v_\theta = v_m \left(\frac{r_m}{r}\right)^\alpha$$

$$\zeta = 2\frac{v_m}{r_m}$$

$$\tau_0 = 30 \text{ min}$$

Kuo et al. 2006

# Nondimensional moat size v.s. nondimensional filamentation moat size

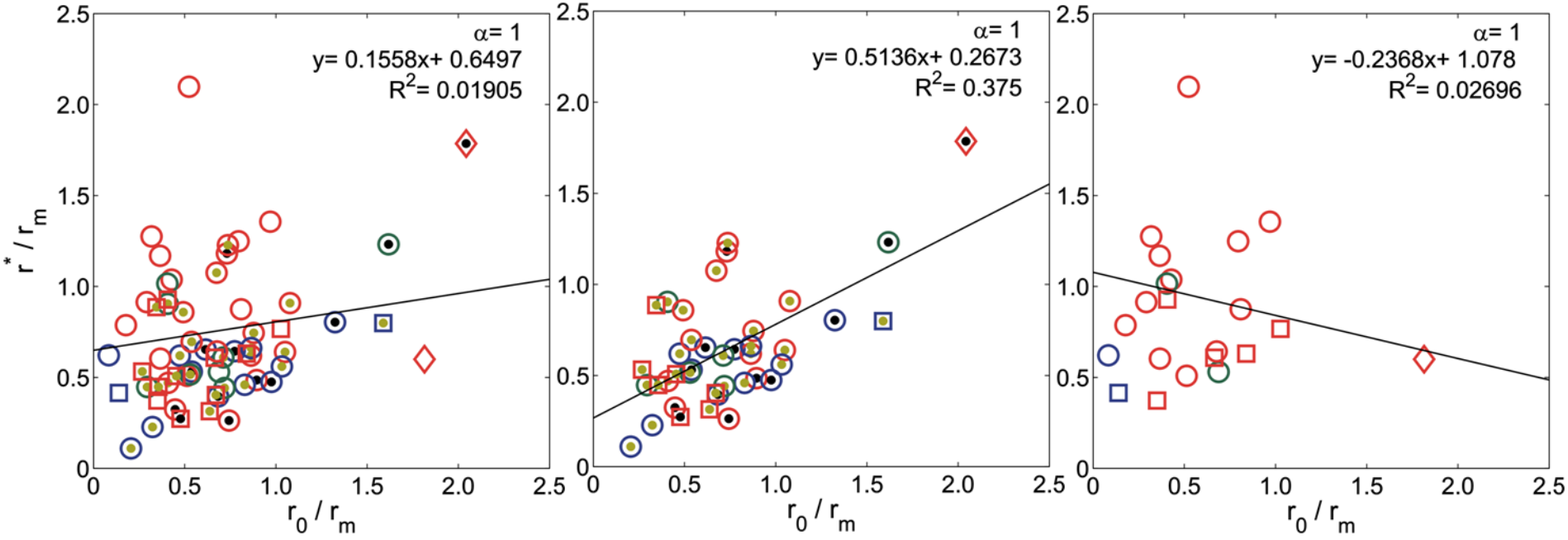


Category 5
Category 4

Apr, May, Jun
Jul, Aug, Sep
Oct, Nov, Dec

# Summary

- As revealed by microwave imaginary, tropical cyclones of sufficient strength (e.g. sustained wind speed $\geq$ 120 kts) often form concentric or double eyewalls. Area of asymmetric convection outside the core vortex that wraps around the inner eyewall to form the concentric eyewalls in about 12 hours.

- The outer eyewalls usually constricts the inflow of moisture, mass, and momentum into the inner eyewalls and the inner eyewall weakens and/or die.

- A new dimension is added to the Dritschel-Waugh binary vortex interaction scheme that provides a proper concentric vorticity structure, the tripole vortex strucuture and the multiple eyewalls structure. Two important parameters are the vorticity strength ratio and the skirt parameters.

- The contraction of the secondary wind maximum and the formation of the moat are features of the vorticity dynamics. The moat formation by subsidence, rapid filamentation, and advective dynamics.

- Concentric vorticity structure formation reuqires a core vortex that is of 4 to 6 times stronger than the outer vortex. The outer vortex is larger than the core and with a separation distance from the core vortex that is within 6 times the core vortex radius. The vortex with (without) skirts allows the formation of outer band at large (small) radii.

- The pivotal role of the vorticity strength of the core vortex in maintaining itself, and in strectching, organizing and stabilizing the outer vorticity field, and the shielding effect of the moat to prevent further merger and enstrophy cascade processes in concentric eyewall dynamics.

- Formation of concentric eyewalls is important for the TC intensity problem. A self-limiting process for TC intensity. A natural “STORMFURY”.**!!**

- The organizational aspects of outer eyewall formation from an asymmetric vorticity field outside the cyclone core. The importance of core vortex structure, the moat, and the spatial characteristics of the vorticity field outside the core in the formation of double eyewalls.

- Need to understand the vorticity generating meso-scale processes in the TC environment.

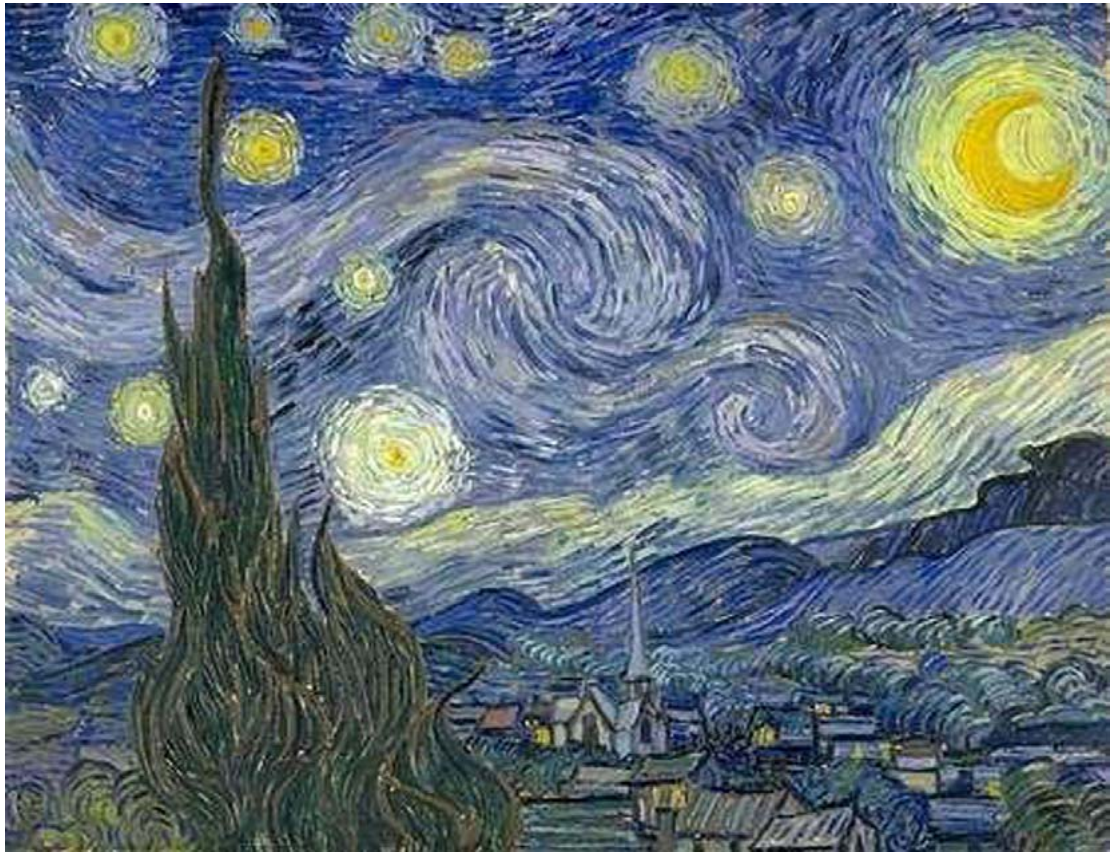

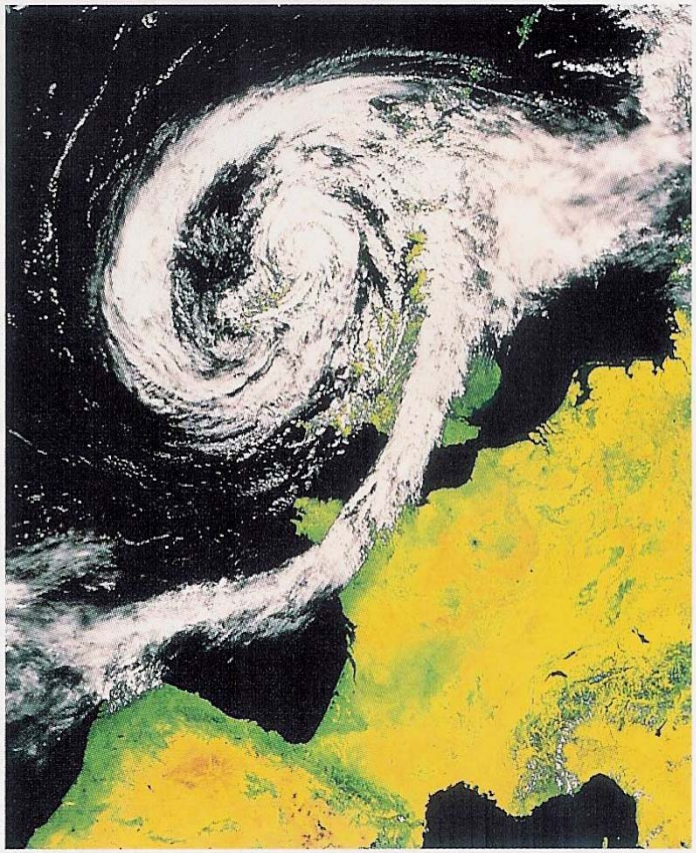

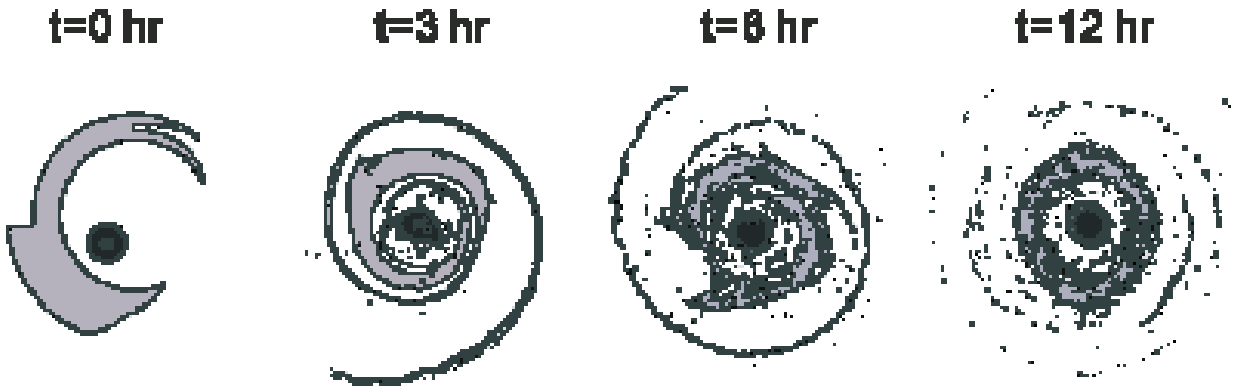
t=0 hr
t=3 hr
t=6 hr
t=12 hr

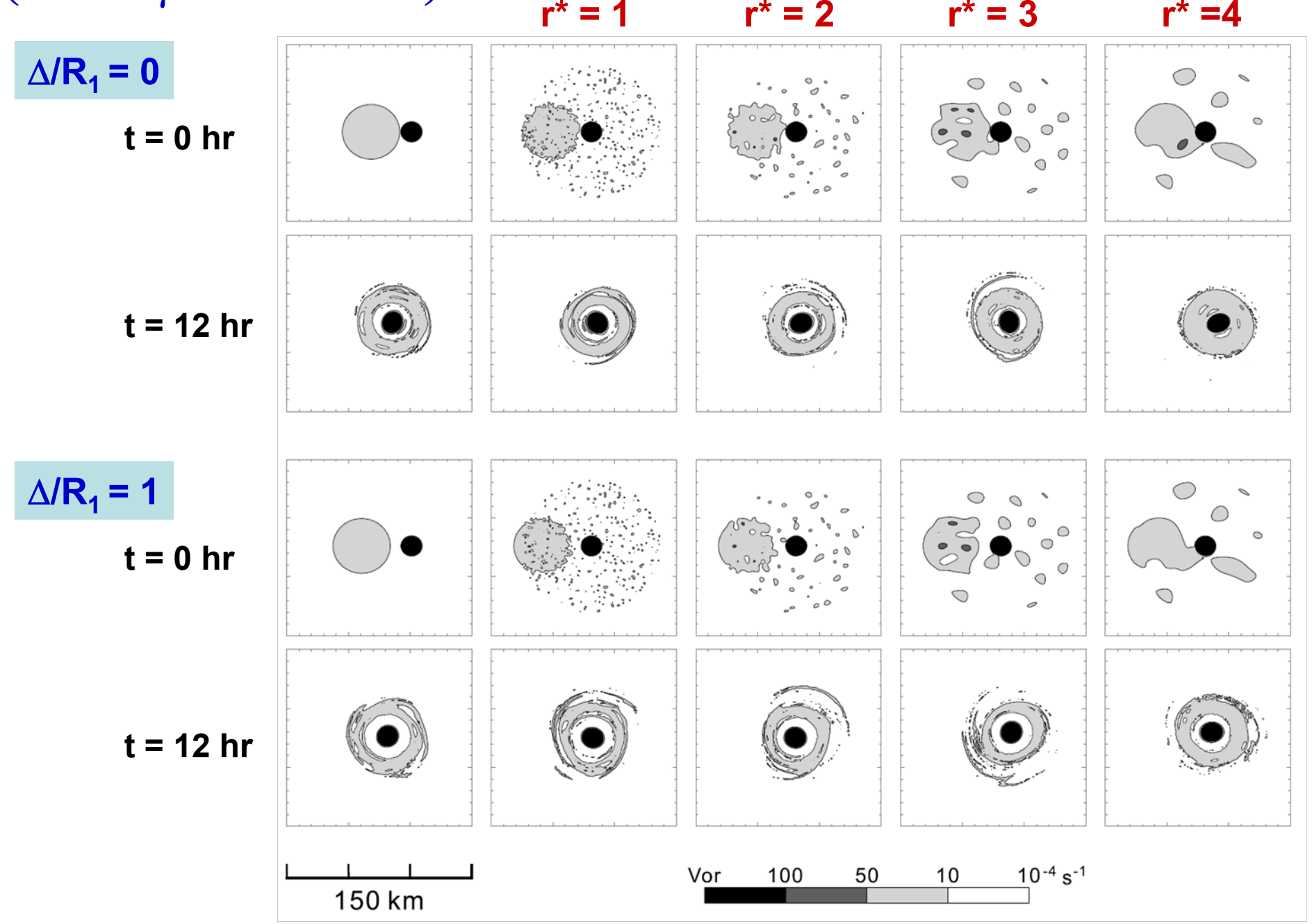
(α = 1 γ = 10 r = 1/3)
r* = 1
r* = 2
r* = 3
r* =4
Δ/R1 = 0
t = 0 hr
t = 12 hr
Δ/R1 = 1
t = 0 hr
t = 12 hr
150 km
Vor 100 50 10 10-4 s-1

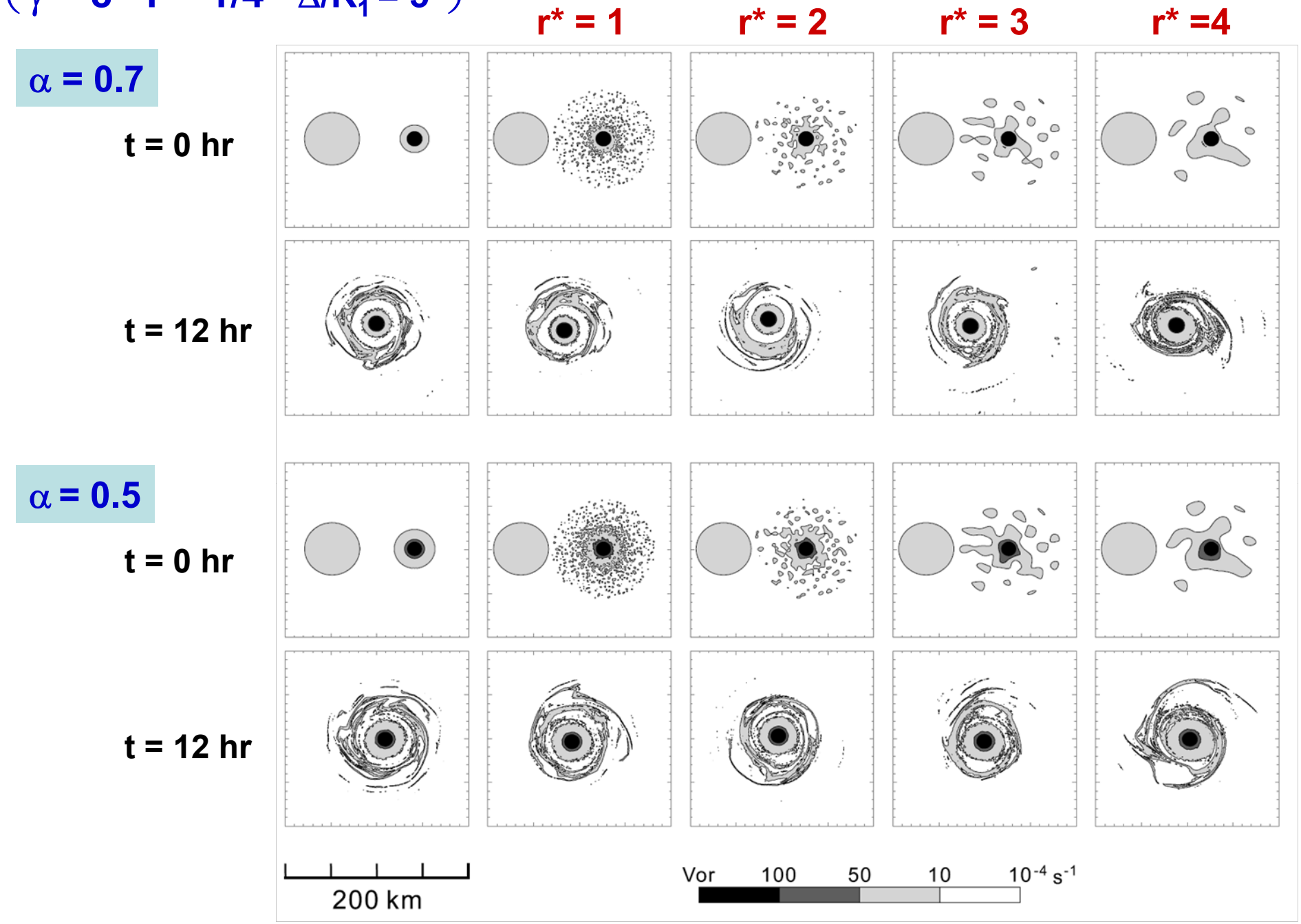
(γ = 8 r = 1/4 Δ/R1 = 5 )
r* = 1
r* = 2
r* = 3
r* =4
α = 0.7
t = 0 hr
t = 12 hr
α = 0.5
t = 0 hr
t = 12 hr
200 km
Vor 100 50 10 10-4 s-1